UNIVERSITA' DEGLI STUDI DI SIENA

DOCTORATE IN GENETICS, ONCOLOGY AND CLINICAL MEDICINE
XXIV CYCLE

MOLECULAR MECHANISMS OF NEURONAL DYSFUNTION IN HIV-ASSOCIATED NEUROLOGICAL DISORDERS

Marco Pacifici

DIRECTOR OF DOCTORAL SCHOOL
Prof. Alessandra Renieri

COORDINATOR OF THE DOCTORAL SCHOOL SECTION
Prof. Antonio Giordano

MENTOR
Prof. Francesca Peruzzi

ACADEMIC YEAR 2011-2012

I am grateful to Dr. Antonio Giordano and the University of Siena for giving me the opportunity to complete my academic education.

I would like to thank Dr. Francesca Peruzzi for this wonderful experience leading me to acquire many scientific skills through her mentorship and support.

I'm thankful to my family for their endless support.

CONTENTS

Preface.....3

Introduction.....5

1. HIV-Associated Neurocognitive Disorders.....5

1.1 Neuro-Biology of HIV Infection.....5

1.2 Pathobiology of HAND.....6

2. HIV-Tat in CNS.....9

2.1 HIV-Tat and neurotoxicity.....9

2.2 HIV Tat, astrocytes and inflammation.....11

2.3 HIV Tat and microglia.....11

2.4 HIV Tat and neurodevelopment.....12

3. MicroRNAs.....14

3.1 MicroRNAs in the Central Nervous System.....14

3.2 MicroRNAs in NeuroAIDS.....15

3.3 MicroRNAs in body fluids.....16

3.4 Diagnostic and therapeutic potential of secreted microRNAs.....17

HIV-1 Tat binds to SH3 domains: Cellular and viral outcome of Tat/Grb2 interaction.....19

CCL8/MCP-2 is a target for mir-146a in HIV-1-infected human microglial cells.....42

Cerebrospinal Fluid miRNA Profile in HIV-Encephalitis 65

Conclusions.....81

References.....83

Preface

Human immunodeficiency virus (HIV) Associated-Neurocognitive Disorders (HAND) remain among the most common disorders in people infected with HIV, even in an era when potent antiretroviral therapy is widely deployed. Although triggered by productive HIV infection of brain macrophages, aberrant and sustained immune activation appears to play a major role in inducing HAND, and may explain the often incomplete neurological response to highly active antiretroviral therapy.

The HIV-1 transactivating factor Tat has been shown to affect cellular functions by interfering with signal transduction pathways and its ability to interact with many proteins may be due, at least in part, to the presence of specific motifs in its amino acid. Following this hypothesis, we have shown evidence for Tat/Grb2 direct interaction, which is mediated by the SH3 C-terminal domain of Grb2 and polyproline regions of Tat. This interaction is functional and bidirectional: it affects cellular pathways as well as viral replication.

Among the cellular molecules and pathways deregulated by Tat, we also found alteration in the expression of selected microRNAs in neurons treated with this viral protein. MicroRNAs are short, non-coding RNAs that regulate gene expression by translational inhibition. Our research group found that a number of Tat-regulated miRNAs impart a negative impact on neuronal functions by targeting molecules involved in the formation of synaptic vesicles. Starting from this study, we have further investigated changes in the expression of miR-146a in HIV-1 infected microglial cells. We found that levels of miR-146a increase upon HIV-infection and we have identified CCL8/MCP-2 as a target for this miRNA, as overexpression of miR-146a prevented HIV-induced secretion of MCP-2 chemokine. The clinical relevance of our findings was evaluated in HIV-Encephalitis (HIVE) brain samples in which decreased levels of MCP-2 and increased levels of miR-146a were observed, suggesting a role for miR-146a in the maintenance of HIV-mediated chronic inflammation of the brain.

One of the most attractive features of miRNAs is that they are secreted in the extracellular environment, in which they remain stable. As such, secretion of miRNAs to body fluids, including the cerebrospinal fluid (CSF), has been associated with several illnesses, for which specific miRNA signatures can predict type of the

disease and progression. We have than hypothesized that, in HAND, a miRNA signature could be a predictor of disease progression and that miRNAs in the CSF could serve as diagnostic and prognostic markers. In a pilot study, we have determined miRNA profiles in the CSF of HIV-infected individuals with and without encephalitis (HIVE). We have also evaluated similarities and differences between CSF and brain tissue miRNAs in the same clinical settings and we have found a global downregulation of miRNAs expression in the CSF of HIV+ individuals compared to HIV-control. This trend was reversed in the presence of encephalitis. After statistical analyses, we have found eleven miRNAs significantly up-regulated in HIVE. This work represented the first report detecting CSF miRNAs in HIV-infected patients and identified a potential miRNA signature for HIVE.

Introduction

1. HIV-associated Neurological Disorders

1.1 Neurobiology of HIV Infection

At least 40 million people worldwide are infected with Human Immunodeficiency Virus-1 (HIV), the causative agent of AIDS. One of the most notable early events in HIV infection is how rapidly the virus is detected in the Central Nervous System (CNS) [1, 2].

The introduction of antiretroviral therapies more than a decade ago resulted in profound declines in morbidity and mortality and raised hopes for the eradication of CNS complications. Despite the initial drop in the incidence of cognitive impairment as a result of highly active antiretroviral therapy (HAART), CNS disease is again increasing as HIV-infected individuals are living longer. In this scenario, HIV-Associated Neurocognitive Disorders (HAND) remain frequent, although often not diagnosed and typically with milder symptoms [1]. These more subtle forms of HAND can greatly impact daily functioning and predict non-CNS morbidity and mortality [3].

HAND has been associated with the presence of elevated CNS inflammatory factors, such as cytokines (including tumor necrosis factor (TNF)-α and interleukin (IL)-1β), PAF, excitatory amino acids (especially glutamate), soluble viral proteins, and chemokines, as determined in post-mortem examination of tissue [4].

These observations *in vivo* have been correlated with *in vitro* findings that support the participation of these factors as mediators of neurodegeneration [5]. In the brain, macrophages/microglia cells are the primary cells infected by HIV, as they can support viral replication. A small percentage of astrocytes can also be infected, but HIV entry and replication are inefficient [6]. There is no evidence that neurons are infected with the virus; however, neuronal damage and dropout occur, indicating that neuronal cell death must be the result of indirect mechanisms, such as neurotoxins released by HIV-infected and uninfected cells [5].

Although HIV enters the nervous system soon after infection, it is uncertain whether progressive neurological damage begins at this stage, or is delayed until after systemic immunosuppression has developed. Within the brain, macrophages may serve as long-lived reservoirs for latent HIV infection [7]. Microglia and macrophages are able to sustain a productive infection without cellular activation. In addition, chronic immune activation with HIV disease progression and depletion of regulatory T cells leads to dysregulation of macrophages, with the overproduction within the central nervous system (CNS) of various proinflammatory cytokines and chemokines. This may be a self-sustaining process with persistent CNS inflammation even after viral replication has been controlled. Interestingly, while the introduction of highly active antiretroviral therapy (HAART) has greatly reduced the incidence of HIV-associated dementia, the prevalence of HIV-associated minor cognitive and motor disorders has increased [8-10].

1.2 Pathobiology of HAND

It is very likely that the CNS infection is established very early after initial infection, and possibly even before seroconversion occurs. Evidence for this stems from cases of acute encephalopathy developing with seroconversion, and additionally from experimental studies with SIV-infected macaques. In a model of subacute SIV encephalitis developed by the dual inoculation of immunosuppressive and neurovirulent strains in pig-tailed macaques, SIV RNA is measurable in the brain parenchyma within days of infection, then levels are suppressed (even while SIV DNA is detectable), and RNA subsequently returns after several months of infection in animals with encephalitis [11]. In humans, the same scenario is likely, although the time course is probably much longer. It is likely that HIV enters the CNS from the blood, with the ingress of activated and infected monocytes through the blood–brain barrier and one critical regulator of the trafficking of monocytes may be osteopontin, a secreted phosphoprotein that can bind to several integrin receptors on leukocytes and is known to induce cell adhesion, migration, and survival in immune cells [11].

The pathological features of HIV encephalitis, most prominent in the basal ganglia, include productive infection within perivascular macrophages, and often the

formation of multinucleated giant cells, from fusion of HIV-infected macrophages. The frequency of HIV encephalitis, with or without opportunistic infections, was 54% before the introduction of HAART and declined by about 60% subsequently [12, 13].

Neurons are not infected by HIV, and regionally, most productive HIV infection is seen within the basal ganglia, brainstem, and deep white matter, causing a prominent upregulation of chemokines and cytokines, particularly in the basal ganglia [14, 15]. This regional susceptibility probably accounts for the mostly subcortical pattern of clinical deficits in HANDs and the selectivity of these pathological changes probably parallels differences in the distribution of perivascular macrophages in various brain regions [16]. Even HAART-treated individuals can show sustained inflammation within the brain. Specimens from individuals receiving HAART had intense inflammation in the hippocampus and temporal cortex [17], a diffuse rarefaction of white matter is observed frequently, with breakdown of the blood–brain barrier and astrocyte apoptosis, but the most representative pathological features are synaptodendritic simplification and neuronal loss [18], as confirmed by morphometric studies [18-20].

Reduced numbers of neural progenitor stem cells have also been identified, which might indicate a reduced capacity in HIV infection for repair of the nervous system.

In this context, the parenchymal release of proinflammatory cytokines impairs cellular functions, inducing the neuropathological changes in HAND, and its severity is strongly associated with the density of activated CNS macrophages and with the expression of activated astrocyte-derived and macrophage-derived products [21-23]. The density of apoptotic astrocytes also correlates with the rapidity of progression of HAND [18]. In the HAART era, there appears to have been some reduction in the degree of immunological response, but there is still frequent evidence of immune activation and oxidative stress in HAART-treated individuals. In Immune reconstitution inflammatory syndrome (IRIS), severe inflammatory responses occur within the brain as a feature of immunological reconstitution after HAART and this reflects invasion of CD8 T lymphocytes in response to antigens expressed within the parenchyma [24]. These cells release granzyme B, which interacts with Gi protein-coupled receptors on neurons and induces a cascade of events leading to neurite trimming and neuronal cell death [25]. Infected or activated perivascular macrophages may additionally contribute to neurological injury through

diverse mechanisms. For example, these cells release several potent toxins, including viral gene products such as Tat and gp120, and a range of cellular gene products, including proinflammatory cytokines such as TNF-α, eicosanoids, nitric oxide, platelet-activating factor, quinolinic acid, and extracellular matrix-degrading proteases [23, 26-32].

CNS macrophages and astrocytes are activated by the extracellular release of HIV proteins such as Tat and the envelope glycoprotein, gp120. Viral proteins do not necessarily need to be present in a continuous concentration to cause neuronal damage or glial-cell activation; even a brief exposure to these proteins can produce a cascade of events that cause a positive feedback loop and thus lead to a selfsustaining, long-lasting action of these cells (*hit and run phenomenon*) [33-35]. They may also be transported along axonal pathways and thus act remotely from where they are released [36]; moreover, specific neurovirulent HIV strains, characterized by increased neurotoxicity of Tat and gp120, may evolve within the CNS in people with HAND [37-40]. The products of activated macrophages and viral proteins can activate astrocytes, leading to the release of astrocyte-derived cytokines and chemokines, altered homeostasis and neurotransmitter uptake, and the local release of excitotoxins. Monocyte chemotactic protein-1 (MCP-1), stromal cell derived factor-1 (SDF-1), and RANTES may be particularly important soluble factors [41, 42]. Although neuronal loss and neuronal apoptosis have been demonstrated at autopsy in HIV-infected individuals, patients with HAND can have at least a partial reversal of symptoms with HAART. This suggests that impairment of neuronal function may occur without neuronal loss, and this may reflect injury to the synaptodendritic complex. Indeed, pathological studies confirm synaptodendritic degenerative changes, with significant loss of synapses, decreased numbers of dendritic branches, and retraction of dendritic spines [43, 44]. Additionally, beading of dendrites and aberrant sprouting may also occur and these anatomical changes, most prominent in the striatum and the hippocampus, lead to disruption of axoplasmic flow [45].

As mentioned above, HIV proteins can travel along axonal pathways to cause synaptic injury at distant sites. Interestingly, the viral protein Tat, affects the CNS in many different ways, including rapid degradation of microtubule-associated protein 2 (MAP2) and the collapse of cytoskeletal filaments, as our lab showed in a previous study [46]. Immunohistochemical analysis of clinical samples further suggests the

occurrence of a similar neurodegenerative mechanism in the setting of HIV encephalopathy [46].

2. HIV-Tat in CNS

2.1 HIV-Tat and neurotoxicity

The HIV- transactivator protein Tat, which is required for viral replication, can be released by infected cells to the extracellular space and be picked up by neighboring cells, maintaining its function. This viral protein can be detected in archived brain samples by IHC and Western blotting analyses [46, 47]. It is unclear whether the majority of the detected Tat is released by infected cells within the CNS or is specifically transported across the blood brain barrier (BBB) from the sera [48], but either ways Tat is taken up by CNS cells often resulting in neuronal toxicity [46, 49, 50]. Interestingly, it has been shown that Tat can be transported along anatomical pathways within the brain, suggesting that sites of neuronal damage may be distant from the site of viral infection [36]. Tat uptake by uninfected cells results in both cytoplasmic and nuclear events, including alterations in gene transcription and secretion of cytokines and chemokines ([51]; also reviewed in [52]), activation of NMDA receptors in neurons [49, 53-55], activation of other receptors [52], and expression of apoptotic proteins [53, 56]. In neurons, some combination of these events results in apoptosis, although the exact mechanism is still unclear. There is now consensus that glutamate and its receptors play an important role in this process, suggesting that HAND may share similarities with other neurodegenerative diseases with respect to dysregulation of glutamate and excitotoxicity.

Tat interacts with many different receptors on various cell types, including integrins, a VEGF receptor (KDR/flk-1) in endothelial cells [57] and possibly the chemokine receptor CXCR4 [58]. In neurons, Tat internalization has been shown to occur primarily through the lipoprotein related protein receptor (LRP) expressed by neurons and activated astrocytes [59, 60]. After internalization with the LRP receptor, Tat escapes the endosome and is found in the cytoplasm and nucleus of neurons, as shown in our previous study [61], and may act in both subcellular

compartments to affect signaling pathways. Indeed, my previous collaborators have observed a predominant cytoplasmic localization of Tat in primary rat cortical neurons and in brain tissues from HIVE patients. In the same study, they have also found that, at least in cultured neurons, retention of Tat in the cytoplasm was mediated by the tubulin-binding domain of Tat. By transfecting primary neurons with YFP-Tat101, YFP-Tat86, and YFP-Tat72 expression plasmids, they have further determined that the affinity of these fusion proteins to the nucleus varied with the length of Tat, with Tat72 having a stronger nuclear localization than Tat86 or Tat101 [61]. Importantly, the length of the Tat C-terminus appears to be critical for Tat-induced neuronal toxicity, as the full length 101 is less toxic than the two-exons 86, which is less toxic than the one-exon Tat72 [61].

Tat treatment, particularly in neurons, results in the release of calcium from IP3 regulated intracellular stores and determines a generalized calcium dysregulation [49, 50, 55, 62-64].

Activation of neuronal nitric oxide synthase (nNOS) and subsequent nitric oxide (NO) production is necessary for Tat induced neuronal apoptosis. nNOS associates with the NDMAR through PSD-95 and is activated by calcium flux through the NMDAR, leading to NO production. Aberrant NO production has been implicated in neuronal cell death caused by a variety of insults (see review [65]). It has been shown that NO toxicity is initiated through interaction with cytochrome c in the mitochondria, resulting in the generation of $ONOO^-$, a molecule that damages the mitochondrial membrane and DNA. Nitric oxide may additionally activate the p38 MAPK pathway, leading to cell death [66], and both the p38 and JNK MAPK pathways have been shown to be activated by Tat treatment of mouse neurons in vitro; however, only p38 MAPK pathway activation was necessary for Tat toxicity [67], while the inhibition of the JNK MAPK pathway significantly reduced the Tat-induced caspase 3 activation. Interestingly, neuronal viability was not affected, indicating that neither the JNK pathway nor caspase activity is necessary for Tat-induced toxicity. This confirmed data from a previous study, which indicated that Tat-induced significant caspase 3 activity as well as release of cytochrome c and endonuclease G from mitochondria [68], but since Tat activates several apoptosis pathways, the cytochrome c/caspase pathway is not crucial for neurotoxicity. Interestingly, as mentioned above, my colleagues investigated the effect of Tat on the extension and maintenance of neuronal processes of rat embryonic cortical

neurons, and in both instances, Tat promoted neuronal damage by a mechanism that involved recruitment of the proteasome to microtubules and microtubule-associated protein-2 (MAP-2) degradation [46]. Moreover, they also showed, in another study, that cleavage of Tat101 by calpain 1 increases neurotoxic effect of this viral protein and presence of the calpain inhibitor protects neuronal cells from Tat-mediated toxicity [61].

2.2 HIV-Tat, astrocytes and inflammation

Treatment of astrocytes with Tat, whether extracellularly or intracellularly through virally infected cells or plasmid transfection, respectively, results in cellular consequences including the induction of inflammatory mediators. Extracellular Tat has been shown to induce human fetal astrocytes to produce the chemokine CCL2 (monocyte chemoattractant protein-1, MCP-1) [69]. CCL2 is important for the recruitment of monocytes to sites of inflammation, and, in the CNS, it induces monocytes to cross the blood-brain barrier and recruits them to the source of secretion. Here, monocytes may elaborate inflammatory mediators and toxins causing CNS damage. It has been shown that CCL2 is elevated in the CSF of individuals with HIVE, and elevated even further in those with HAD [69, 70]; however, there is some evidence that, at least initially, CCL2 may be protective. It has been demonstrated that concomitant treatment with CCL2 protects neurons and astrocytes from Tat-induced toxicity [71] by reducing internalization of Tat and preventing the formation of the complex between LRP, PSD-95 and the NMDAR, as well as by reducing levels of extracellular glutamate. The additional molecular mechanisms that mediate CCL2 neuroprotection are currently being investigated.

2.3 HIV Tat and microglia

Microglia cells are the resident macrophages of the CNS and the predominant cells infected productively by HIV. However, cognitive impairment does not correlate with the level of viral infection in the CNS, but instead inflammation [72]. Upon activation, microglia cells secrete inflammatory mediators including cytokines and chemokines, reactive oxygen and nitrogen species, and excitatory amino acids,

leading to recruitment of other inflammatory cells into the brain. Some of these factors have also been shown to be neurotoxic, such as quinolinic and arachidonic acids [73], suggesting that microglial activation may contribute both directly and indirectly to neuronal toxicity in HIV. Several studies demonstrated the effect of Tat on microglia (see reviews [74, 75]). Treatment of human microglia with Tat led to dramatic increases in the secretion of the chemokines CCL2, CXCL8, CXCL10, CCL3, CCL4 and CCL5 [76], chemotactic factors for monocytes and/or lymphocytes. Tat induced expression of these chemokines was mediated by activation of the ERK1/2 MAPK, PI3K and p38 MAPK pathways. Tat also induced migration of human microglia [77, 78] and this migratory phenotype was mediated through autocrine signaling, by the release of CCL2 by microglia and activation of CCL2 receptors on the microglia [78]. Most likely, HIV-infected monocytes transmigrate into the CNS and release toxic and chemotactic molecules, such as Tat and CCL2 that induce uninfected microglia to migrate to HIV infected areas. This recruitment of microglia contributes to the infection of this cell type by HIV and enables viral propagation within the CNS. Following recruitment, activation and propagation of HIV infection in microglia, inflammation is enhanced within the CNS parenchyma, resulting in HIVE, necrotizing lesions and ultimately neurodegeneration and cognitive impairment.

2.4 HIV Tat and neurodevelopment

The developing brain appears to be particularly vulnerable to the pathologies of HIV as the incidence of CNS disease is significantly higher in HIV infected children than adults. This may be explained by the complex interaction of those pathways stimulated by growth factors and those pathways affected by Tat treatment.

Tat synergistically cooperates with nerve growth factor (NGF) to enhance LTR transcription in neuronal cell models [79] and in immature neuronal and glial cells [80]. Further, neuronal cells transfected with Tat cDNA or treated with low concentration of soluble Tat, showed not only an increased resistance to apoptosis [81], but also a considerable increase in cell proliferation [82]. In agreement with these data, our lab, in a previous work, showed that PC12 cells expressing Tat gained the ability to survive and proliferate in the absence of serum, thus enhancing

the transformed phenotype of this cell line [83]. Furthermore, while PC12 cells undergo differentiation in response to NGF treatment, PC12 cells that express Tat do not extend neurite processes in response to NGF and their differentiation program is inhibited. Also, it was noted that the serum-independent growth promoted by Tat in PC12 cells is, at least in part, mediated by an increased expression of the inhibitor of differentiation Id1 [83]. Id proteins are helix–loop–helix (HLH) transcription factors, which lack a DNA binding domain. The binding of the Id proteins to tissue-specific basic HLH (bHLH) leads to the inhibition of transcription [84]. In many instances, Id proteins have been shown to control cell-cycle progression (reviewed in [85]), and survival of post-mitotic cells [86]. The Id proteins are known to affect the balance between cell growth and differentiation in a number of cell types (reviewed in [87-89]). An interesting study from my previous collaborators pointed to the importance of the Id proteins as additional targets for the action of Tat in neuronal cells. Evidence suggests that aberrant re-entry into the cell cycle may represent a mechanism of the neuronal apoptosis [90-92] observed in neurodegenerative diseases [93, 94]. In this scenario, increased levels of Id1, in response to the action of Tat in neuronal cells, might result in neuronal cell death. An alternative and maybe more attractive hypothesis suggested that, in several neurodegenerative disorders, there is an increase in neurogenesis [95-97]. The process of neurogenesis involves proliferation of neuronal progenitors, their differentiation, and their migration toward the regions of the brain that need repair and neuronal replacement. All these processes are governed by the balance of expression of transcription factors including members of the Id family proteins [98, 99]. Indeed, the improper expression of Id1 in the presence of Tat may have detrimental effects on ongoing neurogenesis and differentiation. Moreover, it has been demonstrated that Tat is acetylated by p300 and PCAF [100-105], important transcriptional coactivators for the signaling of nerve growth factor (NGF) and brain-derived neurotrophic factor (BDNF), and Tat interferes with this pathway resulting in inhibition of the protection against apoptosis provided by NGF [83]. There is further evidence supporting opposing signaling of neurotrophins and Tat. BDNF and NGF protected against Tat induced toxicity in cultured rat cerebellar granular neurons [106], leading to enhanced transcription of the antiapoptotic gene Bcl-2. In this context, my colleagues demonstrated that expression of Tat101 in neuronal progenitors induced the highest degree of cell death in proliferating cells compared to cells undergoing

neuronal differentiation, while treatment of cells with the calpain inhibitor ALLN significantly enhanced their survival [61]. When expressed endogenously, Tat101 is toxic to neuronal progenitors maintained in proliferating medium and ALLN treatment enhances cell survival, suggesting that cleavage by calpain 1 may augment toxicity of Tat. In differentiating cells, however, expression of Tat101 is less toxic and addition of ALLN has only a marginal effect on cell survival. Of interest, mature neurons appear to be more resistant to Tat-mediated cell death. These studies demonstrate that Tat may have effects in the developing CNS.

3. MicroRNAs

3.1 MicroRNAs in the Central Nervous System

MiRNAs are short RNA strands of 18-25 nucleotides that are both evolutionarily conserved and emergent, potentially currently undergoing evolution in vertebrates [107]. MiRNAs can be transcribed from non-protein-coding genomic regions or intronic regions of ‘‘host’’ genes, with which they are usually co-expressed [108]. Pre-miRNAs are synthesized in the nucleus, possessing characteristic hairpin loops [109]. After being exported to the cytoplasm they are further processed by Dicer enzyme into mature miRNAs usually of 21–23 nucleotides in length [110] . They function in association with the RNA-induced silencing complex (RISC) by hybridizing to 8-mer ‘‘seed’’ sequences in the 3’ untranslated regions (3’UTR) of target mRNAs [111]. Imperfect match results in interruption of translation by the ribosomes, while perfect seed sequence matching leads to cleavage of the target mRNA [112]. The search for miRNA targets has been largely bioinformatics-based (the Sanger database http://www.sanger.ac.uk/resources/ is an excellent archive of information on pre-,mature- miRNAs, host genes, chromosomal location, and targets [113]).

A growing body of evidence supports a role for miRNAs in neural patterning, neuronal maintenance and neurodegeneration. Kapsimali *et al.* found that miRNAs have variable expression profiles in the developing and mature brain, demonstrating differences across the lifespan of a cell [114]. MiR-92b varies in expression during

the transition from proliferation to differentiation of neurons, while miR-124 is constitutively expressed in mature neurons. Lau and colleagues identified 43 miRNAs with dynamic expression during transition from progenitor cells to mylenating mature oligodendrocytes miRNAs [115]. Unsurprisingly, miRNAs can be regionally specific, as evidenced by miR-222 which is restricted to the telecephalon and they can also be cell-type specific, e.g. the motor-neuron specific miR-218 [114].

MiRNAs have been implicated in neurodegenerative diseases such as: Alzheimer's, Parkinson's, and Huntington's diseases. MiRNA expression profiling of CNS tissue from patients with sporadic Alzheimer's disease revealed 13 dysregulated miRNAs, which included those with putative binding sites in the 3'UTR of amyloid precursor protein [116]. Kim and coworkers described a regulatory feedback network in midbrain dopaminergic cells whereby miR133-b and the gene Pitx3 regulate tyrosine hydroxylase function, possibly contributing to Parkinson's pathophysiology [117]. In the Frontal Cortex of Huntington's Disease patients, miR-132 was found to be significantly downregulated possibly resulting in increased levels of RE1-silencing transcription factor (REST), a protein with potential implications in neuropathogenesis [118].

Neurologic dysfunction is likely influenced by overlapping mechanisms of miRNA dysregulation in neurodegenerative disorders, psychiatric disorders, and/or infectious diseases.

3.2 MicroRNAs in NeuroAIDS

Given that miRNAs play a role in development and homeostasis of the CNS, and also are affected by and affect the properties of viral infection, it is important to clarify the interplay between miRNAs and HIV in the CNS and how they correlate with common clinical co-morbidities such as HIV-associated neurological disorders (HAND). Interestingly, my colleagues found that HIV-Tat may promote miR-128a activity, leading to a reduction in SNAP25 expression in neurons [119]. Intuitively, decreased expression of pre-synaptic proteins like SNAP25 by the action of microRNAs may compromise proper synaptic activity. Whether this is an effect due to a decreased dendritic arborization observed in HIVE tissues or an early event

remains to be determined. Moreover, an in vitro study using recombinant Tat showed increased microRNA expression (within 12 h from the treatment of primary neurons) and decreased levels of synaptic proteins as early as 24 h in the absence of a clear reduction of dendritic branches, suggesting that increased upregulation of specific microRNAs could precede neuronal damage [119].

Several miRNAs were also shown to affect HIV-1 gene expression and replication in vitro and in animal models [120]. Reciprocally, HIV-1 was shown to affect the levels of several miRNAs to change their expression profile [121]. Interestingly, some targets of the up-regulated miRNAs in primary fetal neurons treated with Tat have been associated with neurological diseases. For instance, miR-378 has been shown to target the CYP2E1 gene, a cytochrome p450 isoform whose polymorphism is associated with Parkinson disease [122] and is found tightly associated with dopamine-containing cells in the substantia nigra [123]. Accordingly, Chang et al. observed a 2-fold decrease in the expression of CYP2E1 in neurons treated with Tat in addition to an increase in miR-1 expression. One interesting target of miR-1 is the Mef2A gene. Recently, it was reported that Mef2A induces the expression of miR-(379–410) cluster in neurons, and the expression of this cluster is important for dendritogenesis [124].

3.3 MicroRNAs in body fluids

While the majority of miRNAs are found intracellularly, a number of miRNAs have been detected outside of cells, including in various body fluids (e.g., serum, plasma, saliva, urine and milk) [125-131]. Furthermore, alterations in the level and composition of these extracellular circulating miRNAs are tightly correlated with various health problems, including cancers [125, 127, 128, 130], diabetes [125] and tissue injury [132-134]. These results firmly establish the quantification of circulating miRNAs as an extremely promising model to assess and monitor the body's pathophysiological status.

Extracellular miRNAs circulate in the body fluids with a high concentration and sufficient integrity despite high extracellular ribonuclease (RNase) activity, indicating that extracellular miRNAs are likely packaged in some manner to shield them from digestion. Indeed, naked miRNAs added to plasma are immediately

degraded, whereas circulating miRNAs are stable for hours under the same conditions [129]. Further studies have also shown that circulating miRNAs are protected from and resistant to harsh conditions such as extreme temperatures, extreme pHs or freeze-thaw cycles [125]. This phenomenon raises intriguing questions regarding the mechanism of circulating miRNA stability. Furthermore, the origin of such extracellular miRNAs also requires exploration. At present, there are at least three possibilities for the remarkable stability of circulating miRNAs and their sources: (1) they are passively leaked from broken cells during tumorigenesis or tissue injury [125, 129]; (2) they are packaged in small membranous vesicles, including exosomes, shedding vesicles and apoptotic bodies, which accounts for the release of miRNAs into circulation and offers protection against RNase activity [135-138]; (3) they are protected by the formation of a protein-miRNA complex. Some studies have demonstrated that many extracellular miRNAs are detectable in conjunction with proteins or lipoproteins, but devoid of membrane vesicles, suggesting the existence of non-vesicle enclosed, RNA-binding protein-associated miRNAs in extracellular fluids, including those bound to AGO2, nucleophosmin1 (NPM1), and high-density lipoprotein (HDL) [134, 139-141]. Recent studies indicate that miRNAs released from donor cells that are either enclosed in vesicles (exosomes, shedding vesicles and apoptotic bodies) or associated with lipoproteins (HDL) are active and can function as secreted molecules to influence the recipient's cell phenotype [134, 136, 137, 141]. The difference between vesicle-enclosed and lipoprotein-associated miRNAs is largely unknown. Their different secretion mechanisms suggest that they may originate from different cell types and, therefore, have different fates and functions.

3.4 Diagnostic and therapeutic potential of secreted microRNAs

Because secreted miRNAs can be detected in biological fluids such as plasma and can reflect the physiological status of the cells and organs they originate from, they could potentially serve as predictive and prognostic biomarkers for diseases.

Several studies have suggested the use of secreted miRNA for diagnostic purposes. For instance, detection of secreted viral miRNAs in the plasma of patients could allow for the detection of infections [142]. Skog et al. reported that the miRNAs characteristic of gliomas could be detected in microvesicles from glioblastoma

patient serum [143], implying for the first time that miRNAs secreted from tumor cells may provide diagnostic information and aid in therapeutic decisions for cancer patients. Rabinowits et al. isolated exosomes from human plasma and evaluated the levels of total exosome, exosomal small RNA, and specific exosomal miRNAs in controls and lung cancer patients [144]. They found that the total exosome level and exosomal miRNA concentration were significantly higher in the lung cancer group and that tumor-derived exosomes from the lung cancer patients contained miRNA similar to the corresponding tumor cells [144]. In another study, Taylor et al. reported that patients diagnosed with ovarian cancer exhibited significantly elevated levels of serum exosomes compared to benign disease or controls and that the levels of circulating exosomes increased as the cancer stage progressed [145]. Interestingly, miRNA expression profiling in serum exosomes of ovarian cancer patients correlated well with that of their tumors [145]. Michael et al. showed that exosomes can be readily isolated from the saliva of healthy donors and Sjögren's syndrome patients, and these exosomes contain detectable miRNAs [146]. Because the isolation of exosomes is non-invasive, subsequent characterization of the miRNA expression patterns is straightforward, exosome profiling holds great promise as an alternate or complementary diagnostic strategy to biopsy profiling and as a screening tool for asymptomatic patients.

The presence of extracellular circulating miRNAs has been detected in a variety of conditions. As observed in many studies, these miRNAs are remarkably stable and are often found inside small membranous vesicles (exosomes, shedding vesicles, and apoptotic bodies) or in association with RNA-binding proteins (HDL, AGO2, and NPM1). Additional findings strongly support the hypothesis that extracellular miRNAs in these forms are actively secreted from cells, are transported within the extracellular environment and are taken up by recipient cells before their finally binding to target mRNAs, resulting in gene silencing in the recipient cells.

Numerous miRNAs can be delivered at once, thus simultaneously regulating multiple target genes and activating a complex network of signaling events in the target cells.

Deviations from the normal expression pattern of miRNAs likely play a role in diseases such as neurodegenerative disorders.

HIV-1 Tat binds to SH3 domains: Cellular and viral outcome of Tat/Grb2 interaction

Biochim Biophys Acta. 2011 Oct;1813(10):1836-44

Slava Rom, Marco Pacifici, Giovanni Passiatore, Susanna Aprea, Agnieszka Waligorska, Luis Del Valle, Francesca Peruzzi

Abstract

The Src-homology 3 (SH3) domain is one of the most frequent protein recognition modules (PRMs), being represented in signal transduction pathways and in several pathologies such as cancer and AIDS. Grb2 (growth factor receptor-bound protein 2) is an adaptor protein that contains two SH3 domains and is involved in receptor tyrosine kinase (RTK) signal transduction pathways. The HIV-1 transactivator factor Tat is required for viral replication and it has been shown to bind directly or indirectly to several host proteins, deregulating their functions. In this study, we show interaction between the cellular factor Grb2 and the HIV-1 trans-activating protein Tat. The binding is mediated by the proline-rich sequence of Tat and the SH3 domain of Grb2. As the adaptor protein Grb2 participates in a wide variety of signaling pathways, we characterized at least one of the possible downstream effects of the Tat/Grb2 interaction on the well-known IGF-1R/Raf/MAPK cascade. We show that the binding of Tat to Grb2 impairs activation of the Raf/MAPK pathway, while potentiating the PKA/Raf inhibitory pathway. The Tat/Grb2 interaction affects also viral function by inhibiting the Tat-mediated transactivation of HIV-1 LTR and viral replication in infected primary microglia.

Introduction

Protein–protein interaction mediated by a conserved sequence motif in one protein and a protein recognition module (PRM) in another is a common mechanism of assembling protein complexes participating in signal transduction pathways. Src homology 3 (SH3) modules are conserved elements of about 60 amino acids present in a large number of proteins which participate in a variety of biological processes [1, 2]. Although SH3 domains generally recognize a PxxP motif in their binding partners, individual SH3 domains might possess distinct specificities for putative ligands. At

least part of this specificity is thought to be determined by the amino acids flanking the core sequence [3, 4], making the overall three-dimensional structure of the PxxP-bearing protein specific only for certain SH3-carrying partners.

While protein–protein interactions mediated by SH3 domains participate in many cellular processes, one of the best characterized signaling pathways is the tyrosine kinase receptor mediated Ras activation. Growth factor receptor-binding protein-2 (Grb2), consisting of three domains, two SH3 and a single SH2 domain, is one of the central factors in the Ras signaling cascade. Grb2 can recruit Ras guanine nucleotide exchange factor, Sos, to the activated tyrosine kinase receptor at the plasma membrane, where Sos activates Ras [5]. Activated Ras then leads to activation of MAPK signaling cascade [6]. Besides its critical role in normal development [7], Grb2-mediated mitogenic signals have been implicated in several human tumors (reviewed in [8]).

The transactivating factor Tat is an 86–101 amino acid polypeptide encoded by the HIV-1 virus [9]. Several studies have demonstrated the importance of HIV-1 Tat in the viral replication cycle and in the pathogenesis of AIDS [10, 11]. Tat displays several important biological activities affecting uninfected and infected cells by a paracrine/ autocrine mechanism due to secretion of Tat from infected cells and its uptake by uninfected neighboring cells [12-14]. Tat has been shown to modulate expression and activity of several cellular factors deregulating a variety of signal transduction pathways [15]. For instance the modulation of signaling pathways such as the MAPK or the PI3-K pathways by Tat is well documented [16-26]. Given the ability of Tat to directly interact with host factors, we sought to examine the amino acid sequence of this viral protein for the presence of protein–protein recognition elements. Similar to another HIV protein, Nef [27], Tat also contains proline-rich motives which are putative SH3-binding domains, one at the N-terminal and the other at the C-terminus of the protein. In an SH3 domain binding screening, we found that Grb2-derived peptides gave the highest probability score of binding to Tat. GST-pull-down assay further revealed a preferred binding of Tat to the C-terminal SH3 domain of Grb2. The outcome of Tat/Grb2 interaction was evaluated in terms of cellular and viral activities. In respect to cellular function, Tat/Grb2 interaction resulted in the attenuation of the MAPK pathway while potentiating the Raf inhibitory pathway. Of interest, in terms of viral functions, we found that Tat/Grb2 interaction decreased the activity of Tat on the HIV-1 LTR, as determined by reduced levels of p24 in the

medium of HIV-1 infected human microglia.

Altogether our results provide evidence for a direct interaction of Tat with Grb2, and possibly other SH3-bearing proteins, suggesting a broad-spectrum mechanism for Tat-mediated deregulation of signaling pathways.

Materials and methods

Cell culture, transfection, infection, recombinant proteins and inhibitors

The human Glioblastoma cell line LN229 was maintained in Dulbecco's modified Eagle's medium (DMEM) supplemented with 10% fetal bovine serum (GIBCO Invitrogen Co., Carlsbad, CA). Primary human fetal microglia cells were isolated and cultured as previously described [28]. Preparation of HIV-1, strain JRFL, stock and infection of primary microglia were performed at a multiplicity of infection (MOI) of 0.1, as described previously [28].

For transient expression experiments, LN229 cells were seeded on 60 mm dishes (BD Falcon™, Oakville, Ontario, Canada) at a density of 5×10^5 cells/plate, and the transfection was performed using FuGENE 6 Transfection reagent (Roche Diagnostics Corp., Indianapolis, IN) according to the manufacturer's instructions. When required, 24 h after transfection cells were washed with PBS twice and starved for 24 h in DMEM without FBS. Stimulation was done by IGF-1 (40 ng/ml; Invitrogen, Carlsbad, CA) for 0, 2 and 10 min and was stopped by medium removal and placing on ice. Recombinant Tat101 was from Immunodiagnostics (Woburn, MA). Inhibitors, LY 294002 and H-89, were purchased from BioMol (BIOMOL Int., Plymouth Meeting, PA).

Antibodies and Western blots

Monoclonal antibody specific to Grb2 was purchased from BD Transduction Laboratories™ (BD Biosciences, San Jose, CA). Antibodies specific to phospho-Akt (Ser473), Akt, phosphorylated forms of Erk1/2 (Thr202/Tyr204), total Erk1/2, phospho-c-Raf (Ser259), total IFG-IR and Gab-1 were purchased from Cell Signaling Inc. (Danvers, MA). Polyclonal antibody specific to total c-Raf protein was purchased from Santa Cruz Biotechnology (Santa Cruz, CA).

Cells were collected by scraping the plates in the presence of PBS, followed by

centrifugation and lysis of the cell pellet in the appropriate volume of RIPA buffer (50 mM Tris pH 7.4, 1% NP-40, 0.25% sodium deoxycholate, 150 mM NaCl, 1 mM EDTA, 1 mM EGTA, 1 mM PMSF, 1 mM sodium orthovanadate, phosphatase inhibitors and protease inhibitor cocktails). Fifteen to fifty micrograms of whole cell lysates was separated on 4–15% SDS-PAGE (BioRad, Hercules, CA). Sample proteins separated by SDS-PAGE were transferred onto nitrocellulose membranes (BioRad) using BioRad semi-dry blotting system (BioRad, Hercules, CA).

Immunohistochemistry

Five samples of formalin-fixed, paraffin-embedded HIV-Encephalopathy samples were collected from the NIH funded, HIV National tissue consortium at the Manhattan Brain Bank, Mount Sinai School of Medicine. All samples were from the cortex and sub-cortical white matter of the frontal lobe, and histopathologically all contain microglial nodules and perivascular cuffs of inflammatory cells, including giant multinucleated cells, pathognomonic of HIV-Encephalitis. According to the clinical data provided by the HIV Brain Bank, all five patients showed signs of dementia, ranging from mild to moderate.

For immunohistochemistry, four micron thick sections were cut using a microtome and placed on charged glass slides. Immunohistochemistry was performed using the avidin–biotin peroxidase methodology, according to the manufacturer's instructions (Vector Laboratories, Burlingame, CA). Our protocol includes deparaffination, rehydration in alcohol up to water, antigen retrieval in citrate buffer pH 6.0 at 98 °C, endogenous peroxidase quenching and blocking in normal horse serum for 2 h at room temperature. Primary antibodies used included a mouse monoclonal anti-Grb2 (Santa Cruz; 1:100 dilution) and a mouse monoclonal anti-Tat (ImmunoDiagnostics, Inc., Woburn, MA; 1:500 dilution). After rinsing with PBS, secondary biotinylated antibodies were incubated for 1 h (1:200 dilution), followed by avidin–biotin peroxidase complex incubation (ABC Elite kit, Vector Laboratories, Burlingame, CA) and developed with diaminobenzidine (DAB, Boehringer Ingelheim, Ingelheim, Germany), counter-stained with hematoxylin and coverslipped.

For double labeling, the first steps of the protocol are similar to the protocol described above. However, after incubation with the first primary antibody, a secondary fluorescein tagged antibody was incubated for 1 h at room temperature, and after rinsing thoroughly, the second primary antibody was incubated overnight. Finally a

second secondary antibody tagged with rhodamine was incubated for 1 h. Sections were coverslipped with aqueous based mounting media containing DAPI and visualized under a fluorescent microscope (Olympus BX61 equipped with a DP72 camera, Center Valley, PA). Deconvolution of selected pictures was performed using the deconvolution software Slide Book 5 (Intelligent Imaging Innovations, Denver, CO).

Plasmids and GST-fusion protein construction

GST-fusion Grb2 full length and the various truncated constructs (ΔN–SH3, ΔC–SH3 and ΔNC–SH3) were generated by PCR using as template the sequence of human Grb2 contained into the pGex-2T– Grb2 plasmid (a kind gift of Dr. Robert J. Sheaff). The primers were: Grb2 Forward 5′-ACGGATCCATGGAAGCCATCGCCAAAT ATGAC, Grb2 Reverse 654 Stop 5′-ACCTCGAGTTAGACGTTCCGGTTCACG GGGG, Grb2 Δ1–69 Forward 5′-ACGGATCCATGGAAGAAATGCTTAGCAAA CAGCGG, and Grb2 Δ128–198 Reverse-stop 5′-ACCTCGAGCCGCAGGAATA TCTGCTGGTTTCTGAGACAGATGT. Those primers were used in various combinations to obtain the desired amplified sequences that were subsequently cloned into pGex-5x1 expression vector (GE Healthcare Bio-Sciences Corp., Piscataway, NJ) between BamHI and XhoI sites (labeled in bold). Wild type and deletion mutants of Grb2 were also subcloned into pmCherry vector (BD Biosciences Clontech, Mountain View, CA) between NotI and EcoRI sites.

The GST–Tat (truncated Tat86, Tat72, Tat50) constructs have been previously described [29]. To generate GST–Tat101 wild type fusion protein the PCR primers were: Forward 5′-ACAAG GTACCATGGAGCCAGTAGATCCTAGC, and Reverse 5′-ACGCGGCCGCTCAAGCGCTCGGATCTGTCTCTG. To generate pEYFP-Tat101 fusion protein, the PCR primers were: Forward 5′-ACAAGGTA CCATGGAGCCAGTAGATCCTAGC, and Reverse 5′-ACGGATCCTCAAGCGC TCGGATCTGTCTCTG. The PCR product was cloned into pEYFP-C1 plasmid (BD Biosciences Clontech, Mountain View, CA) between KpnI and BamHI sites.

GST-pull-down assays

Expression and purification of GST fusion proteins were performed according to the manufacturer's instructions. 300–400 μg of protein lysates from LN229 cells was

incubated with purified GST–Tat fusion proteins (1 μg) bound to glutathione-agarose beads or from Tat-expressing LN229 cell lysates that were incubated with GST–Grb2 fusion proteins bound to glutathione-agarose beads for 2 h at 4 °C at rotator. The glutathione-agarose resin was centrifuged at 14,000 ×g for 3 min and washed 3 times with ice-cold RIPA buffer. Precipitated proteins were suspended in 2× SDS protein-loading buffer, boiled for 5 min, and subjected to 4–15% SDS-PAGE; this was followed by electrotransfer and immunoblot analysis as described above.

SH3 domain prediction

Prediction of SH3 domain interacting sites was performed using SH3-Hunter (http://cbm.bio.uniroma2.it/SH3-Hunter/) [30].

Protein kinase A (PKA) kinase assay

PKA activity was measured using commercially available kit (PKA assay kit, Upstate, Lake Placid, NY), according to the manufacturer's instructions. In brief, LN229 cells were transfected, serum starved for 24 h and IGF-1 stimulated, as described above. Prior to lysis cells were washed twice with ice-cold PBS, scraped and lysed with RIPA buffer. For measurement of PKA activity in cellular extracts, 60 μg protein lysates were incubated with kemptide, ATP, cAMP and 2 μCi of [γ-^{32}P] ATP in the presence of PKC/CaMK inhibitor cocktail for 10 min at 30 °C. Samples from each reaction were spotted on P81 phospho-cellulose membrane, and the reaction was stopped by immersion of the membrane discs in 0.75% phosphoric acid. Amount of incorporated [γ-^{32}P] into the substrate was counted using a multipurpose scintillation counter (Beckman LS6500).

HIV-1 LTR transactivation assay

LN229 cells were co-transfected with pEYFP-Tat101, pmCherryGrb2 wild type or truncated mutants, an pHIV LTR–Firefly luciferase reporter plasmid [31] and a Renilla luciferase control pRL–TK plasmid (Promega, Madison, WI) using Fugene 6 (Roche Diagnostics Corp., Indianapolis, IN). Cells were collected 24 h after transfection and subjected to luciferase assay, as per the manufacturer's recommendations (Promega, Madison, WI). Firefly values were normalized with Renilla as a

mean of transfection efficiency.

Statistics

Results were analyzed by an unpaired, two-or one-sided Student's t-test. p-values ≤0.05 were considered statistically significant.

Results

Tat protein contains two putative SH3 domain-binding sites

Bioinformatic analysis using SH3 Hunter web server (http://cbm.bio.uniroma2.it/SH3-Hunter/) [30] revealed the presence of two putative SH3 binding domains in the amino acid sequence of HIV-Tat full length. Given an input query protein sequence, the server identifies peptides containing poly-proline binding motifs (PxxP) and associates them to a list of SH3 domains, in order to create peptide–domain pairs. As shown in Fig. 1A Tat protein sequence contains two putative SH3 domain binding sites residing in the N-terminal and C-terminal parts of the protein between amino acids 3–8and 81–86, respectively. According to the SH3 Hunter program Tat is predicted to interact with RNA-binding protein Fus1 with a significantly high score of 0.976 and reliability (sensitivity and precision) of 95% and 60%, respectively (Fig. 1B). With a slightly lower score of 0.967, the C-terminus of Tat could interact with growth factor receptor-bound protein 2 domain C (Grb2-C), Grb2 homolog in Caenorhabditis elegans (Sem5), Endophilin-A1 (End2) and Endophilin-A3 (End3) proteins with sensitivity of 57% and with precision of 70%. Further, Tat is also predicted to interact with much lower scores but with higher sensitivity with Grb2-C, signal transducing adaptor molecule SH3 domain and ITAM motif 1 (STAM-1), and End2. Most of the proteins were predicted to bind poly-proline motif located between 81 and 86 amino acids of Tat protein. However, two domains, End2 and Grb2-C, showed ability to bind the proline rich motif of Tat located in the N-terminus.

A

ME**PVDPRL**EPWKHPGSQPKTACTCYCKKCCLHCQVCFLTKGLGISYGRKK
RRQRRRAPPDRQTNQAPLKQPASQPRGD**PTGPKE**SEKKVERETETHPES

B

Peptide	Domain name	Score	S	P
78-84 RGDPTGP	Fus1	0.976	95%	60%
81-86 PTGPKE	Sem5	0.967	57%	70%
81-86 PTGPKE	**Grb2-c**	0.967	57%	70%
81-86 PTGPKE	End3	0.967	57%	70%
81-86 PTGPKE	End2	0.967	57%	70%
3-8 PVDPRL	**Grb2-c**	0.930	98%	50%
81-86 PTGPKE	STAM-1	0.915	98%	50%
3-8 PVDPRL	End2	0.902	98%	50%

Fig. 1. *Tat protein contains two putative SH3 domain-binding sites. A) Amino acid sequence of Tat showing two possible SH3 binding sites (in bold). B) List of SH3 domain containing proteins predicted to bind TAT using SH3 Hunter web server (http://cbm.bio.uniroma2.it/SH3-Hunter/). The first column represents amino acid sequence of peptide and its location in the Tat protein. The second column gives names of domains of interacting proteins. The last three columns in the output define respectively the significance (score) and the reliability (sensitivity and precision) of the prediction.*

Tat directly interacts with Grb2 protein

Since the SH3 domains of Grb2 were recurrent in the list we decided to test Tat–Grb2 interaction in vitro by GST-pull-down assay. The full-length Tat101 and three deletion mutants were cloned into the pGex plasmids (Fig. 2A). Tat101 and Tat1–86 constructs comprised both SH3 putative binding sites; Tat1–50 contained the N-terminal putative SH3 binding site, whereas Tat50–72 was depleted of both. Fig. 2B shows that Tat101 (full length) as well as Tat1–86 deletion mutant was able to pull down Grb2 protein from LN229 whole cell lysate. Some degree of binding was detected with GST–Tat1–50, while the Tat50–72 mutant, lacking both PxxP motifs, failed to pull down Grb2. Next, we generated Tat mutants (pEYFP-Tat101) in which the proline residues within the SH3 binding domains were substituted with alanines as follows: single SH3 mutants had prolines 3 and 6 (P3/6A) and 81 and 84 (P81/84A) changed, respectively; the double mutant contained all four proline residues mutated to alanines (P3/6/81/84A). LN229 cells were transfected with these mutants and with the control Tat wild-type. Results of GST-pull-down assays show that both single pEYFP-Tat–SH3 mutants were efficiently pulled down by GST–Grb2 (Fig. 2C, lanes 2 and 3), although less efficiently than wild-type Tat (lane 5). The double mutant of Tat, in which a total of four proline residues were changed to alanines (P3/6/81/84A), was not pulled down by Grb2 (Fig. 2C, lane 4), confirming the prediction analysis that both putative SH3 binding domains of Tat may bind Grb2.

Grb2 protein carries two SH3 domains, SH3-1 (N-terminal) and SH32 (C-terminal), separated by one Src homology 2 (SH2) domain positioned in the middle of the

protein. We cloned three GST-tagged truncated fragments of Grb2 consisting of either SH3-1 (ΔC) or SH3-2 (ΔN), or depleted of both SH3 domains (ΔN/C) as well as the full length (WT) (Fig. 2D). The four Grb2 expressing constructs were examined for their ability to pull down Tat from Tat-expressing cells (Fig. 2E). Results confirmed that Grb2 full length directly interacted with Tat, and, among the mutants, the C-terminal SH3 domain of Grb2 (ΔN) pulled down Tat more efficiently than the N-terminal domain (ΔC) or the mutant lacking both SH3 domains (ΔN/C).

The Grb2-associated binder 1 (Gab1) protein has been reported to bind with high affinity to the C-terminal SH3 domain of Grb2 [32].The specificity of such Grb2/Gab1 interaction was confirmed in our system by GST pull-down experiments showing that Gab1 can be efficiently pulled down by Grb2–SH3-C but not Grb2–SH3-N or Grb2–SH2 (Fig. 2F). We then performed a competition assay in which Gab1 was pulled down by GST–Grb2–SH3-C in the absence or presence of recombinant Tat (Fig. 2G). As expected, Grb2–SH3-C pulled down Gab1 in the absence of Tat; however, addition of 1 μg of recombinant Tat efficiently competed with Gab1 for binding to the C-terminal domain of Grb2.

Taken together these results suggest that the interaction between Tat and Grb2 is mediated by the PxxP motifs of Tat and the C-terminal SH3 domain of Grb2.

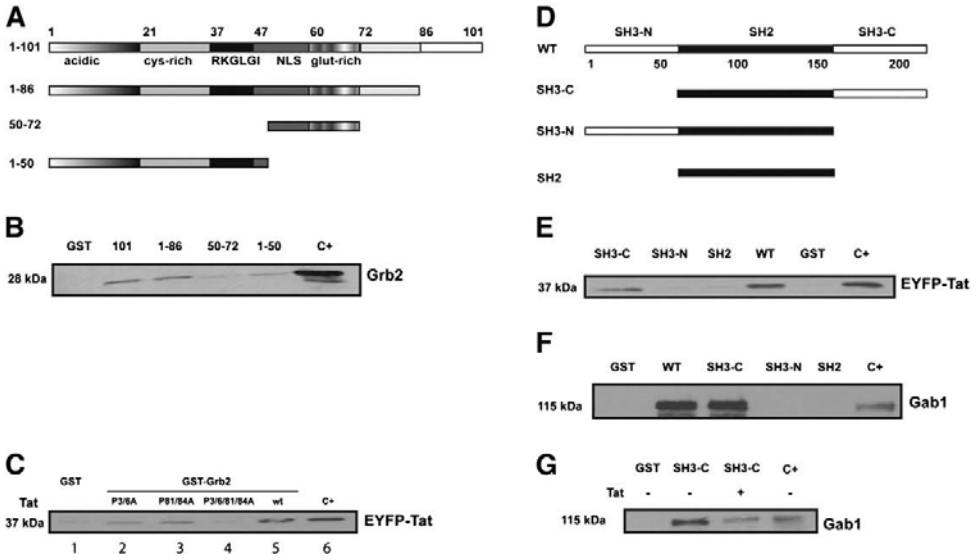

Fig. 2*. Tat directly interacts with Grb2. A) Scheme of GST–Tat full-length and various mutants cloned into pGex-5x-1 plasmid for GST-fusion protein expression. B) Western blot to detect Grb2 pulled down using wild type Tat101 or the various mutants. C+ represents whole cell lysate (15 μg). C) GST–Grb2 pull-down of Tat from cells transfected with Tat bearing a single SH3-binding domain mutated (P3/6A and P81/84A, respectively), the double mutation (P3/6/81/84A) or the wild type Tat (WT). D) Scheme of GST–Grb2 mutants. Grb2 full-length and three mutants ΔN, ΔC, and ΔN/C were cloned into pGex-5x-1 plasmid for GST-fusion protein expression. E) Western blot to detect Grb2 interaction with Tat in cells transfected with Tat101. F) Immunoblot shows that Grb2 wt and Grb2–SH3-C can efficiently pull down Gab1, while recombinant Tat competes with Gab1 for the binding to Grb2 (Panel G).*

The Tat–Grb2 interaction was additionally evaluated in cases of HIV-Encephalitis. Fig. 3 shows representative images of HIVE brain tissue samples immunolabeled with Grb2 (Fig. 3A) and Tat (Fig. 3Band C). Of note, Tat-positive cells, mainly reactive astrocytes, are present only in areas of inflammation (Panel B), while areas within the same brain sample which do not show signs of inflammation are also negative for Tat expressing cells (Panel C). Immunofluorescence performed on a consecutive section demonstrates colocalization between Tat and Grb2 in the cytoplasm of reactive astrocytes (Fig. 3E, D, and F); while immunohistochemistry for p24 (Panel G) shows areas of viral replication. Immunofluorescence analysis further confirmed that p24-positive cells are also positive for Tat (Fig. 3H–J).

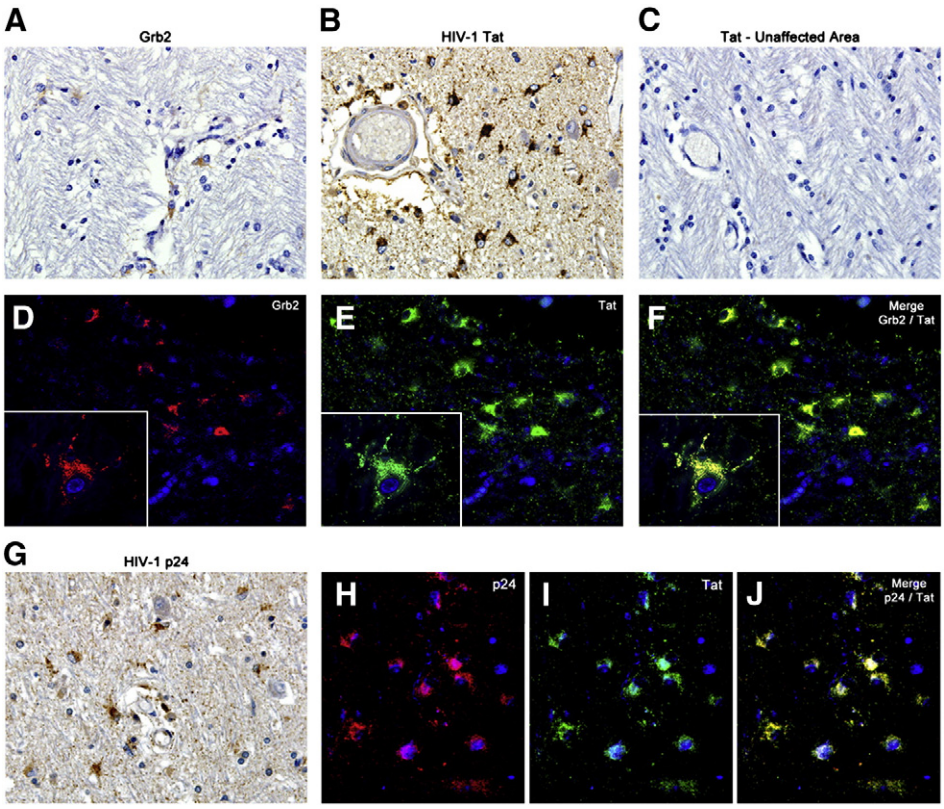

Fig. 3. *Detection of Grb2 and HIV-1 Tat in HIV-Encephalitis. Immunohistochemistry analysis shows the presence of Grb2 in the cytoplasm of reactive astrocytes in areas of neuroinflammation (Panel A). The HIV-1 transactivator protein Tat is detected in endothelial cells, perivascular macrophages and robustly in the cytoplasm of reactive astrocytes in areas of encephalitis (Panel B). In contrast, non-affected areas of the brain within the same section show no expression of Tat (Panel C). Double labeling corroborates the modest presence of Grb2 (Panel D, rhodamine), and abundant expression of Tat (Panel E, fluorescein), in the cytoplasm of astrocytes, where the two proteins co-localize (Panel F), as demonstrated by deconvolution imaging (insets). G) Immunohistochemistry analysis to detect p24 in HIVE. H, I, J) Immunolabeling shows the presence of Tat in reactive astrocytes also positive for p24. Original magnification for all panels is 600× and 1000× in the insets.*

Immunofluorescence analysis of Tat/Grb2 interaction was additionally performed on LN229 cell cultures. Panels A through F of Fig. 4 show representative images of Grb2 immunolabeling (in red) in cells transfected with the control pEYFP or YFP-Tat plasmids (in green), respectively. The colocalization of Tat with Grb2 is enhanced in these cells due to the subcellular distribution of Tat, which takes Grb2 to the nuclear compartment.

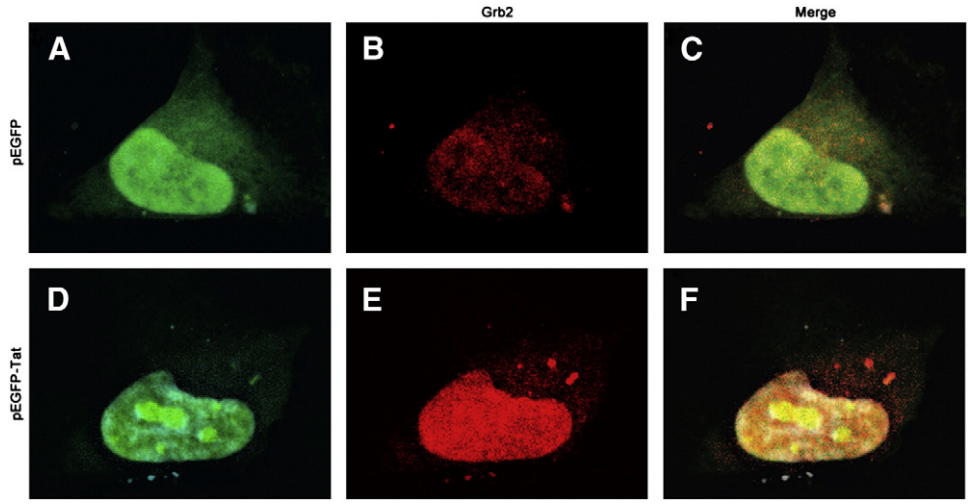

Fig. 4. *Co-localization of Grb2 and Tat in LN229 cells. Representative images show Tat and Grb2 co-localization in LN229 cells transfected with pEYFP and pEYFP-Tat, respectively. Note the diffuse cytoplasmic immunolabeling of Grb2 in control pEYFP transfected cells (Panels B and C), and its nuclear translocation when Tat is present (Panels E and F). Original magnification is 100×.*

Impairment of ERK1/2 activation by Tat

Next, we asked whether the direct binding of Tat with Grb2 was functional. To this end we have utilized the LN229 Glioblastoma cell line and the IGF-1R signaling system. We first examined the phosphorylation status of ERK1/2 in Tat-expressing Glioblastoma cells upon IGF-1 stimulation. LN229 cells were transfected with pEYFP-Tat or pEYFP, as a control, serum-starved for 24 h and then stimulated with IGF-1 for 2 and 10 min (Fig. 5). Results from Western blot analysis show basal levels of phospho-ERKs at time 0. IGF-1 stimulation in pEYFPtransfected cells resulted in increased activation of ERKs after 2 or 10 min of stimulation; whereas less phosphorylation of ERK1/2 was observed in Tat-transfected cells at the same time points. Reduced phosphorylation of ERKs might be due, at least in part, to the Tat-mediated nuclear translocation of Grb2, as we observed by immunofluorescence (Fig.

4). No difference was observed in respect to phospho-Akt levels (data not shown). Expression of Tat in LN229 did not affect levels of expression of IGF-IR (Fig. 5, lower panel).

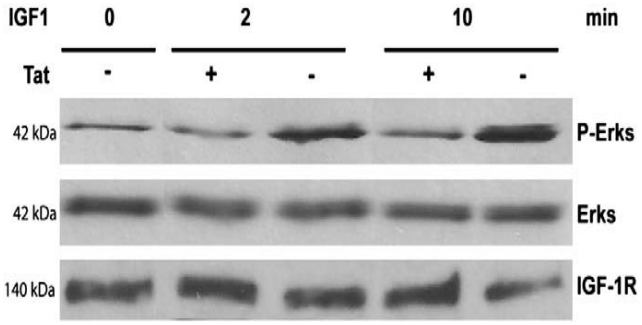

Fig.5. *Inhibitory effect of Tat in IGF-IR-mediated ERK1/2phosphorylation. Representative Western blot showing activation of MAP kinases Erk1/2 by IGF-1(40ng/ml)in pEYFP or pEYFP-Tat expressing cells at the time points of 0, 2and 10min(upperpanel).Total ERKs indicate equal loading (middle panel). Expression of IGF-IR is not affected by Tat (lower panel).*

Tat-mediated increased phosphorylation of c-Raf S259 inhibitory site involves the binding of Tat with Grb2

To get inside the functional implication of Grb2–Tat interaction, we analyzed molecules in the Raf–MEK–MAPK pathway. No changes between Tat-transfected and control cells were observed when we transfected cells) at time zero, and addition of IGF-1 resulted in higher studied the phosphorylation status of c-Raf on the activation sites levels of phosphorylated c-Raf, confirming previous studies [33]. Tat Y340/Y341 (data not shown). We then determined the levels of c-Raf expressing cells showed high level of phosphorylation of c-Raf (S259) phosphorylation on Serine 259 (S259) inhibitory site in LN229 cells without IGF-1 stimulation and treatment with IGF-1 did not further transfected with pEYFP, pEYFP-Tat, pEYFP-Tat and pmCherry–Grb2 or increase phospho-c-Raf levels (Fig. 6A, lanes 4–6). If Tat/Grb2 pmCherry–Grb2 only. Cells, transfected and controls, were serum-interaction is involved in increased levels of phospho-c-Raf, over-starved for 24 h prior to stimulation with IGF-1 for 2 and 10 min expression of Grb2 might restore IGF-1-dependent phosphorylation (Fig. 6A). No phosphorylation was observed in control (pEYFP-of c-Raf on S259. PmCherry–Grb2 vector was transfected alone or together with pEYFP-Tat. Fig. 6A (lanes 7–9) shows that over-expression of Grb2 was able to reduce phosphorylation of c-Raf (S259) in Tat-expressing cells. In general, overexpression of Grb2 alone resulted in a slightly higher level of phospho-c-Raf

S259 at time 0, but, upon induction with IGF-1, the cells behaved essentially as the controls (Fig. 6A, lanes 10–12). Next, we determined which SH3 site of Grb2 is more important in preventing the Tat-mediated increase of phospho-c-Raf S259. LN229 cells were transfected with Tat together with Grb2 full-length and the three mutants, ΔN, ΔC, and ΔN/C. Serum-starvation and stimulation were done as described in Panel A. Expression of Grb2 WT inhibited phosphorylation of c-Raf S259 upon IGF-1 stimulation (Fig. 6B, lanes 1–3). Expression of Grb2–ΔCor Grb2–ΔN/C had little effect on phosphorylation of c-Raf (Fig. 6B, lanes 7–12). Conversely, the C-terminal SH3 domain of Grb2 was able to inhibit phosphorylation of S259 inhibitory site of c-Raf in LN229 Tattransfected cells even better than full-length Grb2 protein (Fig. 6B, lanes 4–6). As a result of inhibition of phosphorylation of c-Raf S259 caused by WT or ΔN Grb2 expression, ERK activation was restored in those samples (data not shown).

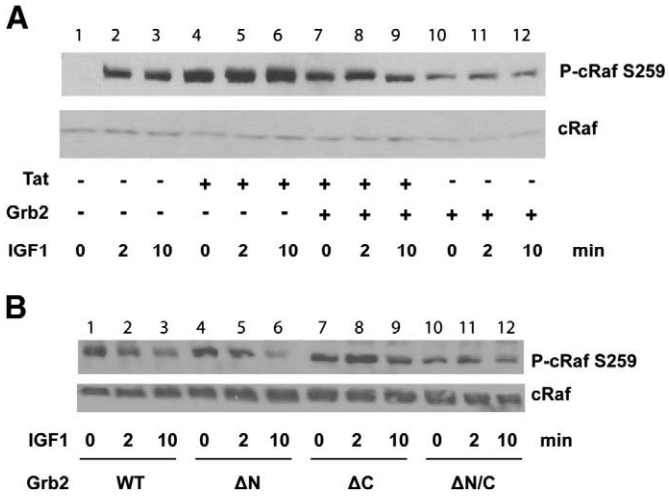

Fig. 6*. Phosphorylation of S259 inhibitory site of c-Raf is increased in Tat-transfected Glioblastoma LN229 cells. A) Western blot analysis to detect phosphorylation levels of c-Raf S259. Fold ratio of time 0 (lane 1) accepted as 1. B) Phosphorylation levels of c-Raf S259 and Erk1/2 in Tat overexpressing LN229 cells transfected together with Grb2 full-length and three mutants ΔN, ΔC, and ΔN/C were detected by Western blot. Total c-Raf indicates equal loading. Experiments were repeated at least 3 times; representative Western blot is shown in the figure.*

Protein kinase A (PKA) phosphorylates c-Raf (S259)

Previous studies have shown that c-Raf could be phosphorylated on its inhibitory site S259 by two kinases protein kinase A (PKA) or AKT/protein kinase B (PKB) [34-36]. To investigate which of these two kinases was involved in the phosphorylation of c-Raf (S259) in our system we used specific compounds to inhibit PKA or PI3-K. LN229 cells were transfected with pEYFP (lanes 1–4) or pEYFP-Tat (lanes 5–8),

serum-starved for 24 h, pretreated with specific inhibitors (50 μM of LY294002, and 25 μM of H89, lanes 3 and 7, and lanes 4 and 8, respectively) for 30 min and stimulated with IGF-1 for the indicated times (Fig. 7A). Results illustrate inhibition of c-Raf S259 phosphorylation only in control cells treated with H89, a specific inhibitor of PKA. PI3-K specific inhibitor LY294002 did not have any noticeable consequence on S259 phosphorylation. Of interest, in cells expressing Tat, both compounds had an inhibitory effect on Raf phosphorylation.

Next, we determined whether expression of Tat alone or along with Grb2 could affect PKA activity. LN229 cells were transfected with pEYFP, pEYFP-Tat, Grb2/pEYFP-Tat and Grb2 alone, serum-starved for 24 h, and stimulated with IGF-1 for 0 and 10 min. Activity of PKA in protein extracts from pEYFP-transfected cells showed slight increase after IGF-1 stimulation (Fig. 7B, lanes 1 and 2). Tat-expressing cells displayed a basal level of PKA activity that was about 5-fold higher than in pEYFP-transfected cells (compare lanes 1 and 3, $p \leq 0.05$), and addition of IGF-1 slightly decreased PKA activity (lane 4). Over-expression of Grb2 in Tat-expressing cells was able to reduce PKA activity (lanes 5 and 6). When Grb2 was overexpressed alone there was no statistically significant difference in PKA activity between IGF-1 stimulated and non-stimulated cells (lanes 7 and 8).

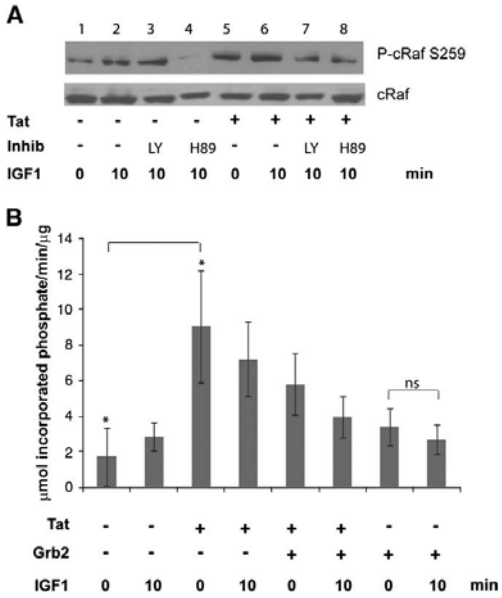

Fig. 7. *Tat-induced PKA activation mediates c-Raf (S259) phosphorylation. A) Western blot to detect c-Raf S259 phosphorylation and activation of Erk1/2 in LN229 cells transfected with pEYFP or pEYFP-Tat, pretreated with specific inhibitors (LY294002 50 μM, H89 25 μM) for 30 min and stimulated with IGF-1 for the indicated times. B) The kinase activity of PKA was tested in LN229 cells transfected with pEYFP, pEYFP-Tat, pEYFP-Tat together with Grb2 or Grb2 alone and stimulated with IGF-1 for 0 and 10 min. Activity was assayed using commercially available kit. Asterisks indicate values statistically significant (p b 0.05). Ns: not statistically significant.*

The activity of Tat on the HIV-1 LTR was evaluated in LN229 cells cotransfected with a reporter plasmid containing the viral LTR and various Grb2 constructs (Fig. 8A). Luciferase activity was determined 24 h post transfection. Among Tat and the various Grb2 constructs, only Tat activates the HIV-1 LTR, as expected. In the presence of Grb2 wild type or the mutant containing the C-terminus SH3 domain the activity of Tat was inhibited about three-fold (70%). The mutant of Grb2 containing the N-terminus SH3 was less efficient in lowering the activity of Tat and luciferase values were reduced about 37%. Even less efficient was the Grb2 mutant lacking both SH3 domains (SH2, 25%).

Finally, we investigated the role of Grb2/Tat interaction on viral replication. To this end we transfected human primary fetal microglia cells with Grb2 1 day prior to their infection with HIV-1. Levels of p24 were measured in the supernatant of cultured cells on days 1 and 3 post-infection. Fig. 8B shows an approximate 30% decrease in p24 in the medium of Grb2-transfected cells compared to control at both days 1 and 3.

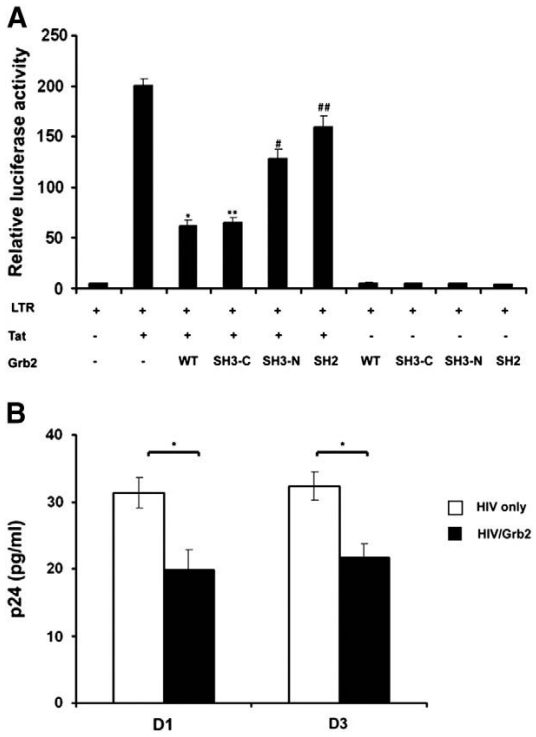

Fig. 8. *Suppression of LTR activity and inhibition of HIV-1 replication by overexpression of Grb2 protein. A) Promoter functional assay showing activation of HIV-LTR by Tat. LN229 cells were co-transfected with pEYFP-Tat, Grb2 wild type or truncated mutants, an HIV LTR–Firefly luciferase reporter plasmid and a Renilla luciferase control pRL-null plasmid. 24 h later luciferase activity was measured according to the manufacturer's protocol. Inhibition of Tat-induced LTR by Grb2 and the indicated mutants is statistically significant: *p =0.00016, **p= 0.00005, $^{\#}$p= 0.000316, $^{\#\#}$p=0.00907. B) ELISA assay to detect p24 in the supernatant obtained from HIV-infected primary human fetal microglia collected at day 1 (D1) and day 3 (D3) post-infection with HIV. In the HIV/Grb2 sample cells were transfected with Grb2 full-length 1 day prior infection with HIV-1 JF-RL. Bar graph shows the average results from three independent experiments. Asterisk indicates p b 0.001*

Discussion

The human immunodeficiency virus-1 transactivating factor Tat has been shown to affect cellular functions by interfering with signal transduction pathways [11, 21, 23]. This ability of Tat to interact with many proteins may be due, at least in part, to the presence of specific motifs in its amino acid sequence. Using SH3 Hunter bioinformatic server [30] we have identified two putative SH3 binding domains in the Tat protein sequence and a list of possible interacting SH3 domains (Fig. 1) such as those contained in Fus1, Sem5, Grb2-C, STAM-1, End3 and End2 proteins. Interestingly, four of them were either Grb2 (Grb2-C), Grb2 C. elegans homolog (Sem5), or Grb2-like proteins (End3 and End2), suggesting some degree of specificity in the SH3 recognition sites present in Tat. Sem5 protein is the GRB2 homolog in C. elegans [37, 38]. End2 and End3 (full names Endophilin-A2 and Endophilin-A3, respectively) are SH3 domain-containing GRB2-like proteins implicated in endocytosis [39, 40]. STAM-1 is a member of the STAM (SH3 domain containing signal-transducing adaptor molecule) family of proteins, which are composed of several domain structures, including the VHS (Vps27/Hrs/STAM) domain, ubiquitin-interacting motif (UIM), Src homology 3 domain, and a coiled-coil (CC) region. Through their CC regions, both STAM-1 and STAM-2 bind Hrs (hepatocyte growth factor-regulated substrate), a protein that is localized on the cytoplasmic face of the early endosome [41]. Although we investigated thoroughly only the interaction of Tat with Grb2, it is tempting to speculate that the interaction of Tat with the above mentioned molecules, and possibly other SH3-bearing proteins, may result in deregulation of a wide variety of cellular processes.

Grb2 is a ubiquitously expressed adaptor protein that has mitogenic properties and is required for several basic cellular processes [6].It can interact with tyrosine phosphorylated substrates, such as tyrosine kinase receptors, via the SH2 domain and with a variety of other signaling molecules via the two SH3 domains. Grb2 is constitutively bound to Son of sevenless (Sos), a guanine-nucleotide exchange factor that promotes GDP–GTP exchange on Ras, whose activation then leads to the activation of MAPK pathway [42, 43]. Direct interaction of Tat with Grb2 may displace the host protein from its usual binding partners and alter the Ras/MAPK pathways. Indeed, our in vitro data show that Tat can compete with Gab1 for binding

to the SH3 domain of Grb2, possibly altering Gab1 downstream cascade. An additional mechanism by which Tat may deregulate Grb2 downstream signaling could be mediated, at least in cell culture, by the subtraction of Grb2 from the cytoplasmic events. This hypothesis is supported by our data showing nuclear localization of Grb2 in Tat-expressing cells (Fig. 4).

Immunohistochemistry analysis of HIVE brain samples revealed a modest presence of Grb2, mainly detected in astrocytes (Fig. 3, Panels A through F). The pattern of HIV-Tat expression appears very robust in area of encephalitis, where the viral protein is also detected in endothelial cells, perivascular macrophages and reactive astrocytes. In contrast, Tat is undetectable in areas of the same brain that are not affected by inflammation. Colocalization between Tat and Grb2 was observed in reactive astrocytes, corroborating the in vitro binding assays. Of interest to note that, although Grb2 is abundantly expressed in all cell types, immunohistochemistry analysis revealed strong labeling only in reactive astrocytes. It may indicate the activation/ proliferation status of these cells, as previously suggested by C. Russo et al. in their study demonstrating increased Grb2/ShcA/APP interaction in reactive astrocytes of Alzheimer's disease (AD) brain samples [44].

Many studies have reported the pleiotropic activity of Tat in deregulating a wide range of signaling pathways by both direct and indirect mechanisms. The presence of SH3-binding domains in the sequence of Tat may account for at least some of the various activities of this viral protein. De la Fuente et al. made an interesting observation on the ability of Tat to downregulate expression of many cellular genes, particularly on cellular tyrosine kinase receptors (RTK) and their downstream signal transduction members, including the Ras–Raf–MEK pathway [45]. Perhaps impairment of the Ras/MEK pathway by Tat/Grb2 interaction may affect transcription of ERK1/2 downstream targets. As the cellular signaling pathways are not linear but cross-talk and overlap, Tat likely affects them at various levels in a complex network of direct and indirect mechanisms. We have tried to analyze some of them using a Glioblastoma cell line and the well-known IGF-1R signaling. Following the Ras/Raf/MAPK pathway we showed that Tat can interact at different levels; it binds to Grb2, subtracting this adaptor molecule to the Ras/MEK pathway, while it potentiates the Raf inhibitory pathway by activating PKA. Shifting of the substrates along signaling pathways appears to be an interesting feature of Tat. For instance, we have previously shown the ability of Tat to promote the non-canonical activation of

Stat5A in PC12 cells stimulated with NGF, which results in the inhibition of cellular differentiation [46]. Ultimately, since the activity of Tat on cellular processes appears to be cell-type specific, the end point of Tat/host interaction, including the Tat/SH3–client interaction, could be either inhibitory or stimulatory. For example, Tat has been shown to mediate activation of ERK1/2 in endothelial cells [25] or to inhibit their activation in neural cells [47]. On the other hand, the outcome of Tat/ host interaction may also affect some aspects of the viral cycle. We utilized primary human fetal microglia infected with HIV-1 and found that over-expression of Grb2 derails the activity of Tat from its natural target, the viral LTR (Fig. 8A), resulting in a lower production of p24 as a measurement of viral replication (Fig. 8B).

In summary, this report provides evidence for Tat/Grb2 direct interaction, which is mediated by the SH3 C-terminal domain of Grb2 and polyproline regions of Tat. This interaction is functional and bidirectional: it affects cellular pathways as well as viral replication. Considering the high number of cellular proteins that possess one or more SH3-binding domains, it is tempting to speculate that the Tat/ SH3 interaction might be a general mechanism for Tat to interfere with many signaling pathways, and consequently, many cellular processes.

Acknowledgements

Slava Rom, Marco Pacifici, Giovanni Passiatore, Luis Del Valle and Francesca Peruzzi were previously with the Department of Neuroscience and Center for Neurovirology at the Temple University School of Medicine, Philadelphia, PA. This work was supported by NIH grant MH079751 to FP.

References

1. Mayer, B.J., *SH3 domains: complexity in moderation.* J Cell Sci, 2001. **114**(Pt 7): p. 1253-63.
2. Pawson, T., *Protein modules and signalling networks.* Nature, 1995. **373**(6515): p. 573-80.
3. Rickles, R.J., et al., *Phage display selection of ligand residues important for Src homology 3 domain binding specificity.* Proc Natl Acad Sci U S A, 1995. **92**(24): p. 10909-13.
4. Sparks, A.B., et al., *Distinct ligand preferences of Src homology 3 domains*

from Src, Yes, Abl, Cortactin, p53bp2, PLCgamma, Crk, and Grb2. Proc Natl Acad Sci U S A, 1996. **93**(4): p. 1540-4.

5. Pawson, T. and J. Schlessingert, *SH2 and SH3 domains.* Curr Biol, 1993. **3**(7): p. 434-42.
6. Tari, A.M. and G. Lopez-Berestein, *GRB2: a pivotal protein in signal transduction.* Semin Oncol, 2001. **28**(5 Suppl 16): p. 142-7.
7. Cheng, A.M., et al., *Mammalian Grb2 regulates multiple steps in embryonic development and malignant transformation.* Cell, 1998. **95**(6): p. 793-803.
8. Giubellino, A., T.R. Burke, Jr., and D.P. Bottaro, *Grb2 signaling in cell motility and cancer.* Expert Opin Ther Targets, 2008. **12**(8): p. 1021-33.
9. Gatignol, A. and K.T. Jeang, *Tat as a transcriptional activator and a potential therapeutic target for HIV-1.* Adv Pharmacol, 2000. **48**: p. 209-27.
10. Cullen, B.R., *Trans-activation of human immunodeficiency virus occurs via a bimodal mechanism.* Cell, 1986. **46**(7): p. 973-82.
11. Peruzzi, F., *The multiple functions of HIV-1 Tat: proliferation versus apoptosis.* Front Biosci, 2006. **11**: p. 708-17.
12. Aprea, S., et al., *Tubulin-mediated binding of human immunodeficiency virus-1 Tat to the cytoskeleton causes proteasomal-dependent degradation of microtubule-associated protein 2 and neuronal damage.* J Neurosci, 2006. **26**(15): p. 4054-62.
13. Del Valle, L., et al., *Detection of HIV-1 Tat and JCV capsid protein, VP1, in AIDS brain with progressive multifocal leukoencephalopathy.* J Neurovirol, 2000. **6**(3): p. 221-8.
14. Huigen, M.C., W. Kamp, and H.S. Nottet, *Multiple effects of HIV-1 trans-activator protein on the pathogenesis of HIV-1 infection.* Eur J Clin Invest, 2004. **34**(1): p. 57-66.
15. Ptak, R.G., et al., *Cataloguing the HIV type 1 human protein interaction network.* AIDS Res Hum Retroviruses, 2008. **24**(12): p. 1497-502.
16. Borgatti, P., et al., *Extracellular HIV-1 Tat protein activates phosphatidylinositol 3- and Akt/PKB kinases in CD4+ T lymphoblastoid Jurkat cells.* Eur J Immunol, 1997. **27**(11): p. 2805-11.
17. D'Aversa, T.G., K.O. Yu, and J.W. Berman, *Expression of chemokines by human fetal microglia after treatment with the human immunodeficiency virus type 1 protein Tat.* J Neurovirol, 2004. **10**(2): p. 86-97.

18. Del Valle, L., et al., *Insulin-like growth factor I receptor signaling system in JC virus T antigen-induced primitive neuroectodermal tumors--medulloblastomas.* J Neurovirol, 2002. **8 Suppl 2**: p. 138-47.
19. Deregibus, M.C., et al., *HIV-1-Tat protein activates phosphatidylinositol 3-kinase/ AKT-dependent survival pathways in Kaposi's sarcoma cells.* J Biol Chem, 2002. **277**(28): p. 25195-202.
20. Evans, P., et al., *Sequence alignment reveals possible MAPK docking motifs on HIV proteins.* PLoS One, 2010. **5**(1): p. e8942.
21. Herbein, G., et al., *Macrophage signaling in HIV-1 infection.* Retrovirology, 2010. **7**: p. 34.
22. Ju, S.M., et al., *Extracellular HIV-1 Tat up-regulates expression of matrix metalloproteinase-9 via a MAPK-NF-kappaB dependent pathway in human astrocytes.* Exp Mol Med, 2009. **41**(2): p. 86-93.
23. Peruzzi, F., et al., *Cross talk between growth factors and viral and cellular factors alters neuronal signaling pathways: implication for HIV-associated dementia.* Brain Res Brain Res Rev, 2005. **50**(1): p. 114-25.
24. Rusnati, M., et al., *Activation of endothelial cell mitogen activated protein kinase ERK(1/2) by extracellular HIV-1 Tat protein.* Endothelium, 2001. **8**(1): p. 65-74.
25. Toschi, E., et al., *HIV-1 Tat regulates endothelial cell cycle progression via activation of the Ras/ERK MAPK signaling pathway.* Mol Biol Cell, 2006. **17**(4): p. 1985-94.
26. Zauli, G., et al., *HIV-1 Tat protein down-regulates CREB transcription factor expression in PC12 neuronal cells through a phosphatidylinositol 3-kinase/AKT/cyclic nucleoside phosphodiesterase pathway.* Faseb J, 2001. **15**(2): p. 483-91.
27. Saksela, K., G. Cheng, and D. Baltimore, *Proline-rich (PxxP) motifs in HIV-1 Nef bind to SH3 domains of a subset of Src kinases and are required for the enhanced growth of Nef+ viruses but not for down-regulation of CD4.* EMBO J, 1995. **14**(3): p. 484-91.
28. Rom, S., et al., *CCL8/MCP-2 is a target for mir-146a in HIV-1-infected human microglial cells.* FASEB J, 2010. **24**(7): p. 2292-300.
29. Sawaya, B.E., et al., *Cooperative interaction between HIV-1 regulatory proteins Tat and Vpr modulates transcription of the viral genome.* J Biol

Chem, 2000. **275**(45): p. 35209-14.

30. Ferraro, E., et al., *SH3-Hunter: discovery of SH3 domain interaction sites in proteins.* Nucleic Acids Res, 2007. **35**(Web Server issue): p. W451-4.
31. Chipitsyna, G., et al., *Cooperativity between Rad51 and C/EBP family transcription factors modulates basal and Tat-induced activation of the HIV-1 LTR in astrocytes.* J Cell Physiol, 2006. **207**(3): p. 605-13.
32. Lewitzky, M., et al., *The C-terminal SH3 domain of the adapter protein Grb2 binds with high affinity to sequences in Gab1 and SLP-76 which lack the SH3-typical P-x-x-P core motif.* Oncogene, 2001. **20**(9): p. 1052-62.
33. Subramaniam, S., et al., *Insulin-like growth factor 1 inhibits extracellular signal-regulated kinase to promote neuronal survival via the phosphatidylinositol 3-kinase/protein kinase A/c-Raf pathway.* J Neurosci, 2005. **25**(11): p. 2838-52.
34. Chong, H. and K.L. Guan, *Regulation of Raf through phosphorylation and N terminus-C terminus interaction.* J Biol Chem, 2003. **278**(38): p. 36269-76.
35. Wellbrock, C., M. Karasarides, and R. Marais, *The RAF proteins take centre stage.* Nat Rev Mol Cell Biol, 2004. **5**(11): p. 875-85.
36. Zimmermann, S., et al., *MEK1 mediates a positive feedback on Raf-1 activity independently of Ras and Src.* Oncogene, 1997. **15**(13): p. 1503-11.
37. Downward, J., *The GRB2/Sem-5 adaptor protein.* FEBS Lett, 1994. **338**(2): p. 113-7.
38. Rozakis-Adcock, M., et al., *Association of the Shc and Grb2/Sem5 SH2-containing proteins is implicated in activation of the Ras pathway by tyrosine kinases.* Nature, 1992. **360**(6405): p. 689-92.
39. Giachino, C., et al., *A novel SH3-containing human gene family preferentially expressed in the central nervous system.* Genomics, 1997. **41**(3): p. 427-34.
40. Reutens, A.T. and C.G. Begley, *Endophilin-1: a multifunctional protein.* Int J Biochem Cell Biol, 2002. **34**(10): p. 1173-7.
41. Mizuno, E., et al., *Association with Hrs is required for the early endosomal localization, stability, and function of STAM.* J Biochem, 2004. **135**(3): p. 385-96.
42. Aronheim, A., et al., *Membrane targeting of the nucleotide exchange factor Sos is sufficient for activating the Ras signaling pathway.* Cell, 1994. **78**(6): p. 949-61.

43. Wong, L. and G.R. Johnson, *Epidermal growth factor induces coupling of protein-tyrosine phosphatase 1D to GRB2 via the COOH-terminal SH3 domain of GRB2.* J Biol Chem, 1996. **271**(35): p. 20981-4.

44. Russo, C., et al., *Signal transduction through tyrosine-phosphorylated carboxy-terminal fragments of APP via an enhanced interaction with Shc/Grb2 adaptor proteins in reactive astrocytes of Alzheimer's disease brain.* Ann N Y Acad Sci, 2002. **973**: p. 323-33.

45. De la Fuente, C., et al., *Gene expression profile of HIV-1 Tat expressing cells: a close interplay between proliferative and differentiation signals.* BMC Biochem, 2002. **3**(1): p. 14.

46. Bergonzini, V., et al., *HIV-Tat promotes cellular proliferation and inhibits NGF-induced differentiation through mechanisms involving Id1 regulation.* Oncogene, 2004. **23**(46): p. 7701-11.

47. Peruzzi, F., et al., *Tat-induced deregulation of neuronal differentiation and survival by nerve growth factor pathway.* J Neurovirol, 2002. **8 Suppl 2**: p. 91-6.

48. Care, A., et al., *MicroRNA-133 controls cardiac hypertrophy.* Nat Med, 2007. **13**(5): p. 613-8.

CCL8/MCP-2 is a target for mir-146a in HIV-1-infected human microglial cells

FASEB J. 24, 2292–2300 (2010)

Slava Rom, Inna Rom, Giovanni Passiatore, Marco Pacifici, Sujatha Radhakrishnan, Luis Del Valle, Sergio Pina-Oviedo, Kamel Khalili, Davide Eletto, and Francesca Peruzzi

Abstract

MicroRNA-mediated regulation of gene expression appears to be involved in a variety of cellular processes, including development, differentiation, proliferation, and apoptosis. Mir-146a is thought to be involved in the regulation of the innate immune response, and its expression is increased in tissues associated with chronic inflammation. Among the predicted gene targets for mir-146a, the chemokine CCL8/ MCP-2 is a ligand for the CCR5 chemokine receptor and a potent inhibitor of CD4/CCR5-mediated HIV-1 entry and replication. In the present study, we have analyzed changes in the expression of mir-146a in primary human fetal microglial cells upon infection with HIV-1 and found increased expression of mir146a. We further show that CCL8/MCP-2 is a target for mir-146a in HIV-1 infected microglia, as overexpression of mir-146a prevented HIV-induced secretion of MCP-2 chemokine. The clinical relevance of our findings was evaluated in HIV-encephalitis (HIVE) brain samples in which decreased levels of MCP-2 and increased levels of mir-146a were observed, suggesting a role for mir-146a in the maintenance of HIV-mediated chronic inflammation of the brain.

Introduction

MicroRNAs (miRNAs) are post-transcriptional regulators of gene expression that function by inhibiting translation of mRNAs [1, 2]. They are endogenously encoded single-stranded RNAs of ~22 nucleotides in length that inhibit protein translation predominantly through imperfect base-pairing with sequences, which are generally located in the 3' untranslated region (UTR) of mRNA transcripts. Although the role of miRNAs in the control of proliferation, differentiation, and apoptosis has been previously recognized, the importance of these small noncoding RNAs in the immune system is just emerging [3-5]. For instance, mir-150 controls B-cell differentiation by targeting the c-Myb transcription factor [6], and mir-155 regulates a variety of immune reactions, including production of cytokines by T and B cells and the germinal center B-cell response [7, 8]. Expression profile of miRNAs in human monocytes has revealed that miR-146a/b, miR-132, and miR-155 responded to endotoxin treatment with elevated expression [9]. Taganov et al. [9] also demonstrated that LPS-mediated induction of mir146a is NF-KB dependent, which attenuates Toll-like receptor (TLR) signaling by targeting IL-1 receptor associated kinase (IRAK1) and TNF-associated receptor factor 6 (TRAF6). Expression of mir-146a is induced by the Epstein-Barr virus (EBV)-encoded latent membrane protein 1 (LMP1) [10], a 6-transmembrane molecule that mimics cellular tumor necrosis factor receptor (TNFR) family members and contributes to the oncogenic potential of EBV. The primary mechanism by which LMP1 induces expression of mir-146a appears to be NF-KB dependent [10]. miRNA-gene target prediction strategy suggested that mir-146a may be part of a negative feedback loop that plays a role in modulating interferon responses [11].

Infection by the human immunodeficiency virus-1 (HIV-1) is often associated with a chronic inflammatory reaction of the brain (HIV-encephalitis, HIVE), where macrophages/microglial cells are thought to be the major reservoir for the virus [12]. Upon viral infection, microglial cells secrete a variety of cytokines and chemokines, including monocytes chemoattractant proteins, MCPs. Chemokine receptors also play a role in infectious diseases, and CCR5 is the primary coreceptor for macrophage tropic (R5) HIV-1 [13, 14]. The chemokine MCP-2 shares ~60%

homology with MCP-1, and MCP-3 and has ~30% identity with MIP-1c, MIP-1, and RANTES [15-17]. MCP-2 is an efficient ligand for CCR1, CCR2, and CCR5 and a potent inhibitor of CD4/CCR5-mediated HIV-1 entry and replication [18-20]. Increased levels of MCP-2 have been previously observed in the supernatant of mixed brain cell cultures infected with HIV-1 [21].

In this study, we have investigated the expression levels of mir-146a in HIV-1-infected primary human fetal microglia and found that its expression increased during the course of infection. We have also identified the CCL8/MCP-2 mRNA as a direct target for mir-146a and have shown that overexpression of mir-146a prior to infection with HIV-1 prevents release of MCP-2 by infected cells. Evaluation of mir-146a and MCP-2 expression in HIVE brain samples also revealed an inverse correlation between levels of mir-146a and expression of its target gene MCP-2, with mir-146a being up-regulated in HIVE and MCP-2 down-regulated. Since MCP-2 chemokine is an efficient ligand for CCR5, our findings demonstrating that mir-146a mediates suppression of MCP-2 may indicate a role for the mir-146a/ MCP-2 axis in the modulation of viral spread in the brain.

Materials and Methods

Primary human fetal microglia

Fetal tissue specimens were obtained from the Temple University Center for Neurovirology tissue culture core facility in accordance with institutional, state, and U. S. National Institutes of Health (NIH) guidelines. The procedures involved in the preparation of microglial cells at the fetal developmental stage are based on the principle of tissue dissociation, followed by enzymatic digestion with or without a gradient to remove debris, and then purification of microglial cells by preferential adhesion [22]. In brief, the tissue specimens obtained were carefully washed in HBSS without phenol red to remove any blood vessels and residual meninges. The tissues were dissociated gently to generate smaller pieces and incubated with

TrypleExpress (Invitrogen, Carlsbad, CA, USA) for 30 min. At the end of this incubation time, the dissociating enzyme was inactivated by the addition of 10% FBS. Cold HBSS was added in the proportion of 5:1 (40 ml HBSS+10 ml tissue), and the tissue was gently triturated. After centrifugation at 500 *g* for 10 min, the tissue was washed another 2 times with HBSS. The tissue was finally resuspended and tritured in complete microglia medium [Dulbecco's modified Eagle medium (DMEM), 10% FBS, 20 mM/ml l-glutamine, 1% penicillin/streptomycin/neomycin, and 1000 U/ml macrophage colony stimulating factor (MCSF)] using smaller pipettes and, ultimately, a fire-polished Pasteur pipette. The cell suspension was filtered through a 70-fm filter, and the cells were counted. Cells were seeded in T75 flasks at a concentration of 3.5– 4 X 10^6 cells/ml in 25 ml of medium, and incubated undisturbed for 2 wk, with a single change of medium on d 7. Supernatant was collected on d 14, 21, and 28 from the original plating and centrifuged at 500 *g* for 10 min, and the pellet was resuspended in a small volume of medium. Microglial cells were counted, plated at the desired density, and cultured for another week in complete medium without MCSF. Cells were either maintained in culture for experiments or frozen. Microglial cultures were highly pure, consisting of >98% $CD68^+$ cells. Two different preparations of microglia were utilized in the present study, and all of the experiments were performed using both microglia preparations, each in triplicate.

Preparation of JRFL HIV-1 virus stock

U937 (Human leukemic monocyte lymphoma) cell line was used to make a stock of HIV, strain JRFL. Approximately 5 X 10^6 cells were infected with HIV (4 µg p24) in 5 ml of serum-free OptiMEM for 5 h. At the end of adsorption, cells were pelleted, virus inoculum was removed, and cells were resuspended in RPMI containing 10% FBS. One-third of the cell culture medium was changed every 2–3 d until a majority of the cells exhibited cytopathic effect in the form of syncitia (usually 10 d post-infection). After 10 d, cells were pelleted, and supernatant was

divided into 1-ml aliquots and stored at -80°C. The concentration of p24 in the new stock was determined with an enzyme-linked immunosorbent assay (ELISA) kit (PerkinElmer, Waltham, MA, USA), according to the manufacturer's protocol.

Quantitative RT-PCR

RNA was extracted using the miRVana miRNA extraction kit (Ambion, Austin, TX, USA). Real-time RT-PCR was performed using the mirVana qRT-PCR miRNA detection kit (Ambion) per the manufacturer's protocol, as described previously [23]. PCR primer pairs for reverse transcription and detection of mature miRs were purchased from Ambion (hsa-mir-146a and control U6). In general, quantitative real-time RT-PCR (qRT-PCR) on primary human fetal microglia was performed on 2 independent experiments using 25 ng of template. For each sample, qRT-PCR was performed in quadruplicate. Each sample was normalized for the corresponding values of U6 control. Relative quantification of the selected miRNAs was calculated using the Roche analysis software (based on the 2nd derivative maximum; Roche, Indianapolis, IN, USA). qRT-PCR to detect levels of mir-146a in brain samples was performed essentially as described above. RNA was extracted from frozen brain tissue samples of 4 control brains, 3 HIVE brains, and 2 HIV brains without brain pathology, using the miRVana miRNA extraction kit, and qRT-PCR was performed using the mirVana qRT-PCR miRNA detection kit following the manufacturer's instructions. qRT-PCR was performed in quadruplicate using 25 ng of template. Analysis of results was performed as described above.

miRNA functional analysis

The sequence of the hsa-mir-146a stem loop was retrieved using miRBase database no. MI0000477: CCGAUGUGUAUCCUCAGCUUUGAGAACUGAAUUCCAUG GGUUGUGUCAGUGUCAGACCUCUGAAAUUCAGUUCUUCAGCUGGGAU UCUCUGUCAUCGU.

For cloning into BlockIt (Invitrogen), the following oligos were used: forward, 5'-TGCTGTGAGAACTGAATTCCATGGGTTGTTTTGGCCACTGACAACCCATG ATTCAGTTCTCA-3', and reverse, 5'-CCTGTGAGAACTGAATCATGGGTTGT

CAGTGGCCAAAACAACCCATGGAATTCAGTTCTCAC-3'. The oligos were annealed and cloned as double strands into the expression vector following the manufacturer's protocols.

For the cloning of the perfect match sequence into PsiCheck-2 vector (Promega, Madison, WI, USA), the PCR primers were based on the mature sequence of hsa-miR-146a but in the antisense orientation. The primers were as follows: forward, 5'-CCGCTCGAGAACCCATGGAATTCAGTTCTCAAGATCTGCGGCCGCTAAA CTAT-3'; and reverse, 5'-ATAGTTTAGCGGCGCAGATCTTGAGAACTGAAT TCCATGGGTTCTCGAGCGG-3'. The MCP-2 3'UTR sequence was PCR amplified from genomic DNA from human microglial cells and cloned downstream to the *Renilla* sequence in the PsiCheck2 reporter vector. The primers were as follows: forward, 5'-CCGCTCGAGAGTCAGAGCTTGAAG, and reverse: 5'-ATAAGAATGCGGCCGCCATAGTTATATACAGTAACATC, containing *Xho*I and *Not*I restriction sites, respectively (underscored). The MCP-2 3'UTR mutated in the mir-146a seeding sequence was generated by site directed mutagenesis (Stratagene, La Jolla, CA, USA) using the psiCHECK2/MCP-2 3'UTR as a template. The oligonucleotides for the mutagenesis were as follows: forward, 5'-ATTCTTTGGCTAAGTCAGGAGC (mutated bases in the mir-146a seeding sequence are underscored). The reverse primer was complementary to the forward.

Dual luciferase assay

For miR target validation, 293T cells were plated at a concentration of 8 X 10^4 cells/well in a 12-well plate. The next day, a total amount of 0.6 µg/well of DNA was transfected using Fugene 6 (Invitrogen) at the DNA:Fugene 6 ratio of 1:3. pcDNA3 was added to keep the total amount of DNA constant. Samples were harvested 48 h post-transfection and subjected to the dual luciferase assay system (Promega) following the manufacturer's instructions using Femtomaster FB12 chemiluminometer (Zylex Corp., Coeur D Alene, ID, USA). Relative units represent the ratio between *Renilla* values and the luciferase internal control. The experiments were performed in duplicate and repeated 23 times.

Immunohistochemistry

Six archival samples of formalin-fixed, paraffin-embedded brain tissue from patients with HIVE and 6 samples from age-matched control patients who died of non-neurological conditions and had no confirmed brain pathology were collected from the NIH-funded HIV National Tissue Consortium at the Manhattan Brain Bank (Mount Sinai Medical School, New York, NY, USA). In all samples, the frontal lobe was selected for analysis since it constitutes the most frequently affected region in HIVE. For immunohistochemistry, 4-µm-thick sections were cut using a microtome and placed on charged glass slides. Immunohistochemistry was performed according to the manufacturer's instructions (Vector Laboratories, Burlingame, CA, USA). Our protocol includes deparaffination, rehydration in alcohol up to water, antigen retrieval in citrate buffer at pH 6.0, endogenous peroxidase quenching, and blocking in normal horse serum for 2 hrs room temperature. The primary antibody against MCP-2 was a goat polyclonal (1:500; Santa Cruz Biotechnology, Santa Cruz, CA, USA), and was incubated overnight in a humidified chamber. After rinsing with PBS, secondary biotinylated antibody was incubated for 1 h (1:200 dilution), followed by avidin-biotin peroxidase complex incubation (ABC Elite kit, Vector Laboratories) and developing with diaminobenzidine (DAB, Boehringer Ingelheim, Ingelheim, Germany), counterstained with hematoxylin, and coverslipped.

***In situ* hybridization**

For in sit*u* hybridization, we utilized miRCURY 3'-DIG-labeled LNA-miRNAs (mir-146a and mir-128a; Exiqon, Woburn, MA, USA) detection probes. A miRCURY detection probe for the brain-enriched mir-128a and scrambled miRNA were used as positive and negative controls, respectively. Samples from 4 frozen brains of patients with HIVE and 4 brains of age-matched control patients who died of nonneurological diseases were collected from the pathology archives of the Manhattan Brain Bank at Mount Sinai Medical School. Sections of 10 fm thickness from the frontal lobe were cut from using a cryostat and mounted on Superfrost/Plus slides (Fisher Scientific, Pittsburgh, PA, USA). Sections were fixed in 70% alcohol for 2 min. Slides were washed 3 times with PBS, acetylated for 10 min, and rinsed

again in PBS. The probe (20 ng DIG-mir-146a or DIG-mir-128a) was diluted in hybridization solution (50% deionized formamide; 0.3 M NaCl; 20 mM Tris-HCl, pH 8.0; 5 mM EDTA; 10 mM NaPO4, pH 8.0; 10% dextran sulfate; 1X Denhardt's; and 0.5 mg/ml yeast RNA). The hybridization mixture was heated at 65°C for 5 min to linearize the probe and chilled on ice. Fifty to 100 µl of hybridization solution was added to each slide; sections were covered with RNase-free plastic coverslips and incubated overnight at a temperature 20–22°C below the temperature of melting (*T*m) of the miRCURY LNA detection probe in a chamber humidified with 50% formamide and 1X SSC (in soaked KimWipes; Kimberly-Clark, Irving, TX, USA). Slides were washed with 5X SSC at room temperature and 2 times for 30 min each at a temperature 20–22°C below *T*m of the miRCURY LNA detection probe in a solution containing 50% formamide, 0.1% Tween-20 and 1X SSC. Slides were then washed for 15 min in 0.2X SSC at room temperature, and an additional 15 min in PBS at room temperature. For antibody detection, the protocol was the following: slides were incubated for1hat room temperature in blocking solution (0.5% blocking powder, 10% heat-inactivated goat serum, 0.1% Tween-20, and 1X PBS). Slides were incubated for3hat room temperature in blocking solution preincubated for 1 h with AP-conjugated anti-DIG Fab fragment (1:1500 in blocking solution; Roche). Slides were washed 2 times for 30 min in 0.1% Tween-20 in PBS followed by 2 times for 20 min in PBS. For detection, slides were incubated with 250 µl of BM Purple AP Substrate (Roche) on slides overnight in the dark at room temperature. The reaction was stopped by placing the slides into stop solution (PBS, pH 5.5; and 1 mM EDTA). Slides were mounted in a water-based medium (VectaShield; Vector Laboratories).

ELISA assay

ELISA to detect CCL8/MCP-2 in the medium of HIV-1infected cells was performed following standard procedures. In brief, 96-well plates were coated with supernatant from HIV-1-infected and control cells and left at 4°C overnight. Wells were washed with PBST 6 times and blocked with 10% milk in PBST for 2h at 37°C. Anti-MCP-2 (C-17; Santa Cruz Biotechnology) was added to the wells at a dilution of 1:200 in PBST and left overnight at 4°C. Next day, wells were washed 6

times with PBST and incubated with anti-goat HRP secondary antibody for 2 h at 37°C. Wells were washed 6 times with PBST and incubated with 150 ml 1X TMB substrate solution (eBioscience Inc, San Diego, CA, USA). Samples were analyzed using an ELISA microplate reader at 630 nm. As a positive control, wells were coated with CCL8/MCP-2 peptide (C-17; Santa Cruz Biotechnology) at concentrations of 0.002, 0.2, 0.6, 1, and 2 μg.

Statistics

Results were analyzed by an unpaired, 2-or 1-sided Student's *t* test. Values of $p<0.05$ were considered statistically significant.

Results

Two different preparations of primary human fetal microglial cells were infected with HIV-1, and levels of p24 were determined by ELISA at 4, 8, 10, 12, and 16 d post-infection as an indicator of viral replication (Fig. 1*A*). Next, we performed qRT-PCR to determine changes in the expression levels of mir-146a in HIV-1-infected primary human fetal microglial cells compared to uninfected cells. RNA samples from HIV-infected and control cells were collected at 0, 4-, 8-, and 12-d time points. qRT-PCR was performed for each sample in quadruplicate, and relative quantification of mir-146a, normalized for U6 levels, was calculated by the Roche 480 LyteCycler software. Results in Fig. 1*B* represent the average expression of mir-146a in the 2 experimental samples and controls. Quantitatively, an increase in mir-146a levels of ~4-, 6-, and 8-fold was observed in HIV-1-infected microglia at 4-, 8-, and 12-d time points, respectively, when compared to controls. In addition, we monitored cell survival on HIV-1 infection during the course of the experiment, and no statistically significant difference in the number of viable cells was observed between HIV-1-infected and control cultures. Trypan blue exclusion test performed at each time point during infection demonstrated an average of 83 ± 2 and 84 ± 5% live cells in control and HIV-1-infected cells, respectively. These results show HIV-1 mediated induction of mir-146a expression in primary human fetal microglial cells.

Initially, we hypothesized that mir-146a up-regulation by HIV-1 might function to

promote the latency of the virus in microglial cells, which may involve a decrease in viral replication. Accordingly, we cloned a genomic sequence corresponding to the human mir-146a into the pBlockIt miR expression plasmid to generate Blo/146a (see Materials ad Methods). Expression of mature mir146a in 293T cells was verified by qRT-PCR at 24 and 48 h post-transfection (data not shown). To test a possible role of mir-146a in viral replication, microglial cells were transfected with control empty vector, a non relevant miRNA (mir-128a) or mir-146a, 72 h prior to infection with HIV-1, or with mock control medium. HIV-1 p24 protein levels were determined at 4, 7, or 10 d following the infection by p24-specific ELISA.

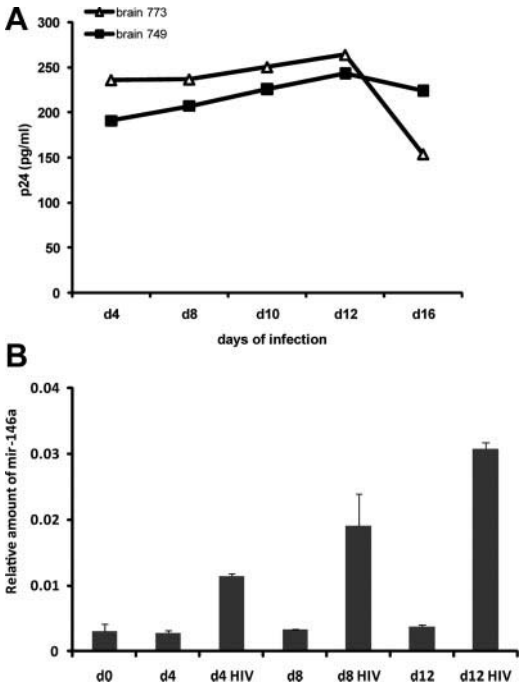

Figure 1. *Increased levels of mir-146a in HIV-1-infected microglial cells. A) ELISA to detect p24 in medium collected at indicated time points from 2 different preparations of HIV-1-infected primary human fetal microglia (brains 7739 and 7490). B) qRT-PCR to detect levels of mature mir-146a in HIV-1-infected and control microglial cells at 0, 4, 8, and 12 d postinfection. qRT-PCR was performed on 25 ng of template, each in quadruplicate. Each sample was normalized for corresponding values of U6 control. Relative amount of mir-146a was calculated by the Roche LightCycler software. Graph represents average values obtained from microglial cell cultures isolated from brain samples 7739 and 7490*

Results in Fig. 2 show no statistically significant differences between the samples, suggesting that the activity of mir-146a does not interfere with viral replication in this cellular system.

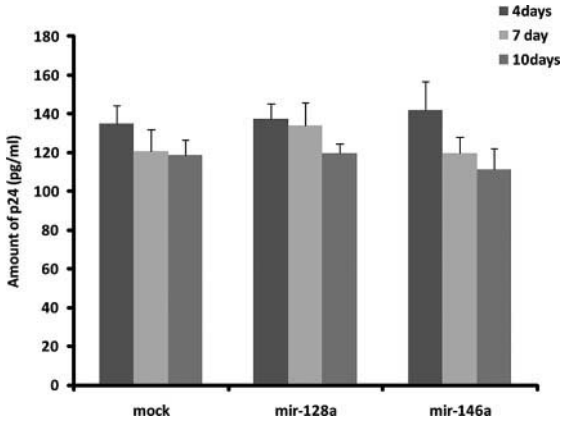

Figure 2. *mir-146a does not affect viral replication. ELISA to determine amounts of p24 protein in medium of HIV-1infected human fetal microglia. Cells were transfected with mir-146a or nonrelevant miRNA, mir-128a, 72 h prior to infection with HIV-1 or control mock (see Materials and Methods). Supernatant was collected after 4, 7, and 10 d of infection. Each time point was performed in triplicate; whole experiment was repeated twice.*

Evaluation of CCL8/MCP-2 protein levels during HIV-1 infection of human fetal primary microglial cells

Since mir-146a appears to play a role in the innate immune response (24), we next asked whether it could regulate expression of cytokines and chemokines that are secreted by HIV-1-infected cells. We analyzed predicted gene targets for mir-146a and found that CCL8/MCP-2 mRNA has a putative binding site for mir-146a in its 3'UTR. Figure 3A shows the sequence alignment between mir-146a and MCP-2 mRNA according to miRNApath (http://lgmb.fmrp.usp.br/mirnapath/tools.php).

Primary human fetal microglial cells were infected with HIV-1, and supernatants from HIV-infected and control cells were collected every second day starting from d 2 for up to d 16 following infection. CCL8/ MCP-2 levels in the medium of HIV-1-infected cells were detected by ELISA following standard procedures. As a positive control, wells were coated with CCL8/ MCP-2 peptide at the concentrations ranging from 0.002 to 2 μg. Results in Fig. 3*B* show a gradual increase in the amount of MCP-2 chemokine secreted by microglial cells during the first 12 d after infection. Interestingly, a reduction in the release of MCP-2 occurred between d 12 and 16, which may reflect the inhibitory action of HIV-induced mir-146a.

In the next series of experiments, we determined the effect of mir-146a on the expression of CCL8/MCP-2 by measuring levels of MCP-2 protein in the medium

of microglial cells overexpressing mir-146a or controls after HIV-1 infection (Fig. 3*C*). As a negative control, we utilized a plasmid containing a miRNA (mir-128a) that is not predicted to target CCL8/MCP-2 3'UTR sequence. Primary human fetal microglial cells were transfected with BlockIt/146a or BlockIt/128a following standard protocols. Seventy-two hours post-transfection, cells were infected with HIV-1. Untransfected, but HIV-1 infected, cells were used as a negative control (mock). MCP-2 ELISA was performed on supernatants obtained at 0, 4, 7, and 10 d after infection of cells with HIV-1. Untransfected, HIV-1-infected microglial cells release CCL8/MCP-2 in the supernatant with a maximal amount secreted on d 10 post-infection. Similar results were obtained when the cells were transfected with control miRNA (mir-128a) prior to infection with HIV-1. Notably, secretion of MCP-2 was almost completely suppressed in cells over-expressing mir-146a.

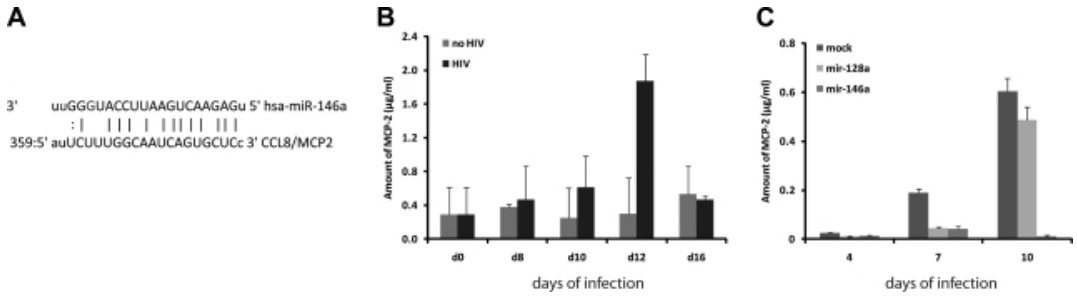

Figure 3. *mir-146a inhibits secretion of CCL8/MCP-2 by HIV-1-infected microglial cells. A) Diagram showing putative mir-146a binding sites in the 3'UTRMCP-2 mRNA sequence. B) Graph of a representative ELISA showing amount (fg/ml) of secreted CCL8/MCP-2 chemokine in medium of HIV-1-infected cells and control mock-infected cells. Experiment was repeated 3 times, each in duplicate. C) ELISA to monitor amount of secreted MCP-2 on supernatant of primary human fetal microglial cells transfected with mir-146a, a non-relevant miRNA (mir-128a), or control empty vector (mock), followed by infection with HIV-1. Experiment was repeated 3 times, each in quadruplicate.*

To test the possibility that expression of MCP-2 was post-transcriptionally regulated by mir-146a, we performed a functional assay using MCP-2 reporter system [23]. The reporter construct contained the full-length MCP-2 3'UTR fused to the *Renilla* gene in the PsiCheck2 vector, which also contained the firefly luciferase gene for normalization.

For *Renilla* luciferase assays, the reporter vectors were co-expressed together with

mir-146a in 293T cells and assayed 48 h post-transfection. As shown in Fig. 4, the ratio *Renilla*/luciferase (R/L) in the control vectors (PsiCheck2 empty vector, Psicheck2 3'UTR MCP-2, and Psicheck2 mut 3'UTR MCP-2) was scaled to 1 (100%). No significant difference between the ratios was observed when PsiCheck2 was co-transfected with mir-146a (psi+146a). Instead, co-expression of 3'UTR MCP-2 with mir-146a (MCP-2+146a) resulted in a reproducible 25% reduction of R/L values ($P<0.05$). The control reporter plasmid carrying the MCP-2 3'UTR mutated in the mir-146a seeding site was not affected by the addition of mir-146a (mutMCP-2+146a), confirming the specificity of the mir-146a activity. As a positive control, the R/L ratio relative to the reporter plasmid carrying the mir-146a perfect match sequence (PM) resulted in a strong (90%) inhibition, confirming that mir-146a is over-expressed and functional in this cell system ($P<0.001$).

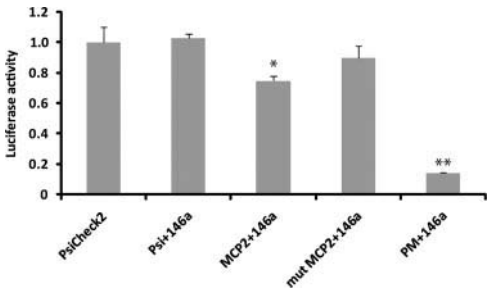

Figure 4. *Inhibition of MCP-2 3'UTR by mir-146a. Luciferase assay on 293T cells transfected with empty vector alone (PsiCheck2), or cotransfected with mir-146a and MCP-2 3'UTR, with mir-146a and the 3'UTR-mutated sequence (mut MCP-2), or with the control mir-146a perfect matching sequence (PM). Luciferase and Renilla values were determined 48 h post-transfection. Relative units represent ratio between Renilla values and luciferase internal control. Experiment was repeated twice, each in triplicate. *P<0.05; **P< 0.001.*

Evidence that MCP-2 inhibits viral replication in microglial cells

CCL8/MCP-2 chemokine is known to bind CCR5 receptor with high affinity and to inhibit HIV-1 replication (18, 19). We tested this possibility in our cellular system, and results are shown in Fig. 5. Human fetal microglial cells were treated with increasing concentrations of MCP-2 peptide (20, 40, 100, and 200 ng/ml) prior to infection with HIV-1. Amounts of p24 protein were determined by ELISA on the supernatant collected at d 4, 7, and 10 after infection. Note that production of p24 decreased with increasing concentration of MCP-2 protein confirming the important

role of MCP-2 in viral replication [18, 20].

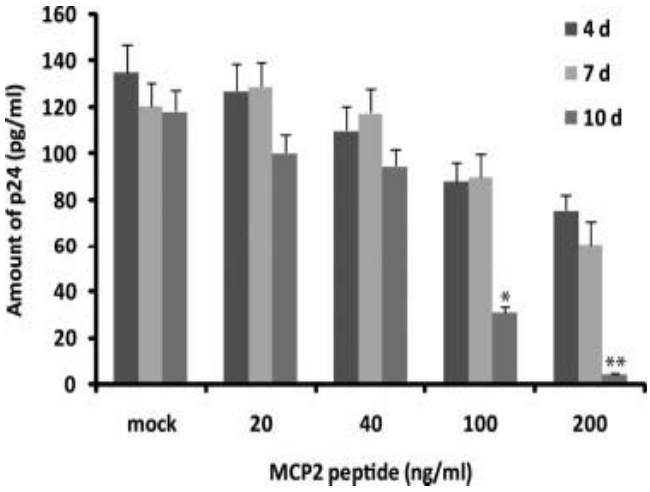

Figure5. *Effects of MCP-2 on HIV-1 infection. ELISA showing amounts of p24 in medium of HIV-1-infected microglial cells in absence or presence of MCP-2 peptide at 4, 7, and 10 d postinfection. Experiment was repeated twice, each in duplicate. *P<0.05; **P<0.001.*

Relevance to HIVE

Our results indicate a possible role for mir-146a in modulating expression of MCP-2 during the course of HIV infection in cultured microglial cells. The next series of experiments was aimed at investigating the effect of such modulation in clinical samples of HIVE. Immunohistochemistry for MCP-2 was performed in cortical sections from archival brains of 3 patients with HIVE and compared to sections from 3 control patients and 3 HIV^+ patients with no brain pathology. Figure 6*Aa* shows representative images from the control brain, where a robust immunolabeling was found in virtually all neurons, compared with the HIV^+ no-pathology brain, in which the expression of MCP-2 was slightly reduced (Fig. 6*Ab*), and the HIVE brain, where MCP-2 was significantly reduced (Fig. 6*Ac*, *d*). Even within the same HIVE section, the expression of MCP-2 was dramatically reduced from non-affected areas (Fig. 6*Ac*), to areas of severe perivascular inflammatory cuffs and microglial nodules, in which the expression of MCP-2 was reduced to a couple of weak speckles (Fig. 6*Ad*).

As expected, expression of MCP-2 was intense in leukocytes found inside

subarachnoid blood vessels in the control patient (data not shown), and the HIV^+ patient with no brain pathology (Fig. 6*Ba*). However, the levels of MCP-2 were significantly decreased in leukocytes from the HIVE patient (Fig. 6*Bb*). Although the general pattern of MCP-2 seemed to decrease in HIVE, it is interesting that parenchymal microglial nodules demonstrated a robust cytoplasmic immunolabeling for MCP-2 in HIVE (Fig. 6*Bc*).

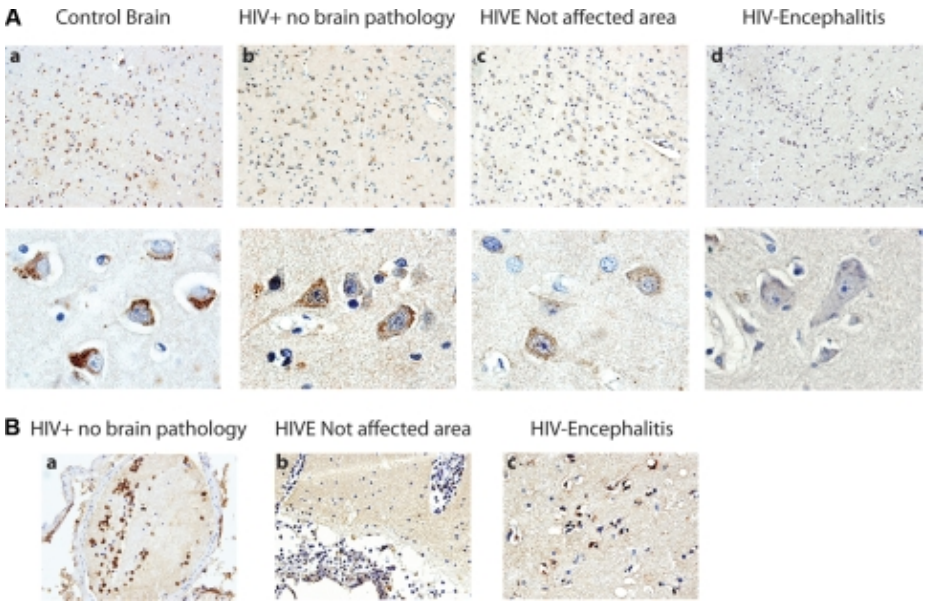

Figure 6. *Detection of MCP-2 protein in HIVE and control brains.* A*) Immunohistochemical analysis of MCP-2 in cortical sections of a control patient, an* HIV^+ *patient with no brain pathology, and an HIVE patient revealed a gradual reduction in levels of MCP-2 from the control patient, in which MCP-2 in robustly labeled (*a*), to lesser expression in the* HIV^+ *patient (*b*), to a significant reduction in HIVE (*c, d*). MCP-2 is also noticeably decreased within the same HIVE sample, from non-affected areas (*c*) to areas of severe inflammation, where MCP-2 is almost undetectable (*d*). Original view: ×200 (top panels); ×1000 (bottom panels).* B*) As expected, MCP-2 is robustly expressed in leukocytes inside a subarachnoid blood vessel in an* HIV^+ *patient with no brain pathology (*a*); in HIVE, leukocytes show a dramatic reduction in MCP-2 (*b*). Microglial nodules in HIVE demonstrate robust cytoplasmic expression of MCP-2 (*c*). Original view: ×400.*

We have evaluated expression of mir-146a in HIVE and control brains by qRT-PCR. Archived frozen control brain and HIVE samples were obtained from the frontal lobe, as it represents the most frequently affected region of the brain, which results in the clinico-pathological term of AIDS-dementia complex. RNA was extracted from brain tissues of three HIVE patients (HIVE 010063, 01057, and

030022), 4 control patients, and 2 HIV patients without encephalitis or any other pathology. Results in Fig. 7*A* show relative amount of mir-146a in all the samples after normalization with levels of U6 RNA. Comparable levels of mir-146a were observed in the 4 control brains; their average is represented as CB in Fig. 7*A*. Levels of mir-146a were slightly higher in the HIV^+ tissue without brain pathology. A 2-fold increase in mir-146a expression was detected in two HIVE samples, while the third (HIVE 010157) strikingly showed 12-fold increase in mir146a expression.

Finally, expression of mir-146a was monitored in the same samples used to monitor expression of mir-146a, 4 archived frozen HIVE brain samples and 4 control brain samples, by *in situ* hybridization. Samples were processed and subjected to hybridization with LNA miRNA probes (see Materials and Methods); representative results are shown in Fig. 7*B*. Images indicate undetectable levels of mir-146a in control non-HIV brain (Fig. 7*B*, CB 528B; left panel) and its abundance in the HIVE sample (HIVE 10157; middle panel), which was also stained with the neuronal mir-128a used as a positive control. Hybridization with a scrambled probe was negative in both control and HIVE samples (not shown). Altogether, these data support a correlation between mir-146a expression and down-regulation of MCP2 chemokine.

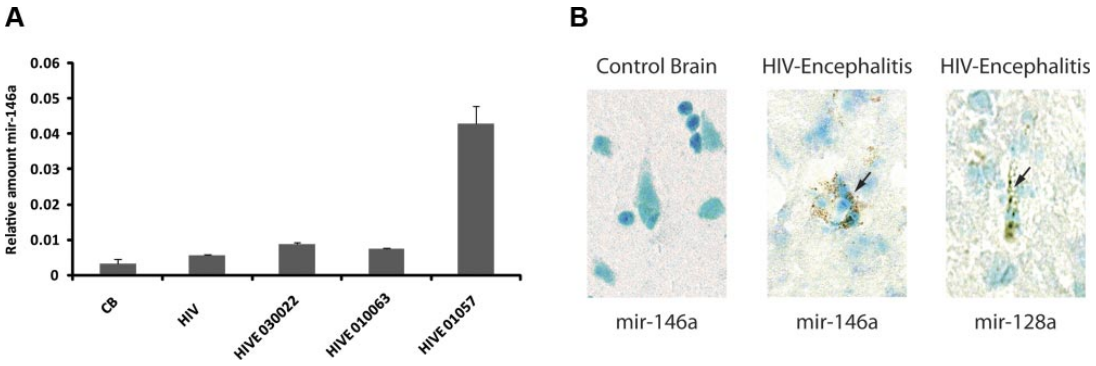

Figure 7. *mir-146a is up-regulated in HIVE brain samples. A) qRT-PCR of mir-146a on RNA samples obtained from 4 HIVE patients (HIVE 030022, 010063, and 01057), 4 control brains (CB), and 2 HIV patients without brain pathology (HIV). qRT-PCR of mir-146a was performed in quadruplicate using 25 ng of RNA. B) Detection of hsa-mir-146a in HIVE 010063 and control CB 528B archived frozen samples. In situ hybridization was performed with miRCURY-LNA-DIG mir-146a (and control mir-128a) detection probes. Arrows indicate positive signal in cytoplasm of neurons. Original view: X1000.*

Discussion

Similar to other neurodegenerative disorders, uncontrolled inflammation in the brain of HIV-1-infected individuals may account for the chronic progression of neuroAIDS [24]. Therefore, understanding the mechanisms that trigger and/or sustain uncontrolled inflammation might be of critical importance for the development of new therapeutic modalities to prevent neuronal degeneration. Increasing evidence has accumulated that miRNAs function as key regulators in a wide variety of biological processes, including proliferation, differentiation, cell fate determination, apoptosis, and signal transduction, as well as organ development [1, 25-31]. As a consequence, abnormal expression of miRNAs appears to be a common feature of many human diseases, ranging from muscular [25] and cardiovascular disorders [32, 33], to cancer [34, 35]; developmental abnormalities; psychiatric disorders, such as schizophrenia [36]; and most recently inflammatory diseases [37]. For instance, expression of several miRNAs has been shown to be modulated (elevated or repressed) in activated T cells in vitro [38]. In addition, mir-146a is thought to be involved in innate immunity by regulating, together with mir-155, the acute immune response after pathogen recognition by TLRs [9, 39, 40].

Here, we present evidence showing that expression of mir-146a is increased in primary human fetal microglia infected with HIV-1 (Fig. 1). This is in agreement with previous findings showing increased expression of mir-146a in T cells following proinflammatory stimuli [9], including viral infection [10, 41]. Despite several studies demonstrating induction of mir-146a expression following inflammatory stimuli, there is still little information regarding its function [40]. Because mir146a expression levels increase during infection until at least d 12, we initially hypothesized that mir-146a could interfere with viral replication in the late stage of infection. However, mir-146a is not predicted to target any of the viral genes [42], and levels of p24 did not significantly change in cells that overexpress mir-146a (Fig. 2). Although we cannot exclude an indirect effect of mir-146a on viral proteins other than p24, we choose to study direct gene targets. Specifically, we have investigated the role of mir-146a in modulating the release of proinflammatory chemokines and found that MCP-2 is a target for mir-146a in HIV-1 infected primary human fetal microglia (Figs. 2–4). Activation of mac-

rophages/microglia is thought to play a key role in development and progression of neuroAIDS (reviewed in ref. [43]). Among the factors secreted by HIV-1infected microglia/macrophages, MCP-1 is one of the most investigated chemokines and is thought to play a central role in the pathogenesis of HIV-1-associated dementia [44-46]. Another member of the MCP family of chemokines, MCP-2, has been shown to inhibit CD4/CCR5-mediated HIV-1 entry and replication [18-20]. Our data also show the inhibitory effect of MCP-2 on HIV-1 entry/replication, with the maximal effect at the highest concentration of MCP-2 at d 10 postinfection (Fig. 5). While we cannot explain the reason for the late effect of MCP-2, we could speculate that the multiplicity of infection (MOI) [47] may play a role; perhaps a highest MOI would result in earlier inhibition of p24 production by MCP-2. Nevertheless, our data are in line with the work of Yang *et al.* [20], which shows maximal inhibition of HIV-1 replication by MCP-2 at d 10 postinfection.

According to our model, acute infection of microglia with HIV-1 would trigger the production and secretion of MCP-2 chemokine (Fig. 3*B*). Interestingly, the rapid decline of MCP-2 levels after the peak at 12 d is coincident with the up-regulation of mir-146a expression. Transfection of mir-146a prior to infection with HIV-1 prevented the expression of MCP-2 (Fig. 3*C*) in microglial cells, further emphasizing a function for this particular miRNA as a negative regulator of MCP-2 chemokine. When tested in a miRNA functional assay, the 3'UTR of MCP-2 mRNA was inhibited by >20% by the action of mir-146a (Fig. 4), and a mutation in the mir-146a seeding sequence of the MCP-2 3'UTR abolished the inhibitory activity of mir-146a. Perhaps the up-regulation of mir-146a at a certain point during infection might be a feedback mechanism to rapidly decrease the otherwise deleterious effects of an overproduction of MCP-2. This mechanism may work during an acute inflammatory response, where expression of mir-146a is negatively regulated later during infection. One such mechanism can involve the activity of NF-KB, which is up-regulated during viral infection and is an inducer of mir-146a promoter [9]. Indeed, NF-KB was found to be activated in microglia and macro-phages during HIV-1-encephalitis [48], and we found increased expression of mir-146a in HIVE brain samples (Fig. 7), emphasizing a role for the NF-KB/mir146a pathway in HIVE. Lukiw *et al.* [49] have provided evidence for a NF-KB-sensitive mir-146a-

mediated inflammatory pathway in Alzheimer's disease and in stressed human brain cells.

There are a limited number of reports in which expression of MCP-2 in normal or diseased brains has been investigated. McManus *et al.* [50] found prominent immunoreactivity for MCP-2 in the center of multiple sclerosis (MS) lesions, with reactivity diminishing at the lesion edges. In our study, immunohistochemical analysis of HIVE and control brain samples revealed a substantial presence of MCP-2 in the control brain, which was strongly attenuated in HIVE, particularly in areas of inflammation (Fig. 6). Although interesting, we can only speculate on the reason why MCP-2 immunolabeling was stronger in microglial nodules of HIVE brain tissues. This could be a result of either the presence of cells that actively produce MCP-2 or it could be due to the presence of factors that increase the stability of this chemokine.

We have also noticed an intense immunolabeling for MCP-2 in neurons of normal brain. Although there are few studies supporting either the presence or the function of this chemokine in neurons, the MCP-2 main receptor, CCR2, is expressed in neurons [51, 52]. Alternatively, as also proposed by Coughlan *et al.* [51], neurons themselves may produce chemokines, which may affect cellular function within the CNS.

In summary, we have identified a mechanism implicated in the negative regulation of inflammation in HIV-1 infected macrophages/microglia. It involves HIV-mediated increased expression of mir-146a, which, in turn, inhibits the expression of the proinflammatory chemokine MCP-2. Our data in cultured cells and in clinical samples support a role for mir-146 in the dynamic modulation of inflammatory processes in neuronal cells.

References

1. Bartel, D.P., *MicroRNAs: genomics, biogenesis, mechanism, and function.* Cell, 2004. **116**(2): p. 281-97.
2. Gebauer, F. and M.W. Hentze, *Molecular mechanisms of translational control.* Nat Rev Mol Cell Biol, 2004. **5**(10): p. 827-35.

3. Bagasra, O. and K.R. Prilliman, *RNA interference: the molecular immune system.* J Mol Histol, 2004. **35**(6): p. 545-53.
4. Sonkoly, E., M. Stahle, and A. Pivarcsi, *MicroRNAs and immunity: novel players in the regulation of normal immune function and inflammation.* Semin Cancer Biol, 2008. **18**(2): p. 131-40.
5. Xiao, C. and K. Rajewsky, *MicroRNA control in the immune system: basic principles.* Cell, 2009. **136**(1): p. 26-36.
6. Xiao, C., et al., *MiR-150 controls B cell differentiation by targeting the transcription factor c-Myb.* Cell, 2007. **131**(1): p. 146-59.
7. Rodriguez, A., et al., *Requirement of bic/microRNA-155 for normal immune function.* Science, 2007. **316**(5824): p. 608-11.
8. Thai, T.H., et al., *Regulation of the germinal center response by microRNA-155.* Science, 2007. **316**(5824): p. 604-8.
9. Taganov, K.D., et al., *NF-kappaB-dependent induction of microRNA miR-146, an inhibitor targeted to signaling proteins of innate immune responses.* Proc Natl Acad Sci U S A, 2006. **103**(33): p. 12481-6.
10. Cameron, J.E., et al., *Epstein-Barr virus latent membrane protein 1 induces cellular MicroRNA miR-146a, a modulator of lymphocyte signaling pathways.* J Virol, 2008. **82**(4): p. 1946-58.
11. Hou, J., et al., *MicroRNA-146a feedback inhibits RIG-I-dependent Type I IFN production in macrophages by targeting TRAF6, IRAK1, and IRAK2.* J Immunol, 2009. **183**(3): p. 2150-8.
12. Del Valle, L. and S. Pina-Oviedo, *HIV disorders of the brain: pathology and pathogenesis.* Front Biosci, 2006. **11**: p. 718-32.
13. Alkhatib, G., et al., *CC CKR5: a RANTES, MIP-1alpha, MIP-1beta receptor as a fusion cofactor for macrophage-tropic HIV-1*. Science, 1996. **272**(5270): p. 1955-8.
14. Dragic, T., et al., *HIV-1 entry into CD4+ cells is mediated by the chemokine receptor CC-CKR-5.* Nature, 1996. **381**(6584): p. 667-73.
15. Decock, B., et al., *Identification of the monocyte chemotactic protein from human osteosarcoma cells and monocytes: detection of a novel N-terminally processed form.* Biochem Biophys Res Commun, 1990. **167**(3): p. 904-9.

16. Proost, P., A. Wuyts, and J. Van Damme, *Human monocyte chemotactic proteins-2 and -3: structural and functional comparison with MCP-1.* J Leukoc Biol, 1996. **59**(1): p. 67-74.
17. Van Damme, J., et al., *Structural and functional identification of two human, tumor-derived monocyte chemotactic proteins (MCP-2 and MCP-3) belonging to the chemokine family.* J Exp Med, 1992. **176**(1): p. 59-65.
18. Gong, W., et al., *Monocyte chemotactic protein-2 activates CCR5 and blocks CD4/CCR5-mediated HIV-1 entry/replication.* J Biol Chem, 1998. **273**(8): p. 4289-92.
19. Gong, X., et al., *Monocyte chemotactic protein-2 (MCP-2) uses CCR1 and CCR2B as its functional receptors.* J Biol Chem, 1997. **272**(18): p. 11682-5.
20. Yang, O.O., et al., *Monocyte chemoattractant protein-2 (CC chemokine ligand 8) inhibits replication of human immunodeficiency virus type 1 via CC chemokine receptor 5.* J Infect Dis, 2002. **185**(8): p. 1174-8.
21. Wang, J. and D. Gabuzda, *Reconstitution of human immunodeficiency virus-induced neurodegeneration using isolated populations of human neurons, astrocytes, and microglia and neuroprotection mediated by insulin-like growth factors.* J Neurovirol, 2006. **12**(6): p. 472-91.
22. Borgmann, K., H.E. Gendelman, and A. Ghorpade, *Isolation and HIV-1 infection of primary human microglia from fetal and adult tissue.* Methods Mol Biol, 2005. **304**: p. 49-70.
23. Eletto, D., et al., *Inhibition of SNAP25 expression by HIV-1 Tat involves the activity of mir-128a.* J Cell Physiol, 2008. **216**(3): p. 764-70.
24. Gao, H.M. and J.S. Hong, *Why neurodegenerative diseases are progressive: uncontrolled inflammation drives disease progression.* Trends Immunol, 2008. **29**(8): p. 357-65.
25. Eisenberg, I., et al., *Distinctive patterns of microRNA expression in primary muscular disorders.* Proc Natl Acad Sci U S A, 2007. **104**(43): p. 17016-21.
26. He, L. and G.J. Hannon, *MicroRNAs: small RNAs with a big role in gene regulation.* Nat Rev Genet, 2004. **5**(7): p. 522-31.
27. Huppi, K., et al., *MicroRNAs and genomic instability.* Semin Cancer Biol, 2007. **17**(1): p. 65-73.

28. Ke, X.S., et al., *MicroRNAs: key participants in gene regulatory networks.* Curr Opin Chem Biol, 2003. **7**(4): p. 516-23.
29. Kloosterman, W.P. and R.H. Plasterk, *The diverse functions of microRNAs in animal development and disease.* Dev Cell, 2006. **11**(4): p. 441-50.
30. Lu, J., et al., *MicroRNA expression profiles classify human cancers.* Nature, 2005. **435**(7043): p. 834-8.
31. Miska, E.A., et al., *Microarray analysis of microRNA expression in the developing mammalian brain.* Genome Biol, 2004. **5**(9): p. R68.
32. Care, A., et al., *MicroRNA-133 controls cardiac hypertrophy.* Nat Med, 2007. **13**(5): p. 613-8.
33. Ikeda, S., et al., *Altered microRNA expression in human heart disease.* Physiol Genomics, 2007. **31**(3): p. 367-73.
34. Calin, G.A. and C.M. Croce, *MicroRNA signatures in human cancers.* Nat Rev Cancer, 2006. **6**(11): p. 857-66.
35. Croce, C.M. and G.A. Calin, *miRNAs, cancer, and stem cell division.* Cell, 2005. **122**(1): p. 6-7.
36. Hansen, T., et al., *Brain expressed microRNAs implicated in schizophrenia etiology.* PLoS ONE, 2007. **2**(9): p. e873.
37. Sonkoly, E., et al., *MicroRNAs: novel regulators involved in the pathogenesis of Psoriasis?* PLoS ONE, 2007. **2**(7): p. e610.
38. Cobb, B.S., et al., *A role for Dicer in immune regulation.* J Exp Med, 2006. **203**(11): p. 2519-27.
39. O'Connell, R.M., et al., *MicroRNA-155 is induced during the macrophage inflammatory response.* Proc Natl Acad Sci U S A, 2007. **104**(5): p. 1604-9.
40. Williams, A.E., et al., *Role of miRNA-146a in the regulation of the innate immune response and cancer.* Biochem Soc Trans, 2008. **36**(Pt 6): p. 1211-5.
41. Motsch, N., et al., *Epstein-Barr virus-encoded latent membrane protein 1 (LMP1) induces the expression of the cellular microRNA miR-146a.* RNA Biol, 2007. **4**(3): p. 131-7.
42. Hariharan, M., et al., *Targets for human encoded microRNAs in HIV genes.* Biochem Biophys Res Commun, 2005. **337**(4): p. 1214-8.

43. D'Aversa, T.G., E.A. Eugenin, and J.W. Berman, *NeuroAIDS: contributions of the human immunodeficiency virus-1 proteins Tat and gp120 as well as CD40 to microglial activation.* J Neurosci Res, 2005. **81**(3): p. 436-46.
44. Bell, M.D., D.D. Taub, and V.H. Perry, *Overriding the brain's intrinsic resistance to leukocyte recruitment with intraparenchymal injections of recombinant chemokines.* Neuroscience, 1996. **74**(1): p. 283-92.
45. Gu, L., S.C. Tseng, and B.J. Rollins, *Monocyte chemoattractant protein-1.* Chem Immunol, 1999. **72**: p. 7-29.
46. Zink, M.C., et al., *Increased macrophage chemoattractant protein-1 in cerebrospinal fluid precedes and predicts simian immunodeficiency virus encephalitis.* J Infect Dis, 2001. **184**(8): p. 1015-21.
47. Liu, Y., et al., *Uptake of HIV-1 tat protein mediated by low-density lipoprotein receptor-related protein disrupts the neuronal metabolic balance of the receptor ligands.* Nat Med, 2000. **6**(12): p. 1380-7.
48. Dollard, S.C., et al., *Activation of nuclear factor kappa B in brains from children with HIV-1 encephalitis.* Neuropathol Appl Neurobiol, 1995. **21**(6): p. 518-28.
49. Lukiw, W.J., Y. Zhao, and J.G. Cui, *An NF-kB-sensitive microRNA-146a-mediated inflammatory circuit in Alzheimer's disease and in stressed human brain cells.* J Biol Chem, 2008.
50. McManus, C., et al., *MCP-1, MCP-2 and MCP-3 expression in multiple sclerosis lesions: an immunohistochemical and in situ hybridization study.* J Neuroimmunol, 1998. **86**(1): p. 20-9.
51. Coughlan, C.M., et al., *Expression of multiple functional chemokine receptors and monocyte chemoattractant protein-1 in human neurons.* Neuroscience, 2000. **97**(3): p. 591-600.
52. van der Meer, P., et al., *Immunohistochemical analysis of CCR2, CCR3, CCR5, and CXCR4 in the human brain: potential mechanisms for HIV dementia.* Exp Mol Pathol, 2000. **69**(3): p. 192-201.

Cerebrospinal Fluid miRNA Profile in HIV-Encephalitis

J Cell Physiol. 2012 Oct 5. doi: 10.1002/jcp.24254

Marco Pacifici, Serena Delbue, Pasquale Ferrante, Duane Jeansonne, Ferdous Kadri, Steve Nelson, Cruz Velasco-Gonzalez, Jovanny Zabaleta and Francesca Peruzzi

Abstract

MicroRNAs are short non-coding RNAs that modulate gene expression by translational repression. Because of their high stability in intracellular as well as extracellular environments, miRNAs have recently emerged as important biomarkers in several human diseases. However, they have not been tested in the cerebrospinal fluid (CSF) of HIV-1 positive individuals. Here, we present results of a study aimed at determining the feasibility of detecting miRNAs in the CSF of HIV-infected individuals with and without encephalitis (HIVE). We also evaluated similarities and differences between CSF and brain tissue miRNAs in the same clinical setting. We utilized a high throughput approach of miRNA detection arrays and identified differentially expressed miRNAs in the frontal cortex of three cases each of HIV+, HIVE, and HIV-controls, and CSF of ten HIV-positive and ten HIV-negative individuals. For the CSF samples, the group of HIV+ individuals contained nine cases of HIV-Associated Neurological Disorders (HAND) and, among those, four had HIVE. All the HIV-negative samples had non-viral acute disseminate encephalomyelitis. A total of 66 miRNAs were found differentially regulated in HIV+ compared to HIV-groups. The greatest difference in miRNA expression was observed when four cases of HIVE were compared to five non-HIVE cases, previously normalized with the HIV-negative group. After statistical analyses, eleven miRNAs were fund significantly up-regulated in HIVE. Although more clinical samples should be examined, this work represents the first report of CSF miRNAs in HIV-infection and offers the basis for future investigation.

Introduction

HIV-associated neurological disorders (HAND) comprise cognitive, motor and behavioral impairments which affect a substantial number of HIV-1 infected individuals. While the introduction of the highly active antiretroviral therapy (HAART) has greatly reduced the incidence of HIV-associated dementia, the prevalence of HIV-associated minor cognitive and motor disorders has increased (reviewed in [1]). Understanding the biology of HIV-1 infection in the brain and identifying markers for its pathological manifestations, including HIV-encephalitis, are of critical importance. Although several molecules in the CSF have been identified as putative indicators of neurocognitive impairments, the need for biomarkers persists [2].

After over a decade of investigation of miRNAs, it is now clear that these non-coding RNA molecules serve a fundamental role in the regulation of gene expression; even though specific regulation and function of miRNAs are largely unknown. Similarly to mRNAs, some miRNAs show specific tissue distribution, such as miR-124 which is enriched in the central nervous system (CNS) [3]. Changes in the expression of cellular miRNAs have been associated with a variety of pathologic conditions [4], including neurodegenerative disorders [5, 6], and systematic high throughput approaches, such as miRNA profiling arrays, have lead to the identification of miRNA signatures in several types of cancer [7-12]. Finally, emerging evidence accumulated supporting the concept of establishing microRNAs expression profiles in body fluids as possible diagnostic and prognostic markers [13-22]. Although the literature confirms a growing interest for miRNAs and their potential role in HIVE [23-27], to our knowledge this is the first report of CSF miRNA profile.

We have utilized RT-PCR-based miRNA arrays to detect expression of 742 unique miRNAs in the CSF of HIV-1-positive individuals with HAND compared to HIV-1-negative individuals. After normalization, 66 miRNAs were considered for further analysis. Comparison between HIVE and HIV+ (non-HIVE) groups showed 47 up- and 7 down-regulated miRNAs in HIVE. Statistical analysis (ANOVA followed by Dunnet's test) indicated significant differences (p<0.2) among the three groups for

11 miRNAs, with miR-182*, miR-362-5p, miR-720, and miR-937 having a *p*-value <0.05. Using a similar approach we have also obtained miRNA profiles from the frontal cortex of HIV+, HIVE, and HIV-clinical samples. Although the CSF specimens and frontal cortices were obtained from different individuals, our results show a surprisingly high number of miRNAs deregulated in both types of specimens.

Altogether, our study demonstrates feasibility in detecting CSF miRNAs, it provides a putative CSF miRNA signature for HIVE, and shows important correlation in differentially regulated miRNAs in the frontal cortex and CSF samples.

Materials and Methods

Clinical Samples

CSF samples were collected over a period of five years from patients at the University of Milan and stored frozen at -80°C in aliquots until analysis. Formalin-fixed paraffin embedded (FFPE) samples from the frontal cortex were previously obtained from the Manhattan HIV Brain Bank (Dr. Susan Morgello, Mt. Sinai, New York).

RNA preparation and miRNA array

RNA was extracted from 0.5 ml of CSF using the mirVANA miRNA isolation kit (Ambion, Austin, TX) following the manufacturer's instructions. Carrier RNA (MS2 RNA, Roche) was added at 1µg per sample prior to total RNA extraction [28]. RNA was quantified using the NanoDrop spectrophotometer and 40 ng were retrotranscribed using the universal cDNA synthesis kit (Exiqon, Woburn, MA). Three RT reactions were performed for each sample. Each cDNA reaction was mixed with SYBR Green master mix (Exiqon) and dispensed into two 384 well plates containing 742 unique miRNAs and several controls (Exiqon microRNA ready to use PCR, human panels I and II). PCR was performed with a Roche LightCycler 480 System (Roche Applied Science, Indianapolis, IN) following Exiqon's recommended settings.

For the FFPE samples, RNA was extracted using the high pure miRNA isolation kit (Roche) from two 10μm thick sections, 1cm x 1cm each.

Data processing and statistical analyses

Absolute quantification using 2nd derivative maximum was calculated with Roche Lightcycler 480 software. Exiqon arrays were performed in triplicate and qPCR data were analyzed in GenEx Professional 5 software (MultiD Analyses AB, Goteborg, Sweden). If a miRNA was not present in at least two out of three replicas it was set as non-expressed. Because of the low abundance of miRNAs in the CSF, we set a cut off of 39. If a miRNA had a cycle threshold Ct >39 for one probe, that reading was replaced with the average of the Ct for the other two probes, provided they were both below 39. Relative quantification was determined by the ΔCt method using miR-622 and miR-1266 as reference genes, as determined by GeNorm and Normfinder incorporated in the GenEx software. The control HIV-negative group was used as the calibrator between the HIVE and non-HIVE groups and the fold change was calculated using the formula $2^{-\Delta\Delta Ct}$. miRNAs with a fold change <0.5 were considered down-regulated, and miRNAs with a fold change >2 were set as up-regulated. The three groups, HIV-, HIVE, and HIV+ for the CSF experiment were compared using oneway ANOVA allowing for unequal variances, and followed by Dunnet tests. For this exploratory study a cut off for the *p*-value was set at 0.2.
For the analysis of brain tissue miRNAs, miR-650 and miR-1266 were used as reference genes. Due to the low number of samples analyzed (n=3 for each group), statistical analysis was not performed on the experiments related to the brain tissue samples.

Bioinformatics

Predicted gene targets for the eleven differentially regulated miRNAs were identified using miRWalk module [29], which allows the search of up to eight established target prediction programs. The list of genes predicted by three out of five databases was filtered for the brain tissue using DAVID functional annotation bioinformatics microarray analysis [30, 31]. Next, Gene Ontology (GO) annotations of predicted gene targets were determined using Genego integrated software

(MetaCore).

Results

RNA was extracted from a total of 20 CSF samples, 10 HIV-negative and 10 HIV-positive, and subjected to miRNA arrays. The group of HIV-positive individuals consisted of nine cases of HAND and was further divided into HIV-encephalitis (HIVE) (*n*=4) and non-HIVE (*n*=5) cases. The HIV-negative group comprised all cases of acute disseminated encephalomyelitis of non-viral origin and none of the individuals in this group had cognitive impairments. Males and females were represented in both HIV-and HIV+ groups. The age of the subjects ranged from 36 to 66 years old, with an overall average of 52.7 (51.3 for the HIV+ and 54.1 for the HIV-group). Each sample was retrotranscribed in triplicates and the resulting cDNA was loaded into three sets of miRNA plates. The Exiqon miRNA ready plates contain pre-assigned 6 wells for 6 different genes which have stable expression levels over a wide range of sample types. Three of these are microRNAs which are often stably expressed, and the other three are small RNA reference genes. However, using Normfinder and GeNorm applications incorporated in the GEnEx analysis software, we found that in CSF the most uniformly expressed miRNAs were miR-622 and miR-1266; therefore, we have selected them as reference genes. The CSF samples were divided in three groups, HIV-(*n*=10), HIV+ (*n*=5) and HIVE (*n*=4) and the ratio HIVE/HIV+ was determined after normalization of HIVE and HIV+ with the control HIV-group. For comparison analyses, only miRNAs present in all the three groups were selected and a new list of 66 miRNAs was generated (Figure 1); while miRNAs expressed preferentially in only one or two groups were removed. In general, infection with HIV-1 results in an overall down-regulation of miRNAs (Figure 1, lane HIV+/HIV-; values < 0.5 highlighted in green), with only five up-regulated miRs (highlighted in red). In contrast, in the group of cases with encephalitis (lane indicated with HIVE/HIV-; values between 0.5 and 2) the majority of miRNAs showed unchanged expression levels and only three, miR-937, miR-598, and miR-595 were up-regulated. Finally, an opposite trend in miRNA expression was observed when HIVE and HIV+ groups were compared and most of miRNAs showed up-regulation, while only seven were down-regulated (Figure 1,

lane indicated with HIVE/HIV+). Expression of 11 miRNAs, miR-502-5p, miR-877*, miR-127-5p, miR-543, miR-1247, miR-615-3p, miR-574-3p, miR-663, miR-197, miR-485-3p, and miR-766 remained unchanged across the three groups of samples (Figure 1, highlighted in yellow).

miRNA	HIVE/HIV-	HIV+/HIV-	HIVE/HIV+
hsa-miR-19b-2*	1.89	0.04	44.18
hsa-miR-595	2.18	0.08	25.72
hsa-miR-300	1.86	0.09	19.90
hsa-miR-937	4.51	0.27	16.78
hsa-miR-598	2.41	0.17	14.50
hsa-miR-1296	1.47	0.12	12.46
hsa-miR-362-5p	1.09	0.09	12.15
hsa-miR-555	1.17	0.13	9.25
hsa-miR-222	1.34	0.16	8.30
hsa-miR-105*	1.48	0.20	7.57
hsa-miR-708*	1.20	0.19	6.32
hsa-miR-520h	0.87	0.14	6.22
hsa-miR-1471	0.91	0.15	6.11
hsa-miR-452	1.52	0.25	5.99
hsa-miR-19a	1.31	0.22	5.96
hsa-miR-650	1.45	0.25	5.71
hsa-miR-629	1.36	0.24	5.63
hsa-miR-137	0.66	0.12	5.46
hsa-miR-562	0.92	0.17	5.32
hsa-miR-29b-1*	1.33	0.27	4.85
hsa-miR-212	0.78	0.17	4.71
hsa-miR-520d-3p	0.86	0.19	4.55
hsa-miR-141*	1.61	0.37	4.38
hsa-miR-888	1.12	0.27	4.13
hsa-miR-139-5p	1.02	0.25	4.10
hsa-miR-16	1.15	0.32	3.58
hsa-miR-558	1.25	0.35	3.55
hsa-miR-346	1.32	0.38	3.50
hsa-miR-518f*	0.68	0.20	3.45
hsa-let-7c	1.60	0.48	3.33
hsa-miR-134	1.38	0.42	3.25
hsa-miR-182*	1.68	0.53	3.19
hsa-miR-720	0.89	0.28	3.15
hsa-miR-1224-3p	1.48	0.48	3.07
hsa-miR-302c*	1.08	0.35	3.05
hsa-miR-297	1.02	0.34	3.04
hsa-miR-1203	1.35	0.45	3.00
hsa-miR-744*	1.60	0.53	2.99
hsa-miR-524-5p	1.12	0.39	2.86
hsa-miR-934	1.45	0.54	2.69
hsa-miR-1539	1.70	0.65	2.62
hsa-miR-1913	0.64	0.26	2.46
hsa-miR-490-3p	1.53	0.62	2.45
hsa-miR-495	1.06	0.44	2.43
hsa-miR-204	1.19	0.53	2.22
hsa-miR-1269	1.12	0.51	2.18
hsa-miR-885-3p	0.98	0.45	2.18
hsa-miR-450b-3p	0.54	0.40	1.35
hsa-miR-760	0.88	1.86	0.48
hsa-miR-324-3p	1.00	2.25	0.45
hsa-miR-331-5p	0.64	1.43	0.45
hsa-miR-187	1.06	2.45	0.43
hsa-miR-484	0.78	3.01	0.26
hsa-miR-92b*	1.28	7.49	0.17
hsa-let-7d*	0.56	10.80	0.05

miRNA	HIVE/HIV-	HIV+/HIV-	HIVE/HIV+
hsa-miR-502-5p	1.69	1.07	1.58
hsa-miR-877*	1.48	1.19	1.24
hsa-miR-127-5p	1.34	1.14	1.18
hsa-miR-543	1.16	1.16	1.00
hsa-miR-766	1.15	1.03	1.11
hsa-miR-1247	1.08	1.03	1.05
hsa-miR-615-3p	1.04	0.61	1.71
hsa-miR-574-3p	1.02	1.06	0.96
hsa-miR-663	1.00	0.63	1.59
hsa-miR-197	0.70	0.93	0.75
hsa-miR-485-3p	0.69	0.76	0.91

Figure 1. *Differentially regulated CSF miRNAs. MiRNAs were profiled in ten HIV+ and ten HIVCSF samples. Nine cases in the HIV+ group had HAND and, among those, 4 had HIVE. After data processing, comparison between three groups, HIVE, HIV+ and HIV-was performed as follows. First the HIVE and HIV+ groups were normalized for the HIV-control group according to the ΔΔCt formula and then the fold change was calculated as the ratio HIVE/HIV+. Over-expressed miRNAs (fold change > 2) are indicated in red, under-expressed miRNAs in green (values < 0.5), and miRNAs whose expression was unchanged (values between 0.5 and 2.0) are highlighted in yellow.*

The list of 66 miRNAs was further subjected to ANOVA analysis followed by the Dunnet's test to determine statistically significant differences among the three groups. Eleven miRNAs, miR-1203, miR-1224-3p, miR-182*, miR-19b-2*, miR-204, miR-362-5p, miR-484, miR-720, miR-744*, miR-934, and miR-937 were found differentially expressed with a $p< 0.2$ (Figure 2). Within this group, miR-182*, miR-362-5p, miR-720, and mir-937 had the lowest p-value, $p<0.05$.

	pvalues		
miRNA	**Overall**	**HIV+**	**HIVE**
hsa-miR-1203	0.137	0.458	0.504
hsa-miR-1224-3p	0.112	0.790	0.199
hsa-miR-182*	0.035	0.590	0.170
hsa-miR-19b-2*	0.145	0.221	0.716
hsa-miR-204	0.182	0.188	0.845
hsa-miR-362-5p	0.011	0.038	0.946
hsa-miR-484	0.167	0.374	0.386
hsa-miR-720	0.029	0.023	0.950
hsa-miR-744*	0.179	0.170	0.404
hsa-miR-934	0.167	0.953	0.133
hsa-miR-937	0.044	0.932	0.042

Figure 2. *List of miRNAs with differential expression significant at the 0.2 level. Global column p-values are for overall tests on the 3 groups (HIVE, HIV+ and HIV-). Dunnet tests comparing each of HIVE and HIV+ to HIV-were carried out. A total of 66 miRNAs was subjected to these analyses.*

We also evaluated miRNA profiles in archived brain tissues previously obtained from the Manhattan HIV Brain Bank. We analyzed three cases each of the following: HIV-control, HIV+, and HIVE. Comparison between groups was performed as described for the CSF study in which the fraction HIVE/HIV+ represents the ratio of the fold changes between the two groups HIVE and HIV+, calculated using the HIV-group as control. The results show 121 differentially regulated miRNAs (Figure 3). In general, and similar to the CSF miRNA profiles, HIV-infection resulted in overall down-regulation of miRNAs. In contrast, in the presence of encephalitis miRNA levels increased. This trend is clear when we compare HIVE versus HIV+ (ratio HIVE/HIV+) in which most of the miRNAs were up-regulated (Figures 1 and 3).

miRNA	HIVE/HIV-	HIV+/HIV-	HIVE/HIV+
hsa-let-7b	0.138	0.004	38.408
hsa-miR-145	0.161	0.004	36.758
hsa-miR-331-3p	0.641	0.022	29.651
hsa-miR-221	0.740	0.032	23.480
hsa-miR-138	0.816	0.036	22.864
hsa-miR-103	0.381	0.018	21.706
hsa-miR-30b	0.160	0.008	20.846
hsa-miR-885-5p	0.166	0.008	20.749
hsa-miR-129-5p	1.280	0.063	20.393
hsa-miR-127-3p	0.273	0.014	19.585
hsa-miR-30c	0.104	0.005	19.472
hsa-miR-149	0.324	0.020	16.393
hsa-miR-132	0.329	0.020	16.280
hsa-miR-135a	0.228	0.014	16.111
hsa-miR-21	0.147	0.010	15.419
hsa-miR-1296	0.416	0.028	14.757
hsa-miR-142-3p	0.771	0.054	14.156
hsa-miR-29c	0.087	0.006	14.042
hsa-let-7f	0.094	0.007	13.269
hsa-miR-342-3p	0.116	0.009	12.996
hsa-miR-143	0.097	0.008	12.743
hsa-miR-99a	0.153	0.012	12.395
hsa-miR-26a	0.072	0.006	11.713
hsa-let-7a	0.086	0.007	11.592
hsa-miR-139-5p	0.644	0.057	11.392
hsa-miR-29a	0.096	0.008	11.379
hsa-miR-181b	0.121	0.011	11.197
hsa-miR-328	0.264	0.026	10.291
hsa-miR-101	0.168	0.017	9.883
hsa-miR-107	0.387	0.040	9.747
hsa-miR-92b	0.123	0.013	9.747
hsa-miR-1913	0.174	0.018	9.736
hsa-miR-136	0.529	0.056	9.448
hsa-miR-128	0.152	0.017	9.021
hsa-miR-126*	0.073	0.008	9.000
hsa-let-7c	0.127	0.014	8.990
hsa-miR-24	0.151	0.017	8.674
hsa-let-7g	0.204	0.024	8.535
hsa-miR-181a	0.106	0.012	8.505
hsa-miR-423-3p	0.103	0.012	8.388
hsa-miR-150	0.069	0.008	8.340
hsa-miR-23a	0.052	0.006	8.311
hsa-miR-497	0.200	0.024	8.225
hsa-miR-19b	0.091	0.011	8.196
hsa-miR-29b	0.130	0.016	8.196
hsa-miR-1247	0.549	0.073	7.516
hsa-miR-638	0.177	0.024	7.353
hsa-miR-26b	0.112	0.015	7.235
hsa-let-7e	0.098	0.014	7.177
hsa-miR-886-3p	0.113	0.016	6.940
hsa-miR-218	0.595	0.087	6.845
hsa-miR-320b	0.046	0.007	6.751
hsa-miR-15a	0.110	0.017	6.394
hsa-miR-32	0.141	0.022	6.364
hsa-miR-212	0.582	0.092	6.298
hsa-miR-1224-3p	0.185	0.029	6.284
hsa-miR-551a	0.202	0.035	5.856
hsa-miR-485-3p	0.265	0.046	5.762
hsa-miR-92a	0.086	0.015	5.736
hsa-miR-1260	0.070	0.013	5.464
hsa-miR-324-5p	0.161	0.029	5.464

miRNA	HIVE/HIV-	HIV+/HIV-	HIVE/HIV+
hsa-miR-204	0.003	0.016	5.296
hsa-miR-151-5p	0.013	0.067	5.260
hsa-miR-186	0.026	0.132	5.081
hsa-miR-106a	0.013	0.065	5.063
hsa-miR-29a*	0.124	0.613	4.925
hsa-miR-27b	0.021	0.103	4.925
hsa-miR-33a	0.160	0.785	4.908
hsa-miR-324-3p	0.030	0.147	4.862
hsa-miR-99b	0.017	0.083	4.801
hsa-let-7d*	0.049	0.233	4.719
hsa-miR-27a	0.047	0.220	4.697
hsa-miR-766	0.140	0.599	4.272
hsa-miR-193b	0.024	0.099	4.108
hsa-miR-197	0.015	0.061	4.005
hsa-miR-598	0.158	0.632	3.991
hsa-miR-222	0.027	0.107	3.991
hsa-miR-16	0.011	0.042	3.936
hsa-miR-140-3p	0.023	0.087	3.771
hsa-miR-23b	0.028	0.105	3.694
hsa-miR-664	0.021	0.073	3.422
hsa-miR-124	0.013	0.044	3.356
hsa-miR-191	0.018	0.059	3.272
hsa-miR-320a	0.006	0.019	3.175
hsa-miR-885-3p	0.042	0.134	3.167
hsa-miR-125a-5p	0.008	0.023	3.109
hsa-miR-34a	0.028	0.088	3.095
hsa-miR-629	0.290	0.848	2.928
hsa-miR-877*	0.423	1.227	2.901
hsa-miR-584	0.093	0.251	2.704
hsa-miR-134	0.039	0.100	2.603
hsa-miR-9	0.012	0.031	2.597
hsa-miR-25	0.014	0.037	2.588
hsa-miR-495	0.074	0.187	2.523
hsa-miR-593	0.141	0.338	2.403
hsa-miR-622	3.157	7.456	2.362
hsa-miR-452	0.579	1.312	2.266
hsa-miR-2110	0.066	0.142	2.171
hsa-miR-451	0.014	0.031	2.158
hsa-miR-331-5p	2.855	5.439	1.905
hsa-miR-934	0.361	0.676	1.875
hsa-miR-346	0.053	0.098	1.866
hsa-miR-574-3p	0.065	0.115	1.765
hsa-miR-605	0.019	0.034	1.757
hsa-miR-484	0.031	0.051	1.666
hsa-miR-125b	0.010	0.013	1.298
hsa-miR-558	0.390	0.493	1.266
hsa-miR-720	0.037	0.045	1.211
hsa-miR-141*	1.539	1.815	1.180
hsa-miR-615-3p	0.310	0.360	1.159
hsa-miR-338-3p	0.042	0.047	1.122
hsa-miR-940	0.021	0.023	1.115
hsa-miR-663	0.067	0.072	1.064
hsa-miR-93	0.041	0.043	1.042
hsa-miR-562	0.679	0.565	0.832
hsa-miR-411*	0.522	0.421	0.808
hsa-miR-937	2.570	2.012	0.783
hsa-miR-490-3p	0.599	0.422	0.704
hsa-miR-224*	0.405	0.270	0.667
hsa-miR-219-5p	0.042	0.027	0.642
hsa-miR-760	0.310	0.161	0.520

Figure 3. *List of differentially regulated miRNAs in archived brain tissue samples. Three cases each of HIVE, HIV+, and HIV-were analyzed and results show 121 differentially expressed miRNAs. Up-regulated and unchanged miRNAs are indicated in red and yellow, respectively. Note that in the lanes indicated as HIV+/HIV-and HIVE/HIV-miRNAs are all down-regulated.*

Next, we compared CSF and frontal cortex miRNA profiles and the results are shown in Figure 4A. Thirty five of the 66 CSF miRNAs (53%) were also present in the list of differentially regulated miRNAs in the frontal cortex. Four miRNAs, miR-1296, miR-134, miR-16, and miR-495 had comparable expression changes for the ratio HIVE/HIV+ in both CSF and brain tissue, with miR-1296 being the most up-regulated. Differences in the expression level of six out of the 11 statistically

significant CSF miRNAs were plotted in Figure 4B. Strikingly, miR-937 is more than 20 times up-regulated in the CSF compared to frontal cortex in HIVE cases.

A

miRNA	HIVE/HIV-	HIV+/HIV-	Frontal Cortex	miRNA	HIVE/HIV-	HIV+/HIV-	CSF
hsa-let-7c	0.127	0.014	8.990	hsa-let-7c	1.60	0.48	3.33
hsa-let-7d*	0.233	0.049	4.719	hsa-let-7d*	0.56	10.80	-19.34
hsa-miR-1224-3p	0.185	0.029	6.284	hsa-miR-1224-3p	1.48	0.48	3.07
hsa-miR-1247	0.549	0.073	7.516	hsa-miR-1247	1.08	1.03	1.05
hsa-miR-139-5p	0.644	0.057	11.392	hsa-miR-139-5p	1.02	0.25	4.10
hsa-miR-141*	1.815	1.539	1.180	hsa-miR-141*	1.61	0.37	4.38
hsa-miR-1913	0.174	0.018	9.736	hsa-miR-1913	0.64	0.26	2.46
hsa-miR-204	0.016	0.003	5.296	hsa-miR-204	1.19	0.53	2.22
hsa-miR-212	0.582	0.092	6.298	hsa-miR-212	0.78	0.17	4.71
hsa-miR-222	0.107	0.027	3.991	hsa-miR-222	1.34	0.16	8.30
hsa-miR-324-3p	0.147	0.030	4.862	hsa-miR-324-3p	1.00	2.25	-2.24
hsa-miR-331-5p	5.439	2.855	1.905	hsa-miR-331-5p	0.64	1.43	-2.24
hsa-miR-346	0.098	0.053	1.866	hsa-miR-346	1.32	0.38	3.50
hsa-miR-452	1.312	0.579	2.266	hsa-miR-452	1.52	0.25	5.99
hsa-miR-484	0.051	0.031	1.666	hsa-miR-484	0.78	3.01	-3.89
hsa-miR-485-3p	0.265	0.046	5.762	hsa-miR-485-3p	0.69	0.76	0.91
hsa-miR-490-3p	0.422	0.599	0.704	hsa-miR-490-3p	1.53	0.62	2.45
hsa-miR-558	0.493	0.390	1.266	hsa-miR-558	1.25	0.35	3.55
hsa-miR-562	0.565	0.679	0.832	hsa-miR-562	0.92	0.17	5.32
hsa-miR-598	0.632	0.158	3.991	hsa-miR-598	2.41	0.17	14.50
hsa-miR-615-3p	0.360	0.310	1.159	hsa-miR-615-3p	1.04	0.61	1.71
hsa-miR-629	0.848	0.290	2.928	hsa-miR-629	1.36	0.24	5.63
hsa-miR-720	0.045	0.037	1.211	hsa-miR-720	0.89	0.28	3.15
hsa-miR-766	0.599	0.140	4.272	hsa-miR-766	1.15	1.03	1.11
hsa-miR-877*	1.227	0.423	2.901	hsa-miR-877*	1.48	1.19	1.24
hsa-miR-885-3p	0.134	0.042	3.167	hsa-miR-885-3p	0.98	0.45	2.18
hsa-miR-934	0.676	0.361	1.875	hsa-miR-934	1.45	0.54	2.69
hsa-miR-937	2.012	2.570	0.783	hsa-miR-937	4.51	0.27	16.78

B

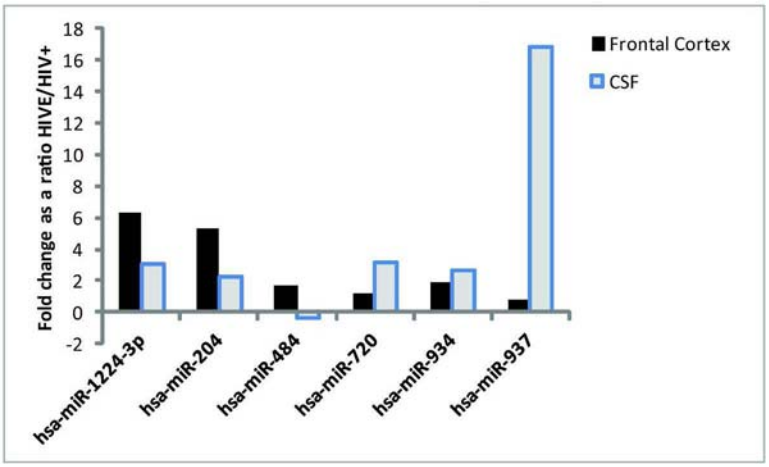

Figure 4. *Comparison of CSF and brain tissue miRNA expression profiles. A) 35 of the 66 differentially expressed CSF miRNAs are also deregulated in the frontal cortex and are listed in alphabetical order. Values are expressed as indicated in Figure 1. Note that, for simplicity, although not in green, most of the values in column 1 (HIVE/HIV-) are down-regulated. B) Six of the 11 statistically significant CSF miRNAs were also present in the frontal cortex and their relative expression is shown in panel B.*

Next, we investigated predicted gene targets for the 11 statistically significant miRNAs (Figure 2) in the context of maps, networks and diseases and the results are

shown in Figure 5. The most represented genes appear to be related to the maps of cytoskeleton remodeling, cell adhesion and chemokines (Figure 5, upper table). Various aspects of neurogenesis including axonal guidance, notch signaling, synaptogenesis and transmission of nerve impulse were the most represented networks (Figure 5, middle table). Interestingly, the predicted gene targets for the combined miRNAs were associated with mental disorders such as mood, affective and depressive disorders, as highlighted in Figure 5 (lowest table).

Maps	pValue	Ratio	
Cytoskeleton remodeling_TGF, WNT and cytoskeletal remodeling	1.998E-13	59	111
Cytoskeleton remodeling_FAK signaling	4.381E-10	34	57
Cell adhesion_Chemokines and adhesion	3.318E-09	48	100
Development_GM-CSF signaling	3.865E-09	30	50
Cytoskeleton remodeling_Cytoskeleton remodeling	7.526E-09	48	102
Chemotaxis_CXCR4 signaling pathway	9.547E-09	23	34
Development_Flt3 signaling	1.178E-08	27	44
Transport_Clathrin-coated vesicle cycle	1.297E-08	37	71
Development_Hedgehog signaling	4.516E-08	27	46
Development_FGFR signaling pathway	4.601E-08	30	54

Networks	pValue	Ratio	
Development_Neurogenesis_Axonal guidance	7.476E-10	129	230
Signal transduction_NOTCH signaling	1.374E-09	131	236
Development_Neurogenesis_Synaptogenesis	1.556E-09	105	180
Development_Neurogenesis in general	2.676E-09	110	192
Neurophysiological process_Transmission of nerve impulse	1.661E-08	117	212
Development_Hedgehog signaling	6.337E-08	134	254
Signal transduction_WNT signaling	1.987E-07	98	177
Cell adhesion_Attractive and repulsive receptors	2.163E-06	94	175
Cytoskeleton_Regulation of cytoskeleton rearrangement	3.245E-06	97	183
Cell adhesion_Amyloid proteins	1.501E-05	100	195

Diseases	pValue	Ratio	
Psychiatry and Psychology	8.113E-20	1261	2837
Mental Disorders	1.233E-19	1252	2817
Pathological Conditions, Signs and Symptoms	2.804E-15	1755	4182
Pathologic Processes	1.726E-12	1157	2694
Mood Disorders	1.008E-11	536	1156
Affective Disorders, Psychotic	7.619E-11	339	695
Bipolar Disorder	8.230E-11	338	693
Depressive Disorder, Major	2.609E-10	440	942
Depressive Disorder	9.021E-10	440	949
Suicide	1.458E-09	84	134

***Figure* 5**. *Annotation results from Gene Ontology analysis. Predicted gene targets for the eleven differentially regulated CSF miRNAs (miR-1203, miR-1224-3p, miR-182*, miR-19b-2*, miR-204, miR-362-5p, miR-484, miR-720, miR-744*, miR-934, and miR-937) were subjected to GO analysis. The three tables show the list of the most significant maps, networks and diseases, respectively.*

In summary, our findings indicate an overall down-regulation of miRNAs in HIV-infected individuals in both CSF and frontal cortex. This trend, however, appears to be reversed in the presence of encephalitis, with miR-937 being the most up-regulated. While more clinical samples should be profiled to validate a miRNA signature in the CSF of individuals with HIV-1, with and without encephalitis, this work provides knowledge and important procedural aspects to investigate CSF miRNAs in the clinical setting of HIV-infection.

Discussion

HIV enters the CNS early during infection, frequently leading to cognitive impairments that can persist even after successful viral suppression [32-34]. HIV-associated neurological disorders comprise a variety of cognitive and motor impairments that range from mild to severe and that are characterized by molecular events leading to neuronal injury, inflammation, and loss of neuroprotection. While several indicators of neuronal injury and immune activation have been identified in the CSF, they do not correlate with the severity and/or progression of HAND, and the need of diagnostic and/or prognostic markers is high priority [2]. MicroRNAs have emerged as critical regulators of gene expression in mammals. Several features of miRNAs, including their stability and tissue specificity, make them suitable for their detection and relative quantification in a variety of tissues and body fluids. In contrast to most mRNAs, detection of miRNAs in specimens such as formalin-fixed tissue and cerebrospinal fluid (CSF) or other body fluids is more accurate and reliable [35, 36]. However, there are some limitations that have been outlined in a recent review by Pritchard et al. [37]. Accordingly, we found that recovery of the RNA for qPCR miRNA profiling was higher in the brain samples (FFPE) in comparison to CSF specimens. Differently from chip-based microarrays, which generally use micrograms of RNA, the advantage of using quantitative PCR panels is that they require nanogram amounts of RNA, allowing diagnostic analyses from low RNA recovery type of tissues, such as CSF and FFPE samples. Furthermore, the low RNA abundance could be, at least partially, overcome by pre-amplification cycles, for which kits have been recently developed and are commercially available. Although the global normalization approach is widely used in microarrays [38, 39],

it couldn't be applied to our system due to the low number of miRNAs that were represented in all samples [40]. Eight miRNAs had an average Ct< 37 and two of them, miR-622 and miR-1266, that showed uniform expression across all samples were chosen as reference genes. Of interest, expression levels of miR-1266 remained unchanged across the samples and in the brain tissue. MiR-937 was the most abundant miR in all CSF samples with an average Ct of 33.6, while in the frontal cortex miR-720 (average Ct=23) was the most expressed miRNA. Although the number of the analyzed brain samples was lower than CSF cases, we have observed significantly less variability across the samples in the brain tissues compared to the CSF. Despite of this difference in RNA samples a high number of miRNAs were found differentially regulated in both brain and CSF. Accordingly, 53% of differentially regulated miRNAs in the CSF were also present in the frontal cortex (Figure 4A).

Figure 1 shows a global downregulation of miRNA expression in the CSF of HIV+ individuals compared to HIV-controls (Figure 1, lane HIV+/HIV-). This trend is reversed in the presence of encephalitis (compare lanes identified as HIVE/HIV-and HIV+/HIV-). A similar general miRNA down-regulation was also observed in the frontal cortex as shown in Figure 3. Overall, these data may suggest impairment in the processing of miRNAs (synthesis and/or maturation). Indeed, we have some indication from gene expression arrays performed on the same brain tissue cases that levels of proteins involved in the miRNA biogenesis, such as Dicer and DCGR8, are down-regulated (data not shown). Among the most up-regulated miRNAs in the CSF of HIVE cases, miR-19b-2*, miR-937, and miR-362-5p had the largest fold change. Although only 11 CSF miRNAs showed statistically significant differences, several other miRNAs may be promising in that they show a large fold change, such as the up-regulated miR-595, miR-300, miR-598, miR-1296, miR-555, miR-222, and miR-105*, or the down-regulated miR-92b* and let-7d*.

Gene ontology analysis performed on the predicted gene targets for the eleven differentially regulated miRNAs revealed maps of genes associated with neurogenesis, cytoskeletal remodeling, chemokine signaling, and networks related to synaptogenesis and axonal guidance (Figure 5). Overall, bioinformatics analysis of CSF miRNA predicted gene targets may further provide additional information on the molecular events that lead to neuronal damage and/or persistent inflammation.

In summary, this is the first report detecting CSF miRNA in HIV patients and identifying a potential miRNA signature for HIVE. By demonstrating the possibility of detecting miRNAs in the CSF, this work offers both scientific and technical details for future longitudinal studies aimed to determine miRNA profiles in clinical settings that include antiretroviral therapies and/or addictive behaviors, such as alcohol and drug usage, often associated with HIV-infection.

References

1. Gannon, P., M.Z. Khan, and D.L. Kolson, *Current understanding of HIV-associated neurocognitive disorders pathogenesis.* Curr Opin Neurol, 2011.
2. McGuire, D., *CSF biomarkers in HIV dementia: through a glass darkly.* Neurology, 2009. **73**(23): p. 1942-4.
3. Mishima, T., et al., *RT-PCR-based analysis of microRNA (miR-1 and -124) expression in mouse CNS.* Brain Res, 2007. **1131**(1): p. 37-43.
4. Montano, M., *MicroRNAs: miRRORS of health and disease.* Transl Res, 2011. **157**(4): p. 157-62.
5. Eacker, S.M., T.M. Dawson, and V.L. Dawson, *Understanding microRNAs in neurodegeneration.* Nat Rev Neurosci, 2009. **10**(12): p. 837-41.
6. Sonntag, K.C., *MicroRNAs and deregulated gene expression networks in neurodegeneration.* Brain Res, 2010. **1338**: p. 48-57.
7. Erkan, E.P., X.O. Breakefield, and O. Saydam, *miRNA signature of schwannomas: Possible role(s) of "tumor suppressor" miRNAs in benign tumors.* Oncotarget, 2011: p. 265-70.
8. Gibcus, J.H., et al., *Hodgkin lymphoma cell lines are characterized by a specific miRNA expression profile.* Neoplasia, 2009. **11**(2): p. 167-76.
9. O'Hara, A.J., W. Vahrson, and D.P. Dittmer, *Gene alteration and precursor and mature microRNA transcription changes contribute to the miRNA signature of primary effusion lymphoma.* Blood, 2008. **111**(4): p. 2347-53.
10. Pedranzini, L., et al., *Differential cytogenomics and miRNA signature of the Acute Myeloid Leukaemia Kasumi-1 cell line CD34+38- compartment.* Leuk Res, 2010. **34**(10): p. 1287-95.

11. Robertus, J.L., et al., *MiRNA profiling in B non-Hodgkin lymphoma: a MYC-related miRNA profile characterizes Burkitt lymphoma.* Br J Haematol, 2010. **149**(6): p. 896-9.
12. Shah, A.A., et al., *miRNA: small molecules as potential novel biomarkers in cancer.* Curr Med Chem, 2010. **17**(36): p. 4427-32.
13. Alevizos, I. and G.G. Illei, *MicroRNAs as biomarkers in rheumatic diseases.* Nat Rev Rheumatol, 2010. **6**(7): p. 391-8.
14. Cho, W.C., *MicroRNAs: potential biomarkers for cancer diagnosis, prognosis and targets for therapy.* Int J Biochem Cell Biol, 2010. **42**(8): p. 1273-81.
15. De Smaele, E., E. Ferretti, and A. Gulino, *MicroRNAs as biomarkers for CNS cancer and other disorders.* Brain Res, 2010. **1338**: p. 100-11.
16. Ferracin, M., A. Veronese, and M. Negrini, *Micromarkers: miRNAs in cancer diagnosis and prognosis.* Expert Rev Mol Diagn, 2010. **10**(3): p. 297-308.
17. Heneghan, H.M., N. Miller, and M.J. Kerin, *MiRNAs as biomarkers and therapeutic targets in cancer.* Curr Opin Pharmacol, 2010. **10**(5): p. 543-50.
18. Ju, J., *miRNAs as biomarkers in colorectal cancer diagnosis and prognosis.* Bioanalysis, 2010. **2**(5): p. 901-6.
19. Kosaka, N., H. Iguchi, and T. Ochiya, *Circulating microRNA in body fluid: a new potential biomarker for cancer diagnosis and prognosis.* Cancer Sci, 2010. **101**(10): p. 2087-92.
20. Taft, R.J., et al., *Non-coding RNAs: regulators of disease.* J Pathol, 2009. **220**(2): p. 126-39.
21. Wittmann, J. and H.M. Jack, *Serum microRNAs as powerful cancer biomarkers.* Biochim Biophys Acta, 2010. **1806**(2): p. 200-7.
22. Xie, L., X. Qian, and B. Liu, *MicroRNAs: novel biomarkers for gastrointestinal carcinomas.* Mol Cell Biochem, 2010. **341**(1-2): p. 291-9.
23. Eletto, D., et al., *Inhibition of SNAP25 expression by HIV-1 Tat involves the activity of mir-128a.* J Cell Physiol, 2008. **216**(3): p. 764-70.
24. Noorbakhsh, F., et al., *MicroRNA profiling reveals new aspects of HIV neurodegeneration: caspase-6 regulates astrocyte survival.* FASEB J, 2010. **24**(6): p. 1799-812.

25. Rom, S., et al., *CCL8/MCP-2 is a target for mir-146a in HIV-1-infected human microglial cells.* FASEB J, 2010. **24**(7): p. 2292-300.
26. Tatro, E.T., et al., *Evidence for Alteration of Gene Regulatory Networks through MicroRNAs of the HIV-infected brain: novel analysis of retrospective cases.* PLoS One, 2010. **5**(4): p. e10337.
27. Yelamanchili, S.V., et al., *MicroRNA-21 dysregulates the expression of MEF2C in neurons in monkey and human SIV/HIV neurological disease.* Cell Death Dis, 2010. **1**(9): p. e77.
28. Andreasen, D., et al., *Improved microRNA quantification in total RNA from clinical samples.* Methods, 2010. **50**(4): p. S6-9.
29. Dweep, H., et al., *miRWalk--database: prediction of possible miRNA binding sites by "walking" the genes of three genomes.* J Biomed Inform. **44**(5): p. 839-47.
30. Huang da, W., B.T. Sherman, and R.A. Lempicki, *Systematic and integrative analysis of large gene lists using DAVID bioinformatics resources.* Nat Protoc, 2009. **4**(1): p. 44-57.
31. Huang da, W., B.T. Sherman, and R.A. Lempicki, *Bioinformatics enrichment tools: paths toward the comprehensive functional analysis of large gene lists.* Nucleic Acids Res, 2009. **37**(1): p. 1-13.
32. Heaton, R.K., et al., *HIV-associated neurocognitive disorders persist in the era of potent antiretroviral therapy: CHARTER Study.* Neurology. **75**(23): p. 2087-96.
33. Power, C., et al., *NeuroAIDS: an evolving epidemic.* Can J Neurol Sci, 2009. **36**(3): p. 285-95.
34. Woods, S.P., et al., *Cognitive neuropsychology of HIV-associated neurocognitive disorders.* Neuropsychol Rev, 2009. **19**(2): p. 152-68.
35. Doleshal, M., et al., *Evaluation and validation of total RNA extraction methods for microRNA expression analyses in formalin-fixed, paraffin-embedded tissues.* J Mol Diagn, 2008. **10**(3): p. 203-11.
36. Mitchell, P.S., et al., *Circulating microRNAs as stable blood-based markers for cancer detection.* Proc Natl Acad Sci U S A, 2008. **105**(30): p. 10513-8.
37. Pritchard, C.C., H.H. Cheng, and M. Tewari, *MicroRNA profiling: approaches and considerations.* Nat Rev Genet, 2010. **13**(5): p. 358-69.

38. Pradervand, S., et al., *Impact of normalization on miRNA microarray expression profiling.* RNA, 2009. **15**(3): p. 493-501.
39. Wylie, D., et al., *A novel mean-centering method for normalizing microRNA expression from high-throughput RT-qPCR data.* BMC Res Notes, 2011. **4**: p. 555.
40. Mestdagh, P., et al., *A novel and universal method for microRNA RT-qPCR data normalization.* Genome Biol, 2009. **10**(6): p. R64.

Conclusions

HIV-associated neurological disorders (HAND) comprise a variety of cognitive and motor impairments that range from mild to severe and that are characterized by molecular events leading to neuronal injury, inflammation, and loss of neuroprotection [1]. The association between the abundance of activated macrophages/microglia in the CNS, neuronal damage, and cognitive dysfunction suggests that neuroinflammation resulting from systemic immune activation and/or inflammation triggers the neurodegeneration observed in HAND [2].

Considering that HAND symptoms are closely associated with neuronal damage and loss, and the observation that HIV is unable to infect neurons, mechanisms other than direct infection must mediate the neuropathogenesis of HIV infection. Currently, two major models account for neurodegeneration and development of neurological symptoms in HAND: the direct model and the indirect model [3]. Each of these models requires the initial productive infection of perivascular macrophages and microglia. The direct model proposes that viral proteins released from infected monocyte-derived cells cause neuronal death through direct interaction of viral proteins with neurons.

The indirect, or 'bystander,' model proposes that neuronal death is mediated by the inflammatory response mounted by infected and uninfected non-neuronal cells against HIV infection and against HIV proteins released by directly infected cells. Clearly, these two models are not mutually exclusive.

The indirect model of neurodegeneration in HAND centers upon soluble factors released by non-neuronal cells as part of an inflammatory response to viral particles. When activated through direct HIV infection or through exposure to viral particles, macrophages and microglia release numerous soluble molecules, including the viral proteins gp120, Tat, and Vpr. Following this model, we have investigated the pleiotropic activity of HIV-Tat showing a very robust pattern of expression in area of encephalopathy, where the viral protein is also detected in endothelial cells, perivascular macrophages and reactive astrocytes [4]. Interestingly, we have identified a direct interaction of Tat with Grb2, and possibly other SH3-bearing

proteins, suggesting a broad-spectrum mechanism for Tat-mediated deregulation of signaling pathways [4].

In response to HIV invasion of the CNS, microglia and macrophages within the brain mount an immune response that includes the release of both α- and β-chemokines. Since neurons express chemokine receptors [3], this HIV-induced inflammatory response may play a critical role in the effects of HIV infection on the CNS. In this scenario, we have identified a mechanism implicated in the negative regulation of inflammation in HIV-1 infected macrophages/microglia. It involves HIV-mediated increased expression of mir-146a, which, in turn, inhibits the expression of the proinflammatory chemokine MCP-2 [5]. According to our model, acute infection of microglia with HIV-1 would trigger the production and secretion of MCP-2 chemokine, and, interestingly, the rapid decline of MCP-2 levels after the peak at 12 d is coincident with the up-regulation of mir-146a expression, suggesting a role for this miRNA in the dynamic modulation of inflammatory processes in neuronal cells.

Understanding the biology of HIV-1 infection in the brain and identifying markers for its pathological manifestations, including HIV-Encephalopathy, are of critical importance. Although several molecules in the CSF have been identified as putative indicators of neurocognitive impairments, the need for biomarkers persists. As emerging evidence accumulated supporting the concept of establishing microRNAs expression profiles in body fluids as possible diagnostic and prognostic markers, our study demonstrates feasibility in detecting CSF miRNAs, it provides a putative CSF miRNA signature for HIVE, and shows important correlation in differentially regulated miRNAs in the frontal cortex and CSF samples [6].

Gene ontology analysis performed on the predicted gene targets for the eleven differentially regulated miRNAs revealed maps of genes associated with neurogenesis, cytoskeletal remodeling, chemokine signaling, and networks related to synaptogenesis and axonal guidance. Overall, bioinformatics analysis of CSF miRNA predicted gene targets may further provide additional information on the molecular events that lead to neuronal damage and/or persistent inflammation.

References

1. Clifford, D.B., *HIV-associated neurocognitive disease continues in the antiretroviral era.* Top HIV Med, 2008. **16**(2): p. 94-8.
2. McArthur, J.C., B.J. Brew, and A. Nath, *Neurological complications of HIV infection.* Lancet Neurol, 2005. **4**(9): p. 543-55.
3. Vivithanaporn, P., et al., *Neurologic disease burden in treated HIV/AIDS predicts survival: a population-based study.* Neurology, 2010. **75**(13): p. 1150-8.
4. McArthur, J.C., et al., *Human immunodeficiency virus-associated neurocognitive disorders: Mind the gap.* Ann Neurol, 2010. **67**(6): p. 699-714.
5. Kaul, M., G.A. Garden, and S.A. Lipton, *Pathways to neuronal injury and apoptosis in HIV-associated dementia.* Nature, 2001. **410**(6831): p. 988-94.
6. Ong, C.L., et al., *Low TRBP levels support an innate human immunodeficiency virus type 1 resistance in astrocytes by enhancing the PKR antiviral response.* J Virol, 2005. **79**(20): p. 12763-72.
7. Masliah, E., et al., *Spectrum of human immunodeficiency virus-associated neocortical damage.* Ann Neurol, 1992. **32**(3): p. 321-9.
8. Heaton, R.K., et al., *HIV-associated neurocognitive disorders persist in the era of potent antiretroviral therapy: CHARTER Study.* Neurology. **75**(23): p. 2087-96.
9. McArthur, J.C., et al., *Dementia in AIDS patients: incidence and risk factors. Multicenter AIDS Cohort Study.* Neurology, 1993. **43**(11): p. 2245-52.
10. Wright, E.J., et al., *NeuroAIDS in the Asia Pacific Region.* J Neurovirol, 2008. **14**(6): p. 465-73.
11. Zink, M.C., et al., *SIV infection of macaques--modeling the progression to AIDS dementia.* J Neurovirol, 1998. **4**(3): p. 249-59.
12. Vago, L., et al., *Pathological findings in the central nervous system of AIDS patients on assumed antiretroviral therapeutic regimens: retrospective study of 1597 autopsies.* AIDS, 2002. **16**(14): p. 1925-8.
13. Everall, I., et al., *Assessment of neuronal density in the putamen in human immunodeficiency virus (HIV) infection. Application of stereology and spatial analysis of quadrats.* J Neurovirol, 1995. **1**(1): p. 126-9.

14. Di Rienzo, A.M., et al., *Virological and molecular parameters of HIV-1 infection of human embryonic astrocytes.* Arch Virol, 1998. **143**(8): p. 1599-615.
15. Kure, K., et al., *Human immunodeficiency virus-1 infection of the nervous system: an autopsy study of 268 adult, pediatric, and fetal brains.* Hum Pathol, 1991. **22**(7): p. 700-10.
16. Brew, B.J., et al., *AIDS dementia complex and HIV-1 brain infection: clinical-virological correlations.* Ann Neurol, 1995. **38**(4): p. 563-70.
17. Anthony, I.C. and J.E. Bell, *The Neuropathology of HIV/AIDS.* Int Rev Psychiatry, 2008. **20**(1): p. 15-24.
18. Thompson, K.A., J.C. McArthur, and S.L. Wesselingh, *Correlation between neurological progression and astrocyte apoptosis in HIV-associated dementia.* Ann Neurol, 2001. **49**(6): p. 745-52.
19. Ketzler, S., et al., *Loss of neurons in the frontal cortex in AIDS brains.* Acta Neuropathol, 1990. **80**(1): p. 92-4.
20. Masliah, E., et al., *Selective neuronal vulnerability in HIV encephalitis.* J Neuropathol Exp Neurol, 1992. **51**(6): p. 585-93.
21. Glass, J.D., et al., *Immunocytochemical quantitation of human immunodeficiency virus in the brain: correlations with dementia.* Ann Neurol, 1995. **38**(5): p. 755-62.
22. Glass, J.D. and R.T. Johnson, *Human immunodeficiency virus and the brain.* Annu Rev Neurosci, 1996. **19**: p. 1-26.
23. Wesselingh, S.L., et al., *Cellular localization of tumor necrosis factor mRNA in neurological tissue from HIV-infected patients by combined reverse transcriptase/polymerase chain reaction in situ hybridization and immunohistochemistry.* J Neuroimmunol, 1997. **74**(1-2): p. 1-8.
24. McCombe, J.A., et al., *Neurologic immune reconstitution inflammatory syndrome in HIV/AIDS: outcome and epidemiology.* Neurology, 2009. **72**(9): p. 835-41.
25. Wang, T., et al., *Granzyme B mediates neurotoxicity through a G-protein-coupled receptor.* FASEB J, 2006. **20**(8): p. 1209-11.
26. Griffin, D.E., *Cytokines in the brain during viral infection: clues to HIV-associated dementia.* J Clin Invest, 1997. **100**(12): p. 2948-51.

27. Adamson, D.C., et al., *Rate and severity of HIV-associated dementia (HAD): correlations with Gp41 and iNOS.* Mol Med, 1999. **5**(2): p. 98-109.
28. Heyes, M.P., et al., *Elevated cerebrospinal fluid quinolinic acid levels are associated with region-specific cerebral volume loss in HIV infection.* Brain, 2001. **124**(Pt 5): p. 1033-42.
29. Smith, D.G., et al., *Quinolinic acid is produced by macrophages stimulated by platelet activating factor, Nef and Tat.* J Neurovirol, 2001. **7**(1): p. 56-60.
30. Yong, V.W., et al., *Matrix metalloproteinases and diseases of the CNS.* Trends Neurosci, 1998. **21**(2): p. 75-80.
31. Vos, C.M., et al., *Cytotoxicity by matrix metalloprotease-1 in organotypic spinal cord and dissociated neuronal cultures.* Exp Neurol, 2000. **163**(2): p. 324-30.
32. Patton, B.L., A.Y. Chiu, and J.R. Sanes, *Synaptic laminin prevents glial entry into the synaptic cleft.* Nature, 1998. **393**(6686): p. 698-701.
33. Chauhan, A., et al., *Intracellular human immunodeficiency virus Tat expression in astrocytes promotes astrocyte survival but induces potent neurotoxicity at distant sites via axonal transport.* J Biol Chem, 2003. **278**(15): p. 13512-9.
34. Williams, K.C. and W.F. Hickey, *Central nervous system damage, monocytes and macrophages, and neurological disorders in AIDS.* Annu Rev Neurosci, 2002. **25**: p. 537-62.
35. Nath, A., et al., *Transient exposure to HIV-1 Tat protein results in cytokine production in macrophages and astrocytes. A hit and run phenomenon.* J Biol Chem, 1999. **274**(24): p. 17098-102.
36. Bruce-Keller, A.J., et al., *Synaptic transport of human immunodeficiency virus-Tat protein causes neurotoxicity and gliosis in rat brain.* J Neurosci, 2003. **23**(23): p. 8417-22.
37. Cheng-Mayer, C. and J.A. Levy, *Distinct biological and serological properties of human immunodeficiency viruses from the brain.* Ann Neurol, 1988. **23 Suppl**: p. S58-61.
38. Chiodi, F., et al., *Biological characterization of paired human immunodeficiency virus type 1 isolates from blood and cerebrospinal fluid.* Virology, 1989. **173**(1): p. 178-87.

39. Power, C., et al., *Neuronal death induced by brain-derived human immunodeficiency virus type 1 envelope genes differs between demented and nondemented AIDS patients.* J Virol, 1998. **72**(11): p. 9045-53.
40. Johnston, J.B., et al., *HIV-1 Tat neurotoxicity is prevented by matrix metalloproteinase inhibitors.* Ann Neurol, 2001. **49**(2): p. 230-41.
41. Meucci, O., et al., *Chemokines regulate hippocampal neuronal signaling and gp120 neurotoxicity.* Proc Natl Acad Sci U S A, 1998. **95**(24): p. 14500-5.
42. Zhang, K., et al., *HIV-induced metalloproteinase processing of the chemokine stromal cell derived factor-1 causes neurodegeneration.* Nat Neurosci, 2003. **6**(10): p. 1064-71.
43. Masliah, E., et al., *Dendritic injury is a pathological substrate for human immunodeficiency virus-related cognitive disorders. HNRC Group. The HIV Neurobehavioral Research Center.* Ann Neurol, 1997. **42**(6): p. 963-72.
44. Everall, I.P., et al., *Cortical synaptic density is reduced in mild to moderate human immunodeficiency virus neurocognitive disorder. HNRC Group. HIV Neurobehavioral Research Center.* Brain Pathol, 1999. **9**(2): p. 209-17.
45. Moore, D.J., et al., *Cortical and subcortical neurodegeneration is associated with HIV neurocognitive impairment.* AIDS, 2006. **20**(6): p. 879-87.
46. Aprea, S., et al., *Tubulin-mediated binding of human immunodeficiency virus-1 Tat to the cytoskeleton causes proteasomal-dependent degradation of microtubule-associated protein 2 and neuronal damage.* J Neurosci, 2006. **26**(15): p. 4054-62.
47. Rom, S., et al., *CCL8/MCP-2 is a target for mir-146a in HIV-1-infected human microglial cells.* FASEB J, 2010. **24**(7): p. 2292-300.
48. Banks, W.A., S.M. Robinson, and A. Nath, *Permeability of the blood-brain barrier to HIV-1 Tat.* Exp Neurol, 2005. **193**(1): p. 218-27.
49. Bonavia, R., et al., *HIV-1 Tat causes apoptotic death and calcium homeostasis alterations in rat neurons.* Biochem Biophys Res Commun, 2001. **288**(2): p. 301-8.
50. Perez, A., et al., *Evaluation of HIV-1 Tat induced neurotoxicity in rat cortical cell culture.* J Neurovirol, 2001. **7**(1): p. 1-10.
51. McManus, C.M., et al., *Chemokine and chemokine-receptor expression in human glial elements: induction by the HIV protein, Tat, and chemokine autoregulation.* Am J Pathol, 2000. **156**(4): p. 1441-53.

52. Rappaport, J., et al., *Molecular pathway involved in HIV-1-induced CNS pathology: role of viral regulatory protein, Tat.* J Leukoc Biol, 1999. **65**(4): p. 458-65.
53. Kruman, II, A. Nath, and M.P. Mattson, *HIV-1 protein Tat induces apoptosis of hippocampal neurons by a mechanism involving caspase activation, calcium overload, and oxidative stress.* Exp Neurol, 1998. **154**(2): p. 276-88.
54. Nath, A., et al., *Synergistic neurotoxicity by human immunodeficiency virus proteins Tat and gp120: protection by memantine.* Ann Neurol, 2000. **47**(2): p. 186-94.
55. Haughey, N.J., et al., *Involvement of inositol 1,4,5-trisphosphate-regulated stores of intracellular calcium in calcium dysregulation and neuron cell death caused by HIV-1 protein tat.* J Neurochem, 1999. **73**(4): p. 1363-74.
56. Bartz, S.R. and M. Emerman, *Human immunodeficiency virus type 1 Tat induces apoptosis and increases sensitivity to apoptotic signals by up-regulating FLICE/caspase-8.* J Virol, 1999. **73**(3): p. 1956-63.
57. Albini, A., et al., *The angiogenesis induced by HIV-1 tat protein is mediated by the Flk-1/KDR receptor on vascular endothelial cells.* Nat Med, 1996. **2**(12): p. 1371-5.
58. Ghezzi, S., et al., *Inhibition of CXCR4-dependent HIV-1 infection by extracellular HIV-1 Tat.* Biochem Biophys Res Commun, 2000. **270**(3): p. 992-6.
59. Liu, Y., et al., *Uptake of HIV-1 tat protein mediated by low-density lipoprotein receptor-related protein disrupts the neuronal metabolic balance of the receptor ligands.* Nat Med, 2000. **6**(12): p. 1380-7.
60. Rebeck, G.W., et al., *Apolipoprotein E in sporadic Alzheimer's disease: allelic variation and receptor interactions.* Neuron, 1993. **11**(4): p. 575-80.
61. Passiatore, G., et al., *HIV-1 Tat C-terminus is cleaved by calpain 1: implication for Tat-mediated neurotoxicity.* Biochim Biophys Acta, 2009. **1793**(2): p. 378-87.
62. Haughey, N.J., et al., *HIV-1 Tat through phosphorylation of NMDA receptors potentiates glutamate excitotoxicity.* J Neurochem, 2001. **78**(3): p. 457-67.

63. Haughey, N.J. and M.P. Mattson, *Calcium dysregulation and neuronal apoptosis by the HIV-1 proteins Tat and gp120.* J Acquir Immune Defic Syndr, 2002. **31 Suppl 2**: p. S55-61.

64. Bacskai, B.J., et al., *The endocytic receptor protein LRP also mediates neuronal calcium signaling via N-methyl-D-aspartate receptors.* Proc Natl Acad Sci U S A, 2000. **97**(21): p. 11551-6.

65. Guix, F.X., et al., *The physiology and pathophysiology of nitric oxide in the brain.* Prog Neurobiol, 2005. **76**(2): p. 126-52.

66. Cao, J., et al., *The PSD95-nNOS interface: a target for inhibition of excitotoxic p38 stress-activated protein kinase activation and cell death.* J Cell Biol, 2005. **168**(1): p. 117-26.

67. Singh, I.N., et al., *Differential involvement of p38 and JNK MAP kinases in HIV-1 Tat and gp120-induced apoptosis and neurite degeneration in striatal neurons.* Neuroscience, 2005. **135**(3): p. 781-90.

68. Singh, I.N., et al., *Apoptotic death of striatal neurons induced by human immunodeficiency virus-1 Tat and gp120: Differential involvement of caspase-3 and endonuclease G.* J Neurovirol, 2004. **10**(3): p. 141-51.

69. Conant, K., et al., *Induction of monocyte chemoattractant protein-1 in HIV-1 Tat-stimulated astrocytes and elevation in AIDS dementia.* Proc Natl Acad Sci U S A, 1998. **95**(6): p. 3117-21.

70. Cinque, P., et al., *Elevated cerebrospinal fluid levels of monocyte chemotactic protein-1 correlate with HIV-1 encephalitis and local viral replication.* AIDS, 1998. **12**(11): p. 1327-32.

71. Eugenin, E.A., et al., *MCP-1 (CCL2) protects human neurons and astrocytes from NMDA or HIV-tat-induced apoptosis.* J Neurochem, 2003. **85**(5): p. 1299-311.

72. Sevigny, J.J., et al., *Evaluation of HIV RNA and markers of immune activation as predictors of HIV-associated dementia.* Neurology, 2004. **63**(11): p. 2084-90.

73. Nath, A. and J. Geiger, *Neurobiological aspects of human immunodeficiency virus infection: neurotoxic mechanisms.* Prog Neurobiol, 1998. **54**(1): p. 19-33.

74. D'Aversa, T.G., E.A. Eugenin, and J.W. Berman, *NeuroAIDS: contributions of the human immunodeficiency virus-1 proteins Tat and gp120 as well as CD40 to microglial activation.* J Neurosci Res, 2005. **81**(3): p. 436-46.

75. Minghetti, L., et al., *Multiple actions of the human immunodeficiency virus type-1 Tat protein on microglial cell functions.* Neurochem Res, 2004. **29**(5): p. 965-78.

76. D'Aversa, T.G., K.O. Yu, and J.W. Berman, *Expression of chemokines by human fetal microglia after treatment with the human immunodeficiency virus type 1 protein Tat.* J Neurovirol, 2004. **10**(2): p. 86-97.

77. Lokensgard, J.R., et al., *Diazepam inhibits HIV-1 Tat-induced migration of human microglia.* J Neurovirol, 2001. **7**(5): p. 481-6.

78. Eugenin, E.A., et al., *HIV-1 tat protein induces a migratory phenotype in human fetal microglia by a CCL2 (MCP-1)-dependent mechanism: possible role in NeuroAIDS.* Glia, 2005. **49**(4): p. 501-10.

79. Recio, J.A. and A. Aranda, *Activation of the HIV-1 long terminal repeat by nerve growth factor*. J Biol Chem, 1997. **272**(43): p. 26807-10.

80. Ensoli, F., B. Ensoli, and C.J. Thiele, *HIV-1 gene expression and replication in neuronal and glial cell lines with immature phenotype: effects of nerve growth factor.* Virology, 1994. **200**(2): p. 668-76.

81. Zauli, G., et al., *Human immunodeficiency virus type 1 Tat protein protects lymphoid, epithelial, and neuronal cell lines from death by apoptosis.* Cancer Res, 1993. **53**(19): p. 4481-5.

82. Shugurova, I., et al., *The expression of HIV-1 tat and nef genes induces cell-specific changes in growth properties and morphology of different types of rat cells.* Cell Prolif, 2002. **35**(4): p. 237-45.

83. Bergonzini, V., et al., *HIV-Tat promotes cellular proliferation and inhibits NGF-induced differentiation through mechanisms involving Id1 regulation.* Oncogene, 2004. **23**(46): p. 7701-11.

84. Benezra, R., et al., *The protein Id: a negative regulator of helix-loop-helix DNA binding proteins.* Cell, 1990. **61**(1): p. 49-59.

85. Zebedee, Z. and E. Hara, *Id proteins in cell cycle control and cellular senescence*. Oncogene, 2001. **20**(58): p. 8317-25.

86. Cai, L., E.M. Morrow, and C.L. Cepko, *Misexpression of basic helix-loop-helix genes in the murine cerebral cortex affects cell fate choices and neuronal survival.* Development, 2000. **127**(14): p. 3021-30.

87. Norton, J.D., *ID helix-loop-helix proteins in cell growth, differentiation and tumorigenesis.* J Cell Sci, 2000. **113 (Pt 22)**: p. 3897-905.

88. Ruzinova, M.B. and R. Benezra, *Id proteins in development, cell cycle and cancer.* Trends Cell Biol, 2003. **13**(8): p. 410-8.

89. Sikder, H.A., et al., *Id proteins in cell growth and tumorigenesis.* Cancer Cell, 2003. **3**(6): p. 525-30.

90. Frade, J.M., *Unscheduled re-entry into the cell cycle induced by NGF precedes cell death in nascent retinal neurones.* J Cell Sci, 2000. **113 (Pt 7)**: p. 1139-48.

91. Klein, J.A., et al., *The harlequin mouse mutation downregulates apoptosis-inducing factor.* Nature, 2002. **419**(6905): p. 367-74.

92. Liu, D.X. and L.A. Greene, *Neuronal apoptosis at the G1/S cell cycle checkpoint.* Cell Tissue Res, 2001. **305**(2): p. 217-28.

93. Husseman, J.W., D. Nochlin, and I. Vincent, *Mitotic activation: a convergent mechanism for a cohort of neurodegenerative diseases.* Neurobiol Aging, 2000. **21**(6): p. 815-28.

94. Yang, Y., D.S. Geldmacher, and K. Herrup, *DNA replication precedes neuronal cell death in Alzheimer's disease.* J Neurosci, 2001. **21**(8): p. 2661-8.

95. Jin, K., et al., *Neurogenesis in dentate subgranular zone and rostral subventricular zone after focal cerebral ischemia in the rat.* Proc Natl Acad Sci U S A, 2001. **98**(8): p. 4710-5.

96. Jin, K., et al., *Increased hippocampal neurogenesis in Alzheimer's disease.* Proc Natl Acad Sci U S A, 2004. **101**(1): p. 343-7.

97. Liu, J., et al., *Increased neurogenesis in the dentate gyrus after transient global ischemia in gerbils.* J Neurosci, 1998. **18**(19): p. 7768-78.

98. Jen, Y., K. Manova, and R. Benezra, *Each member of the Id gene family exhibits a unique expression pattern in mouse gastrulation and neurogenesis.* Dev Dyn, 1997. **208**(1): p. 92-106.

99. Ross, S.E., M.E. Greenberg, and C.D. Stiles, *Basic helix-loop-helix factors in cortical development.* Neuron, 2003. **39**(1): p. 13-25.

100. Bres, V., et al., *Differential acetylation of Tat coordinates its interaction with the co-activators cyclin T1 and PCAF.* EMBO J, 2002. **21**(24): p. 6811-9.

101. Dorr, A., et al., *Transcriptional synergy between Tat and PCAF is dependent on the binding of acetylated Tat to the PCAF bromodomain.* EMBO J, 2002. **21**(11): p. 2715-23.

102. Kaehlcke, K., et al., *Acetylation of Tat defines a cyclinT1-independent step in HIV transactivation.* Mol Cell, 2003. **12**(1): p. 167-76.

103. Kiernan, R.E., et al., *HIV-1 tat transcriptional activity is regulated by acetylation.* EMBO J, 1999. **18**(21): p. 6106-18.

104. Mujtaba, S., et al., *Structural basis of lysine-acetylated HIV-1 Tat recognition by PCAF bromodomain.* Mol Cell, 2002. **9**(3): p. 575-86.

105. Ott, M., et al., *Acetylation of the HIV-1 Tat protein by p300 is important for its transcriptional activity.* Curr Biol, 1999. **9**(24): p. 1489-92.

106. Ramirez, S.H., et al., *Neurotrophins prevent HIV Tat-induced neuronal apoptosis via a nuclear factor-kappaB (NF-kappaB)-dependent mechanism.* J Neurochem, 2001. **78**(4): p. 874-89.

107. Liu, N., et al., *The evolution and functional diversification of animal microRNA genes.* Cell Res, 2008. **18**(10): p. 985-96.

108. Saini, H.K., S. Griffiths-Jones, and A.J. Enright, *Genomic analysis of human microRNA transcripts.* Proc Natl Acad Sci U S A, 2007. **104**(45): p. 17719-24.

109. Stefani, G. and F.J. Slack, *Small non-coding RNAs in animal development.* Nat Rev Mol Cell Biol, 2008. **9**(3): p. 219-30.

110. Peters, L. and G. Meister, *Argonaute proteins: mediators of RNA silencing.* Mol Cell, 2007. **26**(5): p. 611-23.

111. Zamore, P.D., *RNA silencing: genomic defence with a slice of pi.* Nature, 2007. **446**(7138): p. 864-5.

112. Valencia-Sanchez, M.A., et al., *Control of translation and mRNA degradation by miRNAs and siRNAs.* Genes Dev, 2006. **20**(5): p. 515-24.

113. Griffiths-Jones, S., *The microRNA Registry.* Nucleic Acids Res, 2004. **32**(Database issue): p. D109-11.

114. Kapsimali, M., et al., *MicroRNAs show a wide diversity of expression profiles in the developing and mature central nervous system.* Genome Biol, 2007. **8**(8): p. R173.

115. Lau, P., et al., *Identification of dynamically regulated microRNA and mRNA networks in developing oligodendrocytes.* J Neurosci, 2008. **28**(45): p. 11720-30.

116. Hebert, S.S. and B. De Strooper, *Molecular biology. miRNAs in neurodegeneration.* Science, 2007. **317**(5842): p. 1179-80.

117. Kim, J., et al., *A MicroRNA feedback circuit in midbrain dopamine neurons.* Science, 2007. **317**(5842): p. 1220-4.

118. Johnson, R., et al., *A microRNA-based gene dysregulation pathway in Huntington's disease.* Neurobiol Dis, 2008. **29**(3): p. 438-45.

119. Eletto, D., et al., *Inhibition of SNAP25 expression by HIV-1 Tat involves the activity of mir-128a.* J Cell Physiol, 2008. **216**(3): p. 764-70.

120. McCoy, M.K. and M.G. Tansey, *TNF signaling inhibition in the CNS: implications for normal brain function and neurodegenerative disease.* J Neuroinflammation, 2008. **5**: p. 45.

121. O'Connor, M.F., M.R. Irwin, and D.K. Wellisch, *When grief heats up: pro-inflammatory cytokines predict regional brain activation.* Neuroimage, 2009. **47**(3): p. 891-6.

122. Ashraf, S.I. and S. Kunes, *A trace of silence: memory and microRNA at the synapse.* Curr Opin Neurobiol, 2006. **16**(5): p. 535-9.

123. Nunez-Iglesias, J., et al., *Joint genome-wide profiling of miRNA and mRNA expression in Alzheimer's disease cortex reveals altered miRNA regulation.* PLoS One. **5**(2): p. e8898.

124. Kocerha, J., et al., *MicroRNA-219 modulates NMDA receptor-mediated neurobehavioral dysfunction.* Proc Natl Acad Sci U S A, 2009. **106**(9): p. 3507-12.

125. Chen, X., et al., *Characterization of microRNAs in serum: a novel class of biomarkers for diagnosis of cancer and other diseases.* Cell Res, 2008. **18**(10): p. 997-1006.

126. Chen, X., et al., *Identification and characterization of microRNAs in raw milk during different periods of lactation, commercial fluid, and powdered milk products.* Cell Res. **20**(10): p. 1128-37.

127. Park, N.J., et al., *Salivary microRNA: discovery, characterization, and clinical utility for oral cancer detection.* Clin Cancer Res, 2009. **15**(17): p. 5473-7.

128. Lawrie, C.H., et al., *Detection of elevated levels of tumour-associated microRNAs in serum of patients with diffuse large B-cell lymphoma.* Br J Haematol, 2008. **141**(5): p. 672-5.
129. Mitchell, P.S., et al., *Circulating microRNAs as stable blood-based markers for cancer detection.* Proc Natl Acad Sci U S A, 2008. **105**(30): p. 10513-8.
130. Hanke, M., et al., *A robust methodology to study urine microRNA as tumor marker: microRNA-126 and microRNA-182 are related to urinary bladder cancer.* Urol Oncol. **28**(6): p. 655-61.
131. Kosaka, N., et al., *microRNA as a new immune-regulatory agent in breast milk.* Silence. **1**(1): p. 7.
132. Ji, X., et al., *Plasma miR-208 as a biomarker of myocardial injury.* Clin Chem, 2009. **55**(11): p. 1944-9.
133. Laterza, O.F., et al., *Plasma MicroRNAs as sensitive and specific biomarkers of tissue injury.* Clin Chem, 2009. **55**(11): p. 1977-83.
134. Wang, K., et al., *Circulating microRNAs, potential biomarkers for drug-induced liver injury.* Proc Natl Acad Sci U S A, 2009. **106**(11): p. 4402-7.
135. Valadi, H., et al., *Exosome-mediated transfer of mRNAs and microRNAs is a novel mechanism of genetic exchange between cells.* Nat Cell Biol, 2007. **9**(6): p. 654-9.
136. Zernecke, A., et al., *Delivery of microRNA-126 by apoptotic bodies induces CXCL12-dependent vascular protection.* Sci Signal, 2009. **2**(100): p. ra81.
137. Kosaka, N., et al., *Secretory mechanisms and intercellular transfer of microRNAs in living cells.* J Biol Chem. **285**(23): p. 17442-52.
138. Zhang, Y., et al., *Secreted monocytic miR-150 enhances targeted endothelial cell migration.* Mol Cell. **39**(1): p. 133-44.
139. Arroyo, J.D., et al., *Argonaute2 complexes carry a population of circulating microRNAs independent of vesicles in human plasma.* Proc Natl Acad Sci U S A. **108**(12): p. 5003-8.
140. Turchinovich, A., et al., *Characterization of extracellular circulating microRNA.* Nucleic Acids Res. **39**(16): p. 7223-33.
141. Vickers, K.C., et al., *MicroRNAs are transported in plasma and delivered to recipient cells by high-density lipoproteins.* Nat Cell Biol. **13**(4): p. 423-33.
142. Pegtel, D.M., et al., *Functional delivery of viral miRNAs via exosomes.* Proc Natl Acad Sci U S A. **107**(14): p. 6328-33.

143. Skog, J., et al., *Glioblastoma microvesicles transport RNA and proteins that promote tumour growth and provide diagnostic biomarkers.* Nat Cell Biol, 2008. **10**(12): p. 1470-6.

144. Rabinowits, G., et al., *Exosomal microRNA: a diagnostic marker for lung cancer.* Clin Lung Cancer, 2009. **10**(1): p. 42-6.

145. Taylor, D.D. and C. Gercel-Taylor, *MicroRNA signatures of tumor-derived exosomes as diagnostic biomarkers of ovarian cancer.* Gynecol Oncol, 2008. **110**(1): p. 13-21.

146. Gourzones, C., et al., *Extra-cellular release and blood diffusion of BART viral micro-RNAs produced by EBV-infected nasopharyngeal carcinoma cells.* Virol J. **7**: p. 271.

147. Kaul, M., et al., *HIV-1 infection and AIDS: consequences for the central nervous system.* Cell Death Differ, 2005. **12 Suppl 1**: p. 878-92.

148. Lindl, K.A., et al., *HIV-associated neurocognitive disorder: pathogenesis and therapeutic opportunities.* J Neuroimmune Pharmacol, 2010. **5**(3): p. 294-309.

149. Rom, S., et al., *HIV-1 Tat binds to SH3 domains: cellular and viral outcome of Tat/Grb2 interaction.* Biochim Biophys Acta, 2011. **1813**(10): p. 1836-44.

150. Pacifici, M., et al., *Cerebrospinal fluid miRNA profile in HIV-encephalitis.* J Cell Physiol, 2012.